Radiochemical Separation and Purification of Molybdenum-99 for Medical and Industrial Applications

By

ABHISHEK KUMAR SHARMA

CHEM01201204015

Bhabha Atomic Research Centre, Mumbai

A thesis submitted to the
Board of Studies in Chemical Sciences

In partial fulfillment of requirements
for the Degree of

DOCTOR OF PHILOSOPHY

of

HOMI BHABHA NATIONAL INSTITUTE

Febuary, 2020

Homi Bhabha National Institute[1]

Recommendations of the Viva Voce Committee

As members of the Viva Voce Committee, we certify that we have read the dissertation prepared by ABHISHEK KUMAR SHARMA entitled "Radiochemical Separation and Purification of Molybdenum-99 for Medical and Industrial Applications" and recommend that it may be accepted as fulfilling the thesis requirement for the award of Degree of Doctor of Philosophy.

Chairman - Dr. Ashutosh Dash, BARC		Date 28/8/2020
Guide / Convener - Dr. B. S. Tomar, HBNI		Date 28/8/2020
Examiner - Dr. Bhagvant Rai Mittal, PGIMER	online	Date 28/8/20
Member 1- Dr. S. Kannan, BARC		Date 28/8/20
Member 2- Dr. Sudipta Chakraborty, BARC	Sudipta Chakraborty	Date 28/08/20
Member 3- Dr. V. Sudarsan, BARC	Sudarsan. V	Date 28/8/2020

Final approval and acceptance of this thesis is contingent upon the candidate's submission of the final copies of the thesis to HBNI.

I/We hereby certify that I/we have read this thesis prepared under my/our direction and recommend that it may be accepted as fulfilling the thesis requirement.

Date: 28.08.2020

Place: HBNI

Guide

(Dr. B. S. Tomar)

[1] This page is to be included only for final submission after successful completion of viva voce.

STATEMENT BY AUTHOR

This dissertation has been submitted in partial fulfillment of requirements for an advanced degree at Homi Bhabha National Institute (HBNI) and is deposited in the Library to be made available to borrowers under rules of the HBNI.

Brief quotations from this dissertation are allowable without special permission, provided that accurate acknowledgement of source is made. Requests for permission for extended quotation from or reproduction of this manuscript in whole or in part may be granted by the Competent Authority of HBNI when in his or her judgment the proposed use of the material is in the interests of scholarship. In all other instances, however, permission must be obtained from the author.

(Abhishek Kumar Sharma)

DECLARATION

I, hereby declare that the investigation presented in the thesis has been carried out by me. The work is original and has not been submitted earlier as a whole or in part for a degree/diploma at this or any other Institution / University.

(Abhishek Kumar Sharma)

List of Publications arising from the thesis

Journal

1. Development of ^{99}Mo-alfa-benzoin oxime complex as industrial radiotracer for identification of leaky heat exchanger and its validation with ^{99m}Tc. **Abhishek K. Sharma**, Gaurav Agrahari, C. B. Tiwari, B. S. Tomar and V. N. Yelgaonkar. *Journal Radioanal Nucl Chem* 323, 143–149 **(2020)**.

2. Syntheses and biological evaluation of ^{99m}Tc-HYNIC-fatty acid complexes for myocardial imaging. Anupam Mathur, **Abhishek K. Sharma**, V. V. Murhekar, Madhava B. Mallia, Shital Pawade, H. D. Sarma, Pradip Chaudhari, S. S. Sachdev and Sharmila Banerjee. *RSC Adv.*, **(2015)**, 5, 93374

3. Studies on separation and purification of fission ^{99}Mo from neutron activated uranium aluminum alloy. Ankita Rao, **Abhishek Kumar Sharma**, Pradeep Kumar, M.M. Charyulu, B.S. Tomar, K.L. Ramakumar. *Applied Radiation and Isotopes*, 89 **(2014),** 186–191

Conference/Symposium

1. Synthesis and bio-evaluation of novel ^{99m}Tc-HYNIC-fatty acid complexes for their potential use as myocardial imaging agent. ***Abhishek K. Sharma****,Anupam Mathur,V.V. Muhrekar, Madhav B. Mallia, H.D. Sarma, Uma Sheri, S.S.Sachdev ,Sharmila Banerjee.*45th Annual Conference of the Society of Nuclear Medicine-India (SNMICON 2013), Mumbai, December 2013.

2. Separation and Purification of Fission ^{99}Mo from neutron irradiated UAl_3 Alloy
*Ankita Rao, **Abhishek Kumar Sharma**, Pradeep Kumar, M.M. Charyulu, B.S. Tomar,K.L. Ramakumar*. 11th biennial symposium on "Nuclear and Radiochemistry" (NUCAR-2013), Jabalpur, February 2013.

(Abhishek Kumar Sharma)

DEDICATIONS

To my Family.....

ACKNOWLEDGEMENTS

This dissertation would not have been accomplished without the help and motivation from numerous people including my well-wishers, friends, and colleagues who contributed in many ways to the successful completion of this Thesis. Firstly, I would like to express my sincere gratitude to my guide Dr. B. S. Tomar for his support, patience and encouragement throughout this study. His knowledge and experience helped me a lot during the course of my Ph.D. work. Besides my guide, I would like to thank my doctoral committee members; Prof. A. Dash, Prof. S. Kannan, Dr. Sudipta Chakraborty and Dr. V. Sudarsan for their time, encouragement and critical evaluation during the course of my Ph.D.

My sincere thanks to my lab mates and to my senior collegues who always kept me motivating to carry out the thesis related work.

I am grateful to my friend Adish tyagi who always inspired me a lot and supported me in thick and thin of the time.

I would like to thank my beloved parents for their support and patience throughout all of my academic work. Words cannot express my gratitude for the unconditional love and unwavering support. I would like to thank to my wife, Richa and to my daughter Aadhya for their support, and the motivational kick. This list of incredible people who fill my life is endless and I regret not being able to explicitly name everybody.

Febuary, 2020

Abhishek Kumar Sharma

BRIT, Mumbai

CONTENTS

SYNOPSIS

Radioisotopes are the radioactive isotopes of an element which posses an unstable combination of neutron and proton, which upon emitting radiation get transformed to relatively stable isotope. Radioisotopes have vast applications in the field of healthcare, industry and agriculture [1-4]. Most of the radioisotopes are artificially produced in research reactors or in particle accelerators by exposing the target nuclide to the projectiles such as neutrons or charged particles (deuterons, protons, alpha particles etc.) [5,6]. During exposure the stable nuclide of target element get converted to radioisotope of same element or of a different element. Irradiation of target atoms with neutrons results in neutron rich product radioisotopes, which decay by emitting β^- particles and most often accompanying γ-rays emission. Typical nuclear reactions used for radioisotopes production are (n,γ), (n,α), (n,p) and (n,f). Radioisotope production in accelerator involves the irradiation of target nuclides with the charge particles (protons, deuterons, He^{+2} etc.), which results in the product nuclides rich in protons. These protons rich radio-nuclides decay by emitting positron or by electron capture (EC). After irradiation of target material, it is radio-chemically processed to get the desired chemical form of radioisotope suitable for its application in healthcare, industry and research [5,6].

In healthcare, radioisotopes are extensively used as radio-pharmaceuticals for diagnosis and treatment of various disorder and diseases. Radiopharmaceutical is a compound in which a molecule is tagged with a radioisotope, and used for nuclear imaging or treatment of illness. Radiopharmaceuticals can be classified as diagnostic or therapeutic radiopharmaceuticals [7,8]. Diagnostic radiopharmaceuticals are tagged with γ-rays emitting radioisotope or positron emitting radioisotope and are used in "single photon emission computed tomography" (SPECT)

and "positron emission tomography" (PET) imaging techniques to obtain highly precise three-dimensional morphology of organs and tissues. There are several diagnostic radioisotopes, which have been artificially produced (^{99m}Tc, ^{131}I, ^{18}F, ^{82}Rb, ^{111}In, ^{123}I, ^{133}Xe, ^{201}Tl etc.) and used for nuclear diagnostic imaging. Out of these, ^{99m}Tc is the most popular radioisotope in the field of nuclear diagnostic imaging. ^{99m}Tc is used in about 80% of the total nuclear diagnostic imaging procedure carried out world over and is considered as the work horse of the nuclear diagnostic imaging. The factors which have made ^{99m}Tc so popular are its short half life (6 h), suitable γ-ray energy (140 keV), ease of availability from ^{99}Mo-^{99m}Tc generators, versatile chemistry of technetium and suitability of instant labeling using cold kits to make radiopharmaceuticals for SPECT imaging [9, 10].

In nuclear medicine centers, ^{99m}Tc required for preparation of radiopharmaceutical is availed from the ^{99}Mo-^{99m}Tc radioisotope generators. A radioisotope generator is a system in which the short lived daughter radioisotope (^{99m}Tc, $T_{1/2}$: 6 hrs) remains in the state of radioactive equilibrium with its long lived parent radioisotope (^{99}Mo, $T_{1/2}$: 66 hrs) and repeated separation of daughter can be carried out. Different types of ^{99}Mo-^{99m}Tc radioisotope generators have been made, such as, column chromatographic generators, solvent extraction generators, precipitation generator, electrochemical generators and sublimation generators. Out of these generators, alumina sorbent based column chromatography generators, loaded with high specific activity ^{99}Mo, are the most popular due to their ease of operation at radio-pharmacies [11,12].

Large scale production of ^{99}Mo is carried out in research reactors by neutron activation of molybdenum target [^{98}Mo(n,γ)^{99}Mo] or by fission of uranium target [^{235}U(n,f)^{99}Mo]. Whereas the former route yields low specific activity of ^{99}Mo (<1 Ci/ g), the latter route yields high specific activity ^{99}Mo (>10^4 Ci/ g) and is desirable for making the alumina sorbent based ^{99}Mo-

^{99m}Tc column generators. Production of medical grade ^{99}Mo from fission route involves the complex radiochemical separation and purification procedure to get the desired level of purity suitable for making ^{99}Mo-^{99m}Tc generators for clinical use [13, 14].

In the present work, a radiochemical method has been developed for separation and purification of ^{99}Mo from thermal neutron irradiated uranium-aluminum alloy target to get high specific activity ^{99}Mo suitable for making ^{99}Mo-^{99m}Tc radioisotope generators. Further, towards medical application, two sets of HYNIC conjugated fatty acid molecules were synthesized, radio-labeled with ^{99m}Tc and biologically evaluated for their potential as myocardial imaging agent. Also, towards industrial utility of ^{99}Mo, a ^{99}Mo-ABO complex based industrial radiotracer has been developed and tested for leak detection studies in hydrocarbon stream of a petroleum refinery. The details of the above works are compiled in five chapters as follows:

Chapter 1: Introduction

This chapter gives general introduction on production of radioisotopes. A brief discussion on different production routes for ^{99}Mo and importance of specific activity of a radioisotope. Radioactive equilibrium, radioisotope generators and different types of ^{99}Mo-^{99m}Tc radioisotope generators have been described. This is followed by brief description of radiopharmaceuticals and use of ^{99m}Tc based radiopharmaceuticals in the field nuclear diagnostic imaging, fatty acid based myocardial metabolic imaging agents. A general discussion on use of radiotracer for industrial application has been added. A brief note on the objective and motivation of the present work has also been included at the end of this chapter.

Chapter 2: Characterization techniques

This chapter describes general materials and chemicals used during the present investigation followed by a brief discussion on experimental tools and techniques such as NMR spectroscopy, Infrared spectroscopy (IR), Electro-spray Ionization Mass Spectroscopy (ESI-MS), High Performance Liquid Chromatography (HPLC), NaI(Tl) scintillation detector, High Purity Germanium (HPGe) based γ-Ray Spectroscopy.

Chapter 3: Separation and purification of fission ^{99}Mo from thermal neutron irradiated natural uranium-aluminium (U-Al) target

This chapter presents a detailed study of production of high specific activity, medical grade ^{99}Mo from thermal neutron irradiated Uranium-Aluminum alloy target. ^{99}Mo ($T_{1/2}$: 66 hrs, Eγ: 180 keV, 740 keV, 780 keV) is parent isotope of ^{99m}Tc ($T_{1/2}$: 6 hrs, E_γ: 140 keV) and used for production of ^{99}Mo-^{99m}Tc radioisotope generators. ^{99}Mo-^{99m}Tc radioisotope generators are used to avail ^{99m}Tc at radio-pharmacies for the formulation of ^{99m}Tc based radiopharmaceuticals.

Large scale production of ^{99}Mo is carried out either by neutron activation route [^{98}Mo(n,γ)^{99}Mo] or by fission route [^{235}U(n,f)^{99}Mo]. Neutron activation yields ^{99}Mo of low specific activity (< 1 Ci/ g), whereas fission route yields high specific ^{99}Mo (> 10^4 Ci/ g). High specific activity ^{99}Mo is a desirable feature for manufacturing of alumina sorbent based ^{99}Mo-^{99m}Tc column chromatography generators.

Several methods have been used for production of medical grade ^{99}Mo from fission route. All these routes can be broadly classified in two categories, depending upon the initial radio-chemical treatment of irradiated target as described below.

(1) Acidic dissolution of irradiated target followed by precipitation of ^{99}Mo and subsequent purification steps (e.g. CINTICHEM process).

(2) Alkaline dissolution of irradiated target followed by purification of ^{99}Mo by series of ion exchange columns.

In this present work, a novel radio-chemical separation and purification methodology has been developed to avail medical grade ^{99}Mo from fission rote. Uranium-Aluminum alloy target (100 mg) was irradiated with thermal neutrons (flux: $5x10^{13}$ n/cm^2/sec) for 7 days in DHRUVA reactor at Trombay. Target was allowed to cool for 2 days for decay of short lived radioisotopes. Target was then dissolved in 6 M NaOH solution. Molybdenum and iodine were quantitatively leached into the solution along with small fractions of ^{132}Te, ^{239}Np, ^{103}Ru, ^{95}Zr, ^{95}Nb, ^{141}Ce and ^{140}Ba. Uranium and other fission and activation products (e.g. ^{137}Cs, ^{239}Pu, ^{89,90}Sr etc.) remains un-dissolved in the solid residue. Solid residue was separated by filtration and the filtrate, containing ^{99}Mo, was further purified to obtain medical grade ^{99}Mo. The following figure shows the Gamma-ray spectrum of the filtrate:

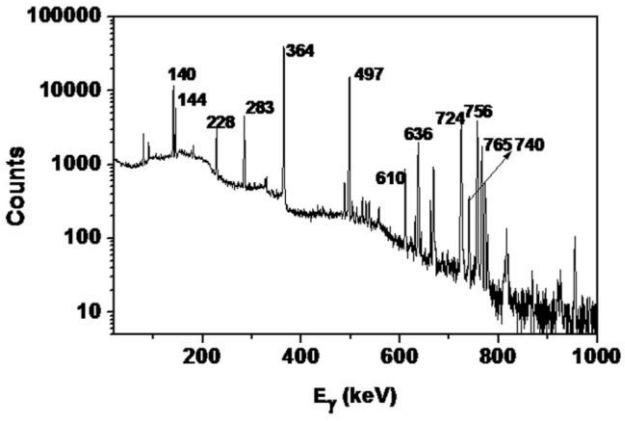

Fig.1 *Gamma ray spectrum of filtrate containing Mo-99*

Filtrate, conta rocesses involving precipitation, evaporation and ion-exchange. Aluminum in the filtrate was removed as $Al(OH)_3$

ppt. by adjusting the pH between 8-9 and filtration. Further, KI and KIO_3 were added to the filtrate as carrier for iodine in different oxidation states. Silver nitrate solution was added into this solution to precipitate radio-iodine, which was removed by filtration. The filtrate was evaporated to dryness and then reconstituted with concentrated nitric acid. $NaBiO_3$ was added to the reconstituted solution and then boiled-off to remove ^{103}Ru as volatile RuO_4. Residue obtained was digested in HNO_3 (3-4 mol L^{-1}). Digested solution was further added with Zr, Ru, Sr, Te, Fe (1 mL each of 2mg/ mL solution) carriers. ^{99}Mo present in the obtained solution was quantitatively precipitated by drop-wise addition of alpha-benzoin-oxime (2 % ethanolic solution) as Mo-α-benzoin-oxime (Mo-ABO) complex. Further, Mo-ABO complex was dissolved in 2 M NaOH followed by boiling-off the solution and again made with 0.4 M NaOH solution. Solution was passed through silver coated activated charcoal (AgC) column to remove organic content. Final purification was done by Amberlyst A-26 anion exchange column to obtain high specific activity ^{99}Mo, suitable for medical applications.

Chapter 4: Synthesis, Radiolabelling and bio-evaluation of novel ^{99m}Tc-HYNIC-Fatty acid complexes for their potential use as myocardial imaging agent

This chapter is related to the medical application of ^{99}Mo. The work involves the synthesis and characterization of two fatty acid (FA)-hydrazinopyridine-3-carboxylic acid (HYNIC) conjugates (11C-FA-HYNIC and 12C-FA-HYNIC). Further these conjugated complexes were radio-labeled with ^{99m}Tc using Tricine, EDDA and TPPTS as co-ligands. Bio-distribution studies in Swiss mice were carried out with these radio-labeled complexes to evaluate their potential as myocardial metabolic SPECT imaging agent.

The work involves the synthesis **of t**wo fatty acids of intermediate chain lengths (11 and 12 carbon synthetically modified with HYNIC bi-functional chelator at the ω-position to facilitate radio-labeling with ^{99m}Tc. Scheme for the synthesis of fatty acid-HYNIC conjugates is shown below (Fig.2):

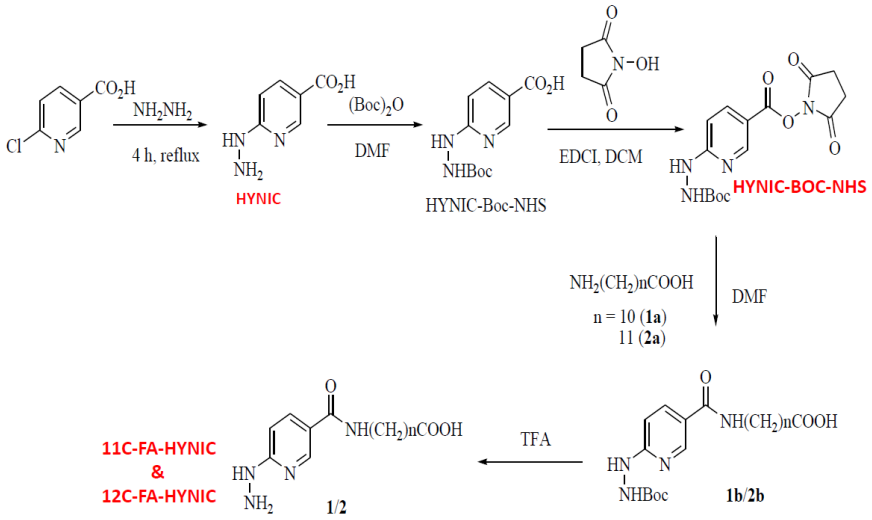

Fig.2 *Synthesis scheme for 11C-FA-HYNIC and 12C-FA-HYNIC conjugates*

All the intermediates and final conjugates were characterized by FT-IR, ^{1}H-NMR and ESI-MS. ^{1}H-NMR of the intermediates as well as the target ligand was consistent with the expected structure and ESI-MS provided additional confirmatory evidence for the formation of the expected ligand.

Fatty acid-HYNIC conjugates (1/2) were subsequently radio-labeled with ^{99m}Tc using tricine, EDDA and TPPTS as co-ligands. The scheme for the preparation of fatty acid-HYNIC-^{99m}Tc complexes is shown below (Fig.3):

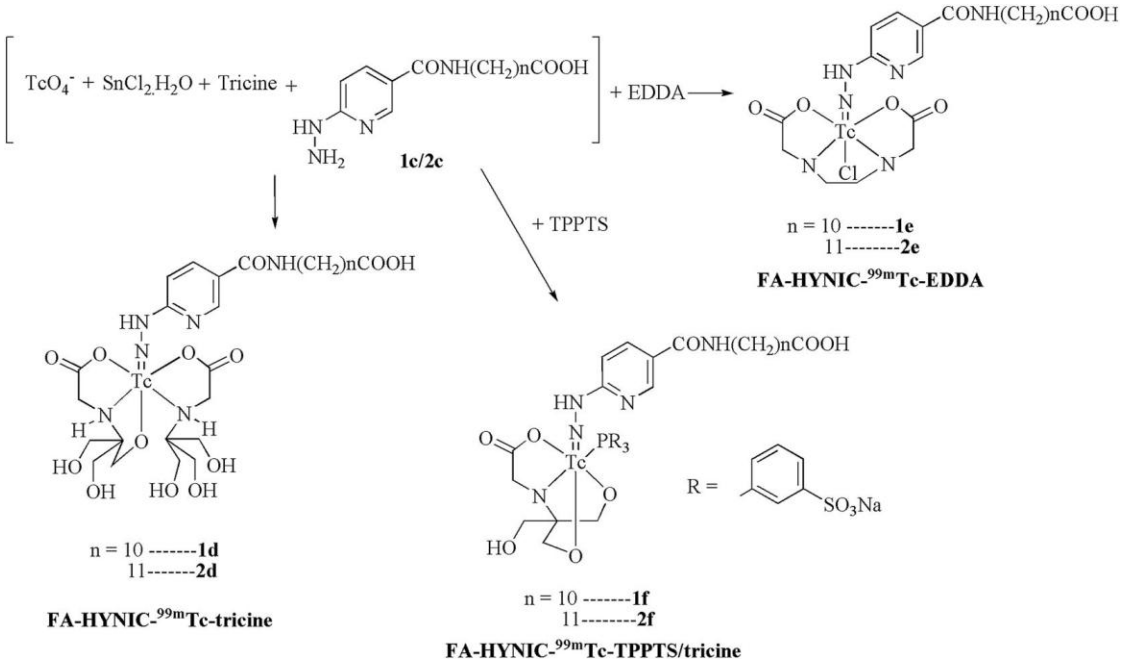

Fig.3 *Radiolabelling of 11C-FA-HYNIC and 12C-FA-HYNIC with* ^{99m}Tc

With the set of two fatty acid-HYNIC conjugates and the above co-ligands, a total of six ^{99m}Tc-fatty acid complexes are prepared (1d/2d, 1e/2e and 1f/2f). The complexes were subsequently analyzed by HPLC. The radiochemical purity of the four complexes, determined from the peak area measurements of the HPLC elution profile were found to be adequate. All the four ^{99m}Tc-HYNIC-fatty acid complexes (1e/2e and 1f/2f) were purified by analytical HPLC using ammonium acetate buffer-methanol system before using for further biological studies.

To obtain the measure of lipophilicity of the complexes (1e/2e, 1f/2f) their partition coefficient, log $P_{o/w}$, was determined. The stability of HPLC purified ^{99m}Tc-fatty acid complexes (1e/2e and 1f/2f) in human serum was tested by incubating the complexes in serum for 30 min. The HPLC chromatogram of the supernatant obtained after the precipitation of serum proteins showed no signs of degradation of the complex.

Biodistribution studies of HPLC purified complexes (1e/2e and 1f/2f) reconstituted in 10% ethanol were carried in normal female Swiss mice. Myocardial uptake of the four ^{99m}Tc-fatty acid complexes and the reference compound, ^{125}I-IPPA was compared. Both fatty acid complexes with EDDA as co-ligand (1e/2e) showed better uptake in the myocardium compared to their TPPTS counterparts (1f/2f). This may be attributed to the lower lipophilicity of the TPPTS complexes which resulted in lower uptake in the myocardium. Among the four ^{99m}Tc-fatty acid complexes, complex 2e showed the highest myocardial uptake [5.95 (0.74)%ID per g] at 2 min p.i. Though all four complexes showed significant activity in myocardium even at 30 min p.i., it was lower than that observed for ^{125}I-IPPA [7.10 (1.79) % ID per g]. High uptake and retention of the radiotracer is essential for myocardial SPECT imaging. However, if not more, clearance of the radiotracer from the background tissue/organs such as blood, liver and lungs, is equally important to obtain high contrast images. Clearance of activity from above mentioned non-target organs with time was analysed. It was found that the clearance of ^{99m}Tc-HYNIC-fatty acid tracers (1e/2e and 1f/2f) from non-target organs such as liver and lungs was better compared to ^{125}I-IPPA. Especially the complex 2e, among all the other complexes, showed significantly lower liver uptake [10.57 (0.45) % ID per g] at 2 min p.i. The latter biological behavior is desirable in IPPA analogues, since early imaging could differentiate between normal/ischemic myocardium and infarct. Consequently, heart to liver ratio of this complex was found better than ^{125}I-IPPA. All ^{99m}Tc-HYNIC-fatty acid complexes (1e/ 2e and 1f/2f) cleared rapidly from liver compared to ^{125}I-IPPA, with TPPTS complexes (1f/2f) showing very sharp fall in liver activity, possibly due to the hydrophilic nature of TPPTS ligand. Uptake of TPPTS complexes (1f/2f) in lungs was also observed to be lower than that of EDDA analogues (1e/2e). All the ^{99m}Tc-

complexes (1e/2e and 1f/2f) showed significant blood pool activity initially compared to ^{125}I-IPPA.

Comparison of bio-distribution results obtained with ^{99m}Tc radiolabelled with that of the most promising ^{99m}Tc-fatty acid tracer i.e. [99mTc]-MAMA-HDA16 evaluated in the same species was carried out. Outcome of comparison suggested that only compound 2e showed a similar myocardial uptake [5.46 (1.15) % ID per g]. HPLC analysis of representative ^{99m}Tc-fatty acid complex (2e) in liver homogenate (collected at 1 h p.i.) was carried out to analyze any metabolic transformation of the tracer inside liver.

Myocardial imaging in mouse was carried out to validate the uptake and washout pattern observed in bio-distribution results and to assess the imaging potential of 12C-EDDA complex (2e). A representative planar image frame of the 12CEDDA complex (2e) was obtained at 2 min p.i. and dynamic SPECT scans of the mouse myocardium were acquired upto 15 min p.i.

Chapter 5: Development and evaluation of organic soluble ^{99}Mo based industrial radiotracer

This work aims towards industrial use of ^{99}Mo. Radiotracers are widely used for various industrial applications such leak detection, flow rate measurement, optimization of chemical process etc. The work involves the development of organic soluble ^{99}Mo based radiotracer for its use in leak detection studies in high pressure, high temperature hydrocarbon stream carrying components of petroleum refineries. Starting with 500 mCi of (n,f)^{99}Mo as Na_2MoO_4, its daughter isotope ^{99m}Tc was separated using solvent extraction with Methyl ethyl ketone. Extraction was carried out in lead shielded glass extractor set-up. For extraction of ^{99m}Tc, the aqueous alkaline solution of ^{99}Mo-sodium molybdate solution was added with methyl ethyl

ketone and mixture was shaken by purging air through mixture. During extraction, ^{99m}Tc got transferred to organic phase from aqueous phase. Organic phase containing ^{99m}Tc was removed and kept separately. Aqueous layer containing ^{99}Mo, was acidified with HNO_3 to decrease the pH to below 1.0. ^{99}Mo was then quantitatively precipitated by the addition of ABO (2 % ethanol solution). Molybdenum formed the Mo-ABO complex and got precipitated, which was dissolved into chloroform. Subsequently, chloroform layer, containing ^{99}Mo as Mo-ABO complex, was mixed in 2 L of diesel and used for radiotracer investigation.

Radiotracer investigation was carried out to detect the leaky heat exchangers out of four serially connected heat exchangers of diesel hydro-treater (DHDT) unit of a leading petroleum refinery. Radiotracer study involves injection of a radiotracer of pre-calculated activity as sharp pulse using a specially designed injection system into the higher pressure side of the heat exchanger system. In case of any leakage in the heat exchanger, fraction of the injected radiotracer will flow from higher pressure side to the lower pressure side [2, 6]. The radiation detectors (NaI(Tl) based scintillator detectors) are kept at the higher pressure side inlet, higher pressure side outlet and lower pressure side outlets of the serially connected heat exchangers.

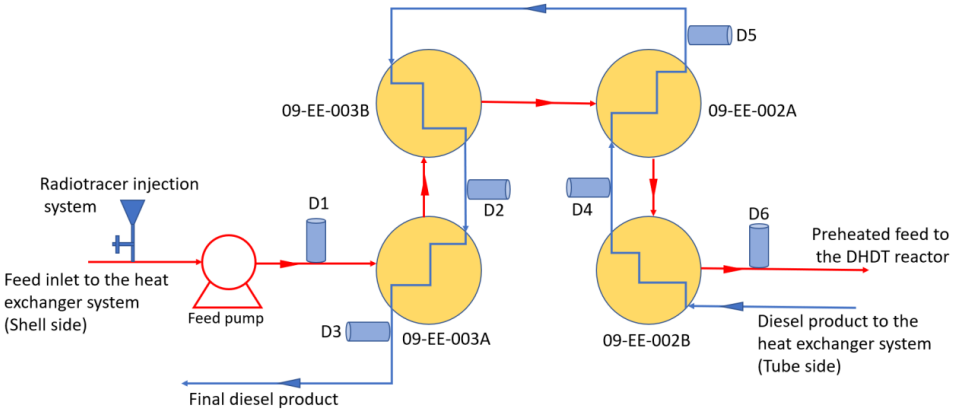

Fig.4: *Schematic of heat exchanger system showing injection system, feed pump and strategically located radiation detectors*

First radiotracer study was carried out by injecting ^{99}Mo-ABO complex dissolved in diesel. The flow of radiotracer in the heat exchanger system, was monitored using NaI(Tl) scintillation detectors (D1,D2,D3, D4, D5 & D6). Table below indicates the location of different detectors in the series of heat exchanger.

Detector No.	Detector location
D1	Shell Inlet of 09-EE-003A
D2	Tube Outlet of 09-EE-003B
D3	Tube Outlet of 09-EE-003A
D4	Tube Outlet of 09-EE-002B
D5	Tube Outlet of 09-EE-002A
D6	Shell Outlet of 09-EE-002B

Table 1*: NaI(Tl) Detectors location*

The count-rate data from each detector was acquired through a multi input data acquisition system (MIDAS). It offers collection and visualization of data in real time. Second radiotracer injection was carried out by injecting 99mTc dissolved in diesel to validate the results obtained for ^{99}Mo-ABO radiotracer injection. The radiotracer investigation with 99Mo based radiotracer indicates the leakage in heat exchanger 09-EE-003B. The results were replicated by using the radiotracer 99mTc in organic phase, indicating the reproducibility of the results and utility of ^{99}Mo-ABO complex radiotracer for

Chapter 6: Summary and outlook

This chapter presents the summary of the outcomes of the work carried out as a part of present thesis. A radio-chemical method was developed for the separation and purification of (n,f)^{99}Mo

from thermal neutron irradiated U-Al alloy target. The purity level of purified ^{99}Mo was found suitable for making ^{99}Mo-^{99m}Tc radioisotope generators. ^{99m}Tc, the daughter of ^{99}Mo, is used for SPECT imaging in the field of nuclear diagnostic. ^{99}Mo is utilized for medical application through its daughter isotope ^{99m}Tc. Towards medical application, two fatty acid-HYNIC conjugates (11C-FA-HYNIC and 12C-FA-HYNIC) were synthesized in good yield and labeled with ^{99m}Tc, using Tricine, EDDA and TPPTS as co-ligands to produce four set of radiolabeled complexes. The bio-distribution studies of radio-labeled complexes in Swiss mice showed reasonable initial myocardial uptake for all four ^{99m}Tc tracers with 12C-EDDA complex exhibiting maximum uptake and retention in the myocardium. This study documents the advantages of the HYNIC BFCA in designing fatty-acid based radiotracers for myocardial imaging.

Towards industrial application of ^{99}Mo, a radiotracer in the form of ^{99}Mo-ABO complex suitable for mixing with organic phase was developed. The developed ^{99}Mo-ABO radiotracer was successfully evaluated for identifying the leaky component of DHDT unit of a leading petroleum refinery. Results were replicated with ^{99m}Tc in organic phase as another radiotracer, showing reproducibility of results.

Overall, this thesis describes a radiochemical separation method for production of high specific activity, medical grade ^{99}Mo. Medical application of ^{99}Mo, through its daughter radioisotope ^{99m}Tc in the form of fatty acid based myocardial SPECT imaging agent. Industrial application of ^{99}Mo in the form ^{99}Mo-ABO complex based industrial radiotracer.

References

1. M Atkins H.L. *Appl. Radiat. Isot.*, **1998**, *49*, 277.
2. Liu S., Edwards D. S. *Bioconjug. Chem*, **2001**, *12*, 7.
3. International Atomic Energy Agency (IAEA) (1990), Technical reports series No. 316,Vienna, Austria
4. J. Thýn (1989) Radioisotope Techniques for Process Optimization, Isotopenpraxis Isotopes in Environmental and Health Studies, 25:4, 144-151
5. INTERNATIONAL ATOMIC ENERGY AGENCY, IAEA-TECDOC-1340, IAEA, Vienna (2003)
6. INTERNATIONAL ATOMIC ENERGY AGENCY, Technical Reports Series No. 468, IAEA, Vienna (2009).
7. Verbruggen A.M. Eur. J. Nucl. Med., 1990, 17, 346.
8. Banerjee S., Pillai M.R.A., Ramamoorthy N. Sem. Nucl. Med., **2001**, 32, 260
9. Jurisson S., Lydon J.D. *Chem. Rev.*, **1999**, *99*, 2205
10. Trends in Radiopharmaceuticals (ISTR-2005), Proceedings of an International Symposium, **2007**, 1
11. Mirzadeh, S. & Knapp, F.F. Journal of Radioanalytical and Nuclear Chemistry, Articles (1996) 203: 471
12. Dash, Ashutosh & Mra, Pillai. (2013). 99Mo/99mTc Separation: An Assessment of Technology Options. Nuclear Medicine and Biology. 40. 167–176.
13. IAEA-TECDOC, **1999,** 1065
14. Seung-Kon Lee, Gerd J. Beyer, Jun Sig Lee, Nuclear Engineering and Technology, Volume 48, Issue 3, 2016, Pages 613-623

List of Figures

List of Tables

Thesis Highlight

Name of the Student: Abhishek K. Sharma

Name of the CI/OCC: BARC **Enrolment No.:** CHEM01201204015

Thesis Title: Radiochemical Separation and Purification of Molybdenum-99 for Medical and Industrial Applications

Discipline: Chemical Sciences **Sub-Area of Discipline:** Radiochemistry

Date of viva voce: August 28, 2020

Artificial radioisotopes are being utilized for wide ranging societal application in the field of healthcare, industry, agriculture and research. In healthcare, radiolabeled compounds are used for diagnosis and treatment of several disorders and diseases. Industrial use of radioisotopes are detection of leakage in the underground pipelines, leaky heat-exchangers of crude oil refineries, industrial radiography for non-destructive testing of specimen etc.Molybdenum-99 ($T_{1/2}$: 66 hrs) is one of the widely produced radioisotope worldwide due to huge medical utility of its daughter isotope ^{99m}Tc ($T_{1/2}$: 6 hrs.). ^{99m}Tc is used for SPECT based nuclear diagnostic imaging of various disorder/ diseases in human body, and said to be the work-horse of nuclear imaging. Large scale production of ^{99}Mo is carried out either by neutron activation route [^{98}Mo(n, γ)^{99}Mo] or by fission route [^{235}U(n, f)^{99}Mo]. The former production route leads to low specific activity of product ^{99}Mo, whereas later route leads to very high specific activity of ^{99}Mo which is a desirable feature for its medical utility through ^{99}Mo-^{99m}Tc column chromatography generator.

The work carried out in the present thesis is aims towards the following goals:(i) Development of a novel method for production high specific activity, medical grade fission ^{99}Mo from thermal neutron irradiated U-Al alloy; (ii) Synthesis, radiolabelling and bio-evaluation of ^{99m}Tc labelled Fatty acid molecules for their use as SPECT based myocardial imaging agents; (iii) Development of ^{99}Mo based organic soluble industrial radiotracer.

Overall, the work carried out in this thesis resulted in development of a novel radiochemical separation method for production of high specific activity, medical grade ^{99}Mo. Towards medical application of ^{99m}Tc in the form of fatty acid based myocardial SPECT imaging agents have been prepared and their potential were explored. Towards industrial application of ^{99}Mo, ^{99}Mo-ABO complex in organic phase was developed as industrial radiotracer and successfully used for identification of leaky heat-exchangers of petroleum refinery.

Chapter 1

General Introduction

Radioisotope of an element consists of unstable nuclei which releases its extra energy in the form particulate radiation (α, β etc.) or electromagnetic radiation (γ rays). Because of the spontaneous emission of radiation, the radioisotopes find wide ranging applications beneficial to society [1,2]. Worldwide, radioisotopes are being utilized for various applications in the field of healthcare, industry, agriculture and research. In healthcare, radiolabeled compounds are used for diagnosis and treatment of several disorders and diseases [3, 4, 5, 6]. Use of radioisotope in healthcare have enabled healthcare professionals for early and precise detection and monitoring of diseased/ disordered internal tissues and organs which in turn has resulted in better healthcare management of patients [7, 8]. Radioisotopes are also being utilized in several industrial applications, such as detection of leakage in the underground pipelines, identification of leaky heat-exchangers of crude oil refineries, industrial radiography for non-destructive testing of specimen etc. [9, 10, 11, 12].

Radioisotopes are be found in nature, and also can be produce artificially. Most of the radioisotopes used for healthcare, industry, agriculture and research are man-made. Production of artificial radioisotopes is either carried out in nuclear reactors or in particle accelerators [13, 14, 15, 16, 17]. However, a major fraction of these man-made radioisotopes are produced in nuclear reactors because of several favorable factors such as large available volume for irradiation, economical cost of production, possibility to produce vast range of radioisotopes and simultaneous irradiation of many samples etc. [15, 18, 19]. Stable isotopes of elements, upon bombardment with neutrons inside the nuclear reactor get transformed into the desired radioactive nuclei of same element or a different element. Post irradiation, the target materials, containing product radioisotopes, are further processed inside a specially

designed radioactive laboratory to convert the produced radioisotope into a specific radiochemical form, suitable for their intended application [19, 20].

1.1 Radioisotopes

Radioactivity was discovered in 1896 by Henri Becquerel, the French physicist, who called the emitted radiations 'Uranic rays' or 'Becquerel rays'. Subsequently, Pierre and Marie Curie concluded that the emission of Becquerel rays from an element was an atomic phenomenon and it did not depend upon the chemical or physical states of that element. They coined the term 'Radioactivity' for such type of phenomenon [21-26]. The emitted radiation can be in the form of particle such as alpha (α), beta (β), proton (p), deuteron (d) etc., or in the form of electromagnetic radiation (γ- rays) [27, 28, 29].

The nucleus of an atom in consists of neutrons and protons, which are collectively called nucleons. The total number of protons in an atom is denoted as Z (atomic number), and total number of neutrons is denoted as N. The total sum of these protons and neutrons (Z+N) is called the mass number of that atom and denoted as symbol A. Symbolically, isotope of an element X is represented as ${}^{A}_{Z}X$. The stability of a nucleus is related to its neutron to proton ratio (N/Z). A plot of neutron number (N) versus the atomic number of all nuclides is shown in Fig. 1.1. All the stable nuclei fall on a narrow region around a line is called '*line of stability'* [1, 2, 30]. Any deviation from this region results in unstable nuclear configuration. The nuclides falling on the region left to the stability line are those species which are rich in number of protons. These proton rich nuclear species have more number of protons compared to their stable isobar, and hence they get decayed either by emitting positron (β^+) or by electron capture (EC) in order to attain a relatively stable nuclear configuration. On the other hand, the nuclei falling on the region right hand side of the stability line are neutron rich

species compared to their stable isobars, and they primarily decays by emitting β^-. The neutron to proton ratio (N/ Z) of a stable atom can be altered either by addition of neutron or by increasing the number of protons into the nucleus [31-34]. For example, ^{98}Mo , one of the stable isotope of molybdenum, get transformed into an unstable isotope of same element (^{99}Mo), after capturing a neutron during irradiation inside a nuclear reactor. ^{99}Mo is radioactive nuclide and decays with a half life of 66 hours. Another example of alteration of N/Z ratio is transmutation of $^{17}_{8}$O , a stable nuclide, into a radioactive nuclide of $^{18}_{9}$F upon addition of one proton to original $^{18}_{9}$F decays by positron (β^+) emission with a half-life of 110 min [15, 35, 36].

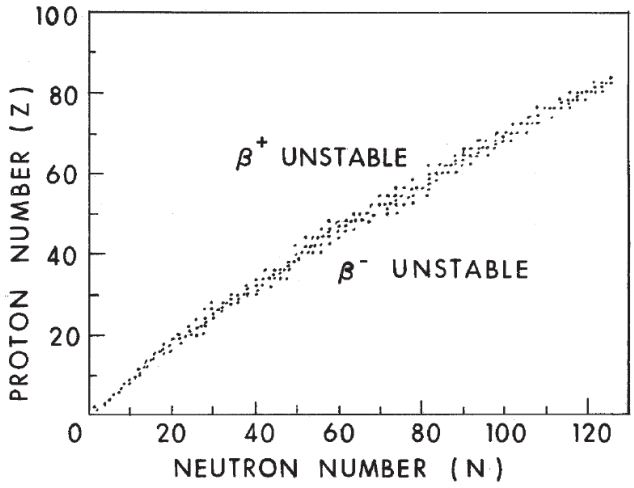

Fig 1.1 *Plot of N vs Z*

1.2 Radioisotopes Production

A stable nuclide can be made radioactive by altering its N/Z ratio. This principle is used for production of artificial radioisotopes by bombarding the suitable target material either by charged particles or by neutrons. Bombardment of target nuclei under the flux of charged particle generally yields in either proton rich or neutron deficient isotopes. These radioisotopes usually get decay either by emitting β^+ (positron) or by Electron Capture (EC) process. In contrast to the above mentioned charged particle bombardment of target nuclei,

the bombardment of neutrons on target nuclei yields in generation of neutron rich isotopes. These neutron rich product nuclei often get decay by emission of β^- (negatron). Generally, β^- emission is accompanied by emission of γ-radiation. In some of the cases, bombardment of neutrons on high atomic mass targets (such as ^{235}U, ^{239}Pu etc.) may lead to the fission of parent nuclei into two fission product fragments of moderate masses, which subsequently undergoes to beta decay to achieve more relative stability. All of the above mentioned cases are illustrated in Fig. 1.2. [1, 2, 37, 38]

Nuclear reactors are used as a source for neutron and particle accelerators (e.g. cyclotron) are used as source for high energy charged particles (proton, deuteron etc.) for radioisotopes production. After the irradiation of target material in a nuclear reactor or in a particle accelerator, the irradiated target materials are safely transported to a specially designed and well shielded radiochemical processing laboratories. Product radioisotopes present in the irradiated target material is then converted into a desired radio-chemical form suitable for its intended application for societal use [1, 2, 20, 37, 38].

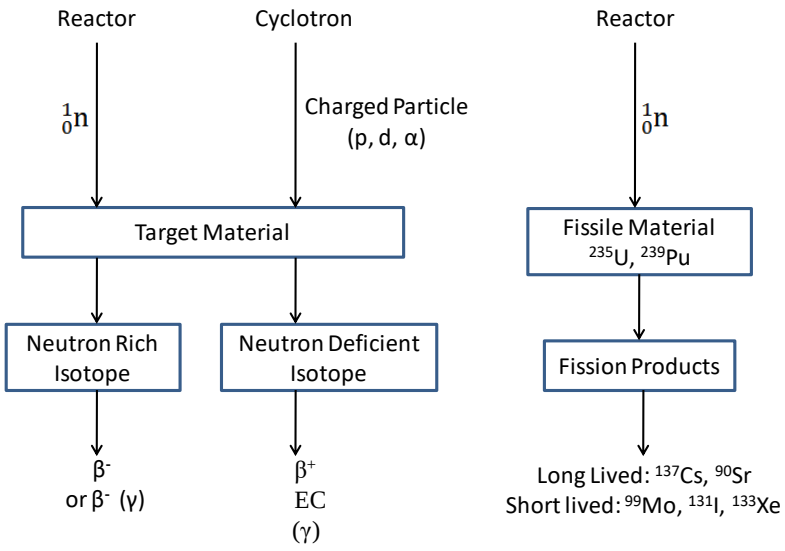

Fig. 1.2 *Production of radioisotopes*

1.3 Reactor Based Production of Radioisotopes

Neutron bombardment on selective target nuclei, having suitable chemical/ physical form, inside nuclear reactors is the most common route for commercial production of radioisotopes used in healthcare and industry. Research reactors are utilized for the production of these radioisotopes. The first operating nuclear reactor, which used natural uranium as fuel and graphite block as neutron moderator, was constructed in Oak Ridge, Tennessee, USA and was in operation from year 1943 to 1963. Typical neutron fluxes in research reactors are of the order of 10^{13} - 10^{14} n/cm^2/s. These neutrons are used to bombard a suitable target material for the production of radioisotopes [15, 39, 40, 41].The research reactors used for radioisotope production could be broadly classified into two categories: (i) Swimming Pool Type Reactors and (ii) Tank Type Reactors. Swimming pool type reactors, e.g. APSARA(U), have a compact core of fuel elements submerged in a large open pool of water. Reactor core is visible and accessible from the top of the reactor pool. These reactors offers ease of handling the target material for irradiation at predetermined locations inside or around the core. In tank type reactors, the reactor core is sealed inside a containment vessel.

For radioisotope production, the material is first enclosed within one or two containments (quartz, aluminum can etc.). Sealed target material is loaded in a specially designed target holder (tray rod, irradiation rigs etc.) for irradiation inside a nuclear reactor. This target holder containing target material is then lowered into a predetermined irradiation location inside a reactor core. After the completion of irradiation period, these irradiated targets are retrieved from the reactor and then loaded into radiation shielded containers for their safe transportation to the radiochemical processing facilities [2, 3, 20]. The type of nuclear reaction and the rate of radioisotope production depend upon the following factors:

1. Energy and flux of neutrons (ϕ)
2. Activation cross section (σ) of the desired nuclear reaction

3. The quantity and the characteristics of the target material

1.3.1 Energy of Neutrons

Depending on the energy, neutrons are classified as thermal neutrons, epithermal neutrons and fast neutrons. Thermal neutrons are those neutrons which have their energy in equilibrium with the surrounding medium such as moderator. Thermal neutrons have average energy of about 0.025 eV at 20^{o}C temperature and their energy distribution pattern can be represented by Maxwellian distribution. Epithermal neutrons have energy in intermediate range of keV with the distribution pattern represented by the 1/v law, where v is the speed of neutron. Fast neutrons have the energy more than 1 MeV. Fast neutrons have similar energy distribution pattern as possessed by fission neutrons [15, 38, 40].

1.3.2 Neutron Flux

Neutron flux (ϕ) is the measure of intensity of neutrons, and is determined by multiplying the neutron density (n neutrons /cm^3) to the average speed (v cm/s) of neutrons. It is expressed as neutrons/cm^2 / sec.

1.3.3 Cross Section

Interaction of neutrons with the nuclei of target material can be expressed quantitatively in terms of cross-section, which determines the probability of occurrence of a given nuclear reaction. In simplest terms, it can be expressed as the area offered by the nucleus around the nucleus to a perpendicular beam of neutrons for the nuclear reaction to occur. The unit of cross-section is barn (1 barn = 10^{-24} cm^2). The numerical value of cross-section depends upon the type of reaction and the energy of neutrons. Generally, lesser the energy of neutrons, higher will be the cross-section. Thermal neutrons have the highest cross- section, and it varies as '1/v' in this region, where v is the speed of neutrons [1, 2, 38].

1.3.4 Characteristics of Target Material

1. Target material should be stable to radiation.
2. Explosive, volatile, pyrophoric etc. materials are not permitted for irradiation.
3. Physical form of the target should be such that the neutron flux depression should be lowest.
4. The chemical form of target should be suitable for post irradiation processing.
5. Isotopically enriched target gives high specific activity of the product radioisotopes.

1.3.5 Types of Nuclear Reactions

Neutrons being the electrically neutral particles do not face any columbic barrier from the nucleus. Hence, even the neutrons of very low energy (e.g. thermal neutrons) can cause the nuclear reaction to occur with the atom present in target material. Mentioned below are the types of neutron induced reactions which are commonly used for radioisotope production.

1.3.5.1 (n,γ) Reaction

This is the most common type of nuclear reaction for reactor based radioisotope production. This reaction is also known as radiative capture. Mostly thermal neutrons are used to bombard the target material. After the reaction, product radionuclide have the same atomic number (Z) as target atoms but the atomic mass is increased by unity. Some of the radioisotope produced by (n,γ)reaction are follows:

$$^{98}_{42}\text{Mo} + ^{1}_{0}\text{n} \rightarrow ^{99}_{42}\text{Mo} + \gamma \qquad (\sigma = 0.14 \text{ barn})$$

$$^{59}_{27}\text{Co} + ^{1}_{0}\text{n} \rightarrow ^{60}_{27}\text{Co} + \gamma \qquad (\sigma = 36 \text{ barn})$$

Product radioisotope formed in the target material will have same Z as of the target nuclei; therefore its chemical separation from target material is not possible. Hence, the specific activity (activity per unit mass of element) of the product radioisotope is limited by the

neutron flux of the reactor [1, 2, 31]. Table 1.1 depicts some of the radioisotopes produced by radiative capture mode of nuclear reaction.

Table 1.1 *Production of radioisotopes by (n,γ) reaction*

Target	Radioisotope	σ_n (b)	$t_{1/2}$	Decay mode
^{59}Co(n,γ)	^{60}Co	36	5.274 y	β^-
^{98}Mo (n,γ)	^{99}Mo	0.14	65.94 h	β^-
^{23}Na (n,γ)	^{24}Na	0.53	14.9512 h	β^-
^{191}lr (n,γ)	^{l92}Ir	370	73.827 d	β^-
^{197}Au (n,γ)	^{198}Au	99	2.69517 d	β^-
^{81} Br (n,γ)	^{82}Br	3.2	35.30 h	β^-

1.3.5.2 (n,γ) Followed by β^- Decay

Some (n,γ) reactions produce a short lived radioisotope which decays to another radioisotope having a longer half-life. For example, ^{130}Te (n,γ) ^{131}Te reaction with tellurium yields ^{131}I, which can be separated from Te and hence is career free.

$$^{130}_{52}\text{Te}\ (n,\gamma)\ ^{131}_{52}\text{Te} \xrightarrow{\beta^-} {}^{131}_{53}\text{I} \xrightarrow{\beta^-} {}^{131}_{53}\text{Xe}$$

1.3.5.3 (n, p) Reaction

In some cases, neutrons having energy more than a specific value, upon absorption by the nucleus leads to the ejection of proton from the nucleus. This specific energy value is called threshold energy and these reactions are called threshold reactions. Below are some examples of this type:

$$^{58}_{28}\text{Ni} + {}^{1}_{0}\text{n} \rightarrow {}^{58}_{27}\text{Co} + \text{p} \qquad (\sigma = 0.113 \text{ barn})$$

$$^{32}_{16}\text{S} + {}^{1}_{0}\text{n} \rightarrow {}^{32}_{15}\text{P} + \text{p} \qquad (\sigma = 165 \text{ milibarn})$$

Here also the product radioisotope is chemically separable from the target, leading to the high specific activity radioisotopes.

1.3.5.4 (n,α) Reaction

In this type of reaction the nucleus ejects an alpha particle after the neutron absorption. These reactions are also the threshold reaction as minimum specific energy (threshold energy) of neutron is required for nuclear reaction to occur.

$^{6}_{3}\mathrm{Li} + {}^{1}_{0}\mathrm{n} \rightarrow {}^{3}_{1}\mathrm{H} + {}^{4}_{2}\mathrm{He}$ (σ = 980 barns)

High specific activity/ carrier free products could also be obtained in this case.

1.3.5.5 Multistage Reactions

Some radioisotopes are produced by successive neutron capture. For example:

$^{186}\mathrm{W(n,\gamma)}^{187}\mathrm{W(n,\gamma)}^{188}\mathrm{W}$

1.3.5.6 Fission

Fission of ^{235}U by thermal neutron yields a large number of radioisotopes. Some of these isotopes (e.g. ^{99}Mo, ^{131}I, ^{137}Cs, ^{90}Sr etc.) have useful application for industry and healthcare. Every fission event yields at least two fission products. Depending upon the mass number, these fission products fall under two groups, a light mass (with mass around 95) and a heavy mass (with mass number around 140) fission product. The fraction or percentage of the total number of fissions, which yield to a particular nuclide, is called the fission yield of that nuclide. The total fission yield is 200% [19, 28, 34]. Some of the most important fission products that find valuable applications for healthcare, industry and research are following.

Short lived fission products→ $^{99}_{42}\mathrm{Mo}$, $^{131}_{53}\mathrm{I}$

Long lived fission products → $^{137}_{55}\mathrm{Cs}$, $^{147}_{61}\mathrm{Pm}$, $^{90}_{38}\mathrm{Sr}$

1.4 Cyclotron Produced Radioisotopes

Cyclotrons are the particle accelerators used for accelerating the charge particles such as: p, d, α and He^{3+} to high energy. These, high energy charged particles, are made to bombard upon the target material to produce neutron deficient radionuclides. The high energy is required to overcome the Coulomb barrier and cause the nuclear reaction. In general, the target, for cyclotron irradiation, is taken in the form of very thin metal foil, considering the small range of charged particles. The product radioisotope formed after the bombardment is normally an element different from the target, and hence can be separated chemically from the target thereby yielding high specific activity of product radioisotope. In cyclotron, depending on the energy of the charge particle, the following reaction channels are possible [4, 17, 35, 36].

(i) (p,α), (p,d), (p, xn), (p,xnyp)

(ii) (d, α), (d,p), (d,xn), (d,xnyp)

(iii) (α,xn), (α,xnyp)

where x,y = 1,2,3,...

Some cyclotron produced radioisotopes such as such as ^{11}C, ^{13}N, $^{15}O$and ^{18}F are short lived with half-life in the range of minutes. These radioisotopes are used in the form of labelled compounds and have extensive application in the field of nuclear diagnostic imaging. Owing to short half-life, these product radioisotopes are rapidly processed to yield labelled molecules. Some of the useful cyclotron produced radionuclides are shown in Table 1.2.

In cyclotron, the irradiation yield of the product radioisotope is depends upon beam current, cross-section of reaction, amount of target material, irradiation time and decay constant the product radioisotope. In cyclotron irradiation, product activity can be expressed by following equation:

$$A_1 = 6.24 \times 10^{18} I\sigma N (1-e^{-\lambda t}) \ (Bq) \qquad (1)$$

Where,

I : Beam intensity (Ampere)

σ : cross section for nuclear reaction (cm^2)

N : Number of target atoms/ cm^2

Table 1.2 *Some cyclotron produced radioisotopes*

Nuclide	$T_{1/2}$	Decay mode	Production
^{22}Na	2.6019 y	β^+ (91%), EC	^{24}Mg (d,α) ^{22}Na
^{57}Co	271.94 d	EC	Ni (p,x) ^{57}Co
^{67}Ga	3.2612 d	EC	^{68}Zn (p,2n) ^{67}Ga
^{111}In	2.8047 d	EC	^{112}Cd (p,2n) ^{111}In
^{123}I	13.27 h	EC	^{124}Te (p,2n) ^{123}I ^{124}Xe (p,2n) $^{123}Cs \rightarrow {}^{123}Xe \rightarrow {}^{123}I$
^{201}Tl	72.912 h	EC	^{203}Tl (p,3n) $^{201}Pb \rightarrow {}^{201}Tl$
^{11}C	20.39 min	β^+	^{14}N (p,α) ^{11}C
^{13}N	9.965 min	β^+	^{16}O (p,α) ^{13}N
^{15}O	122.24s	β^+	^{14}N (d,n) ^{15}O
^{18}F	109.77 min	β^+	^{18}O (p,n) ^{18}F, ^{20}Ne (d,α) ^{18}F
^{103}Pd	16.991 d	EC	^{103}Rh (p,n) ^{103}Pd

1.5 Calculation of Radioisotopes Yield

When target nuclei are irradiated inside a nuclear reactor, the activation per second can be represented by following expression: $$\frac{dN'}{dt} = N_t \sigma_{act} \phi \qquad (2)$$

Where, N_T : Total number of atoms present in target,

ϕ: Neutron flux,

σ_{act} : Activation cross-section,

N' : The number of activated atoms at an instant of time,

The rate of production of radioisotope is independent of time. However, as soon the product radioisotope atoms are formed, they start decaying with their own half-life. Therefore, net growth rate of product will be the difference between rate of production and rate of decay. Equation representing net growth rate of product nuclei can be written as:

$$\frac{dN'}{dt} = N_t\phi\sigma_{act} - \lambda N' \qquad (3)$$

Where, λN' indicates the decay rate of product nuclei.

Equation-3 can be solved to determine the value of radioactive atoms at time 't', as follows:

$$N' = \frac{1}{\lambda} N_t\sigma_{act}\phi\ (1-e^{-\lambda t})$$

Therefore, activity of product radioisotope, $A = \lambda N' = N_t\sigma_{act}\phi\ (1-e^{-\lambda t})$ (4)

Where, σ_{act} : Neutron activation cross-section leading to the production of radioisotope of interest in barn.

ϕ : Neutron flux in $n/cm^2/s$.

t : Time of irradiation.

λ : Decay constant = $[0.693/ T_{½}]$

Equation-4 clearly shows that growth of activity in a target under irradiation is exponential in nature and reaches a saturation value limited by the neutron flux in the reactor.

When $t >> T_{½}$, Saturation activity = $N_t\sigma_{act}\phi$ (Bq)

1.6 Production of ^{99}Mo

Molybdenum-99 ($T_{1/2}$ = 66 h) is one of the widely produced isotopes for its use in the field of nuclear medicine. The global requirement of ^{99}Mo is approximately 9000 Ci (six-day calibration). In nuclear radio-pharmacies, ^{99}Mo is utilized in the form of ^{99}Mo-^{99m}Tc radioisotope generator to avail ^{99m}Tc ($t_{1/2}$ = 6.01 h) radioisotope. ^{99m}Tc, decay product of

^{99}Mo, is used for the preparation of the radiopharmaceuticals for Single Photon Emission Computed Tomography (SPECT) imaging of various disorder and diseases [42-44]. Decay scheme of ^{99}Mo is shown Fig. 1.3. ^{99}Mo can be produced in the nuclear reactor or in cyclotron.

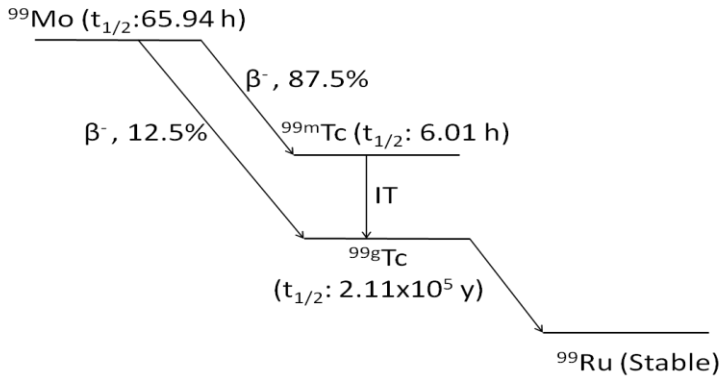

***Fig. 1.3** Partial decay scheme of ^{99}Mo*

1.6.1 Reactor Based Production of ^{99}Mo

The large-scale production of ^{99}Mo is carried out in nuclear reactor. There are two major routes for nuclear reactor-based production of ^{99}Mo as shown below.

(a) Neutron activation route: ^{98}Mo(n,γ)^{99}Mo

(b) Fission route: ^{235}U(n,f)^{99}Mo,

1.6.1.1 Neutron Activation Route:

Molybdenum-99 is produced by radiative neutron capture reaction on ^{98}Mo. The cross-section for this nuclear reaction is 0.14 b with thermal neutron and effective cross-section being 0.5 b after accounting for the contribution from the epithermal neutrons. Molybdenum trioxide (MoO_3) powder is taken as the target material for the irradiation. Natural molybdenum has 24.4 % isotopic abundance for ^{98}Mo, and other remaining isotopes are ^{92}Mo (14.8%), ^{94}Mo(9.1%),^{95}Mo (15.1%), ^{96}Mo (16.7%), ^{97}Mo (9.5%) and ^{100}Mo (9.6%).

Production of ^{99}Mo by activation routes involves the target preparation, target irradiation and processing of irradiated target inside a radiation shielded facility. Target preparation for irradiation involves the filling of high purity MoO_3 powder in alumina can for containment and sealing the can by cold welding process. The sealed can is checked for air tightness and then placed inside nuclear reactor at pre-determined location for neutron irradiation. Target is irradiated for one week and then retrieved. After a short period of cooling time (for the decay of short-lived isotopes) the irradiated target is transported to the radiochemical processing laboratories and taken inside a lead shielded processing facility (Hot-cell). Inside Hot-cell, MoO_3 powder is dissolved in sodium hydroxide solution in hot condition to get ^{99}Mo in the form of Na_2MoO_4. One gram of natural Mo target produces ~800 mCi of ^{99}Mo after one week of irradiation under the neutron flux of 5 x 10^{13} n/ cm^2/ sec [1, 27, 15].

The product ^{99}Mo activity is used to produce ^{99}Mo-^{99m}Tc radioisotopes generators for its use in radio-pharmacies. Specific activity of ^{99}Mo plays an important role in the manufacturing of ^{99}Mo-^{99m}Tc generators, and its higher value is desirable. The specific activity of the ^{99}Mo obtained from neutron activation route is low (< 1 Ci/ g of Mo) due to small value of cross section for nuclear reaction (0.14b) and low isotopic abundance of ^{98}Mo in natural molybdenum. During irradiation only a very small fraction of^{98}Mo will get transmuted to ^{99}Mo, thereby resulting in product activity which consists of large fraction of stable nuclei of Mo, which resulted in lower specific activity of product. The specific activity of ^{99}Mo can be increased by following way:

a) By enrichment of target: Isotopic abundance of Mo-98 in natural target is 24.1%. By enriching Mo-98 in target, specific activity can be increased.
b) By increasing the neutron flux
c) By using Szilard-Chalmer reaction

Szilard-Chalmer reaction is based upon the chemical changes occurring in the target material during (n, γ) reaction due to breaking of chemical bonds, owing to the recoil energy of nucleus during emission of γ-ray.

1.6.1.2 Fission Route:

Thermal neutron induced fission of ^{235}U produces several radioisotopes and ^{99}Mo is one of them with a cumulative fission yield of 6.1 %. Target materials used for the commercial scale production of fission moly (^{99}Mo) are uranium metal or uranium-aluminum alloy etc. Generally, enriched targets are used throughout the globe for production of medical grade (n,f)^{99}Mo. Depending on the level of enrichment, these targets are classified either as Low Enriched Uranium target (LEU) (enrichment < 20 %) or as High Enriched Uranium target (HEU) (enrichment > 20%). These targets (LEU/ HEU) are irradiated inside nuclear reactor at locations having high thermal neutron flux. Typically, 1 g of ^{235}U produces ~200 Ci of ^{99}Mo after 7-day irradiation with neutron flux of $1x10^{14}$ n/ cm^2/ s. After the completion of irradiation, the irradiated target is retrieved from reactor core and placed inside the reactor pool for the decay of short-lived radioisotopes generated during fission of ^{235}U. Further radiochemical processing is carried out inside a radiation shielded production facility to obtain medical grade (n,f)^{99}Mo. High specific activity of ^{99}Mo (> 5000 Ci/ g of Mo) is obtained by fission route. The obtained activity of medical grade (n,f)^{99}Mo is further used for the preparation of ^{99}Mo-^{99m}Tc radioisotope generators [30, 18, 42].

1.7 Radioisotope Generators

A radioisotope generator is a modality in which a short-lived daughter radionuclide co-exists with long lived parent radionuclide, and repeated separation of daughter radionuclide from parent radionuclide can be done. These generators are easily transportable and thus serve as a source for obtaining short-lived daughter radionuclide in radiopharmacies, located far from

the site of reactor or cyclotron facility. A generator works based on the decay-growth relationship between the long-lived parent and short-lived daughter radionuclide. Generator is loaded with long-lived parent radionuclide from which growth of daughter radionuclide take place. The daughter grows until it attains equilibrium with the parent and thereafter it appears to decay as per the half-life of parent radionuclide. Daughter radionuclide is separated from the generator using a suitable solvent while parent remains in the generator [44-46]. After separation, fresh growth of daughter takes place in generator for repeated use of it. A typical radioisotope generator is shown in Fig. 1.4.

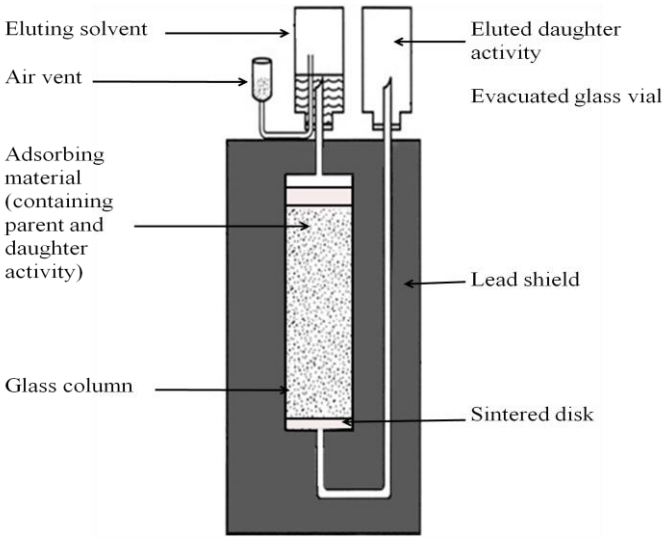

Fig 1.4: *Typical radioisotope generator*

1.7.1 Radioisotope Equilibrium

If the decay product of a radionuclide is also radioactive with a shorter half-life than parent, then growth of daughter take place with time till it reaches a maximum value and thereafter it start decaying with half-life of parent radionuclide. The time to reach maximum activity of daughter is called t_{max} and beyond this time, the ratio of parent to daughter becomes constant. This state is called radioisotope equilibrium. Depending upon the ratio of decay constant for product and daughter radionuclide, there are two categories of radioisotope equilibrium as described below.

Transient Equilibrium

In the cases where the ratio of decay constant of parent (λ_1) to that of daughter (λ_2) is around ~0.1, the equilibrium is called transient equilibrium. A typical example is:

$$^{99}Mo \xrightarrow{\beta^-} {}^{99m}Tc \xrightarrow{IT} {}^{99}Tc$$

Secular Equilibrium

If the half-life of the parent isotope is much longer than that of the half- life of the daughter isotope ($\lambda_2 >> \lambda_1$), then the equilibrium is called secular equilibrium. In this condition, the total activity of the parent and daughter reaches the maximum and does not decrease appreciably for several half-lives of the daughter product [1, 5]. A typical example is: ^{68}Ge-^{68}Ga.

1.7.2 ^{99}Mo-^{99m}Tc Radioisotope Generators

^{99}Mo-^{99m}Tc generators are used at radiopharmacies to avail ^{99m}Tc for preparation of ^{99m}Tc based diagnostic radiopharmaceuticals.^{99m}Tc is the widely used radionuclide for nuclear diagnostic imaging and said to be the work-horse of nuclear imaging. The properties such as optimum half-life (6 hrs), suitable γ-ray energy (140 keV), ease of availability from ^{99}Mo-^{99m}Tc generators, absence of any particulate emission and diverse chemistry makes it a popular choice.

Based on the method of chemical separation, different types of ^{99}Mo-^{99m}Tc generators are available. Some of the commercially used ^{99}Mo-^{99m}Tc radioisotopes generators are: (i) Alumina sorbent based column chromatography generator, (ii) Solvent extraction generator, (iii) Gel generator [1, 5, 43].

Alumina column chromatography generator: Acidic alumina has a maximum adsorption capacity of 20 mg of Mo per gram of sorbent and acts as anion exchanger. Few grams (~2 g) of acidic alumina is filled in a glass column and loaded with ^{99}Mo at pH of 3-3.5. At this pH, molybdenum species exists as paramolybdate form ($^{99}Mo_6O_{24}^{4-}$) and have

maximum adsorption. ^{99m}Tc formed in the alumina by the decay of ^{99}Mo is eluted by 0.9 % saline solution (NaCl). Chloride ions present in the NaCl solution dislodge $^{99m}TcO_4^-$ adsorbed over the alumina matrix; however ^{99}Mo is retained on the alumina due its strong binding. The eluted activity contains ^{99m}Tc in the form of $Na^{99}TcO_4$ and is used in radiopharmaceutical preparation for nuclear diagnostic imaging of patients. These generators are very popular due to their ease of operation, high extraction efficiency for ^{99m}Tc (>85%), very low molybdenum breakthrough, low cost and high radioactive concentration (RAC) of eluted ^{99m}Tc. However, due to the limited adsorption capacity of alumina sorbent for Mo, alumina column chromatography generator can only be prepared by using high specific activity (n,f)^{99}Mo.

Solvent Extraction Generator: This generator works on the principle of liquid-liquid extraction. ^{99}Mo activity in the form of MoO_4^{2-} in 4 N sodium hydroxide solution is kept inside lead shielded glass apparatus.^{99m}Tc present in the aqueous solution is recovered into organic phase by solvent extraction using methyl ethyl ketone (MEK) as organic extractor. During extraction, ^{99m}Tc activity goes into organic phase and ^{99}Mo remains with the aqueous phase. Organic phase, being lighter forms, the upper layer and is separated from the aqueous layer. The aqueous layer containing ^{99}Mo activity is kept for next day repeat extraction of ^{99m}Tc. The organic layer which contains ^{99m}Tc is passed through the basic alumina column to remove any trace amount of ^{99}Mo present in organic phase. MEK present in the organic phase is removed from the by heating the organic layer to dryness followed by reformulating the ^{99m}Tc in $^{99m}TcO_4^-$ form by addition of 0.9 % saline solution. The separation efficiency of solvent extraction generator is similar to that of alumina column generator.

Gel Generator: Gel generators are prepared with a glass column filled with insoluble matrix material of ^{99}Mo bearing Zirconium molybdate. This insoluble matrix acts as a cation exchanger and the ^{99m}Tc can be eluted from the column by passing 0.9 % NaCl solution

through it. Often a secondary glass column, filled with acidic alumina, is connected in tandem with primary column to remove traces of ^{99}Mo present in eluate.^{99}Mo-Zirconium powder is prepared by precipitation of ^{99}Mo, in the form of $ZrOMoO_4$, by the addition of zirconium oxy chloride solution. Obtained precipitate has gel type appearance, which is then filtered, dried and filled into glass columns. These columns are then assembled in lead shielding in the form ^{99}Mo-^{99m}Tc generators. Gel generators can be prepared with low specific ^{99}Mo activity.

1.8 Radiopharmaceuticals

Radiopharmaceuticals are special class of radiochemical formulations that are used in the field of nuclear medicine for diagnostic and therapy of various disorder and disease, and have high purity and pharmaceutical safety. The radiation emitted from these radioactive compounds is utilized in patient healthcare through various medical applications. Radiopharmaceuticals are composed of two components: (i) Carrier molecule, which is a small organic or inorganic molecule, and (ii) Radionuclide. Typically, a radiopharmaceutical has organic moiety as carrier, to which a desired radionuclide is chemically attached. Carrier molecules have preferential specificity towards a target organ/ lesion of interest and get accumulated there post intake by patient. The accumulated radioactive drugs emit radiation which helps in treatment of the patient. The nature of radionuclide attached with radiopharmaceuticals depends upon the diagnostic or therapeutic application. Generally radio-pharmaceuticals containing γ-emitting radionuclide are used for diagnostic purpose, whereas those which are attached with particulate emitting radioisotopes, are used for therapeutic purpose. Usefulness of a radio-pharmaceutical depends upon the characteristics of carrier molecule and the radionuclide. Table 1.3 shows some of the radiopharmaceuticals used for patient healthcare [45, 47, 48].

Table 1.3 *Selected target-specific diagnostic and therapeutic radiopharmaceuticals**

Radiopharmaceutical	Trade name	Primary uses
^{111}In-Capromab pendetide	ProstaScint®	Imaging of prostate cancer
^{111}In-Pentetreotide	Octreoscan®	Imaging of neuroendocrine tumors
^{111}In-Satumomab pendetide	OncoScint®	Imaging of metastatic disease associated with colorectal and ovarian cancer
^{99m}Tc-Apcitide	AcuTect®	Imaging deep vein thrombosis
^{99m}Tc-Arcitumomab	CEA-Scan®	Imaging colorectal cancer
^{99m}Tc-Depreotide	Neotect®	Imaging somatostatin receptor-positive tumors
^{90}Y-IbitumomabTiuxetan	Zevalin®	Treatment of Non-Hodgkin's Lymphoma
^{131}I-Tositumomab	Bexxar®	Treatment of Non-Hodgkin's Lymphoma

*Liu S. *Adv Drug Deliv Rev.*, **2008**, *60(12)*, 1347

1.8.1 Diagnostic Radiopharmaceuticals

Radiopharmaceuticals which are used for the physiological imaging of internal organ or abnormality are called diagnostic Radiopharmaceuticals. These types of Radiopharmaceuticals are tagged either with gamma emitter radionuclide or with a positron emitter. The former is used in Single Photon Emission Computed Tomography (SPECT) imaging technique, whereas the latter are used in Positron Emission Tomography (PET) imaging techniques. Table 1.4 depicts some of the diagnostic radiopharmaceuticals used for nuclear imaging.

Table 1.4 *Selected radiopharmaceuticals used for diagnostic applications*[*]

Organ	Radiopharmaceuticals used
Brain	*Perfusion imaging:* ^{18}F-FDG, ^{99m}Tc-d-l-HMPAO, ^{99m}Tc-ECD *Tumors:*^{201}TlCl, ^{99m}Tc-d-l-HMPAO, ^{99m}Tc-GHA, ^{18}F-FDG *Neuro-Receptors:*^{18}F-DOPA, ^{11}C-N-Methyl spiperone

Thyroid	NaI – $^{131/123}I$; $^{99m}TcO_4^-$
Lungs	*Ventilation:* ^{99m}Tc-aerosols, ^{133}Xe, ^{81m}Kr *Perfusion:* ^{99m}Tc-HSA microspheres / macroaggregates
Heart	*Myocardial Perfusion:* ^{201}TlCl, ^{99m}Tc-Sestamibi, ^{99m}Tc- Tetrofosmin. *Metabolism:* ^{18}FDG, ^{123}I-FA analogs (BMIPP) *Infarcts:* ^{99m}Tc-PYP; ^{99m}Tc-glucarate *Receptors:* ^{123}I-MIBG *Blood Pool:* ^{99m}Tc-RBC; ^{99m}Tc-HSA
Bone	^{99m}Tc-phosphonate (^{99m}Tc-MDP)
Liver/ Spleen	^{99m}Tc-S colloid; ^{99m}Tc-phytate
Hepatobiliary System	^{99m}Tc-IDA derivatives
Kidneys	*Imaging:* ^{99m}Tc-DMSA, ^{99m}Tc-GHA *Renography:* ^{99m}Tc-DTPA, ^{99m}Tc-MAG3, ^{99m}Tc-EC
Infection	^{111}In / ^{99m}Tc-Leucocytes; ^{99m}Tc-Ciprofloxacin
Inflammation	^{99m}Tc/ ^{111}In – HIgG, ^{67}Ga-citrate
Tumors	$^{123/131}$I-MIBG, ^{111}In-Octreotide, ^{18}F-FDG, ^{11}C- Methionine

*Sood D.D., Reddy A.V.R., Ramamoorthy. N. *Fundamentals of Radiochemistry*,**2004**, 298.

1.8.1.1 Single Photon Emission Computed Tomography (SPECT)

SPECT imaging technique is used to generate 3-D information of tumor/ disease lesion in patient body using a radiopharmaceutical containing gamma emitting radionuclide. SPECT imaging modality consists of several NaI(Tl) detectors mounted in a gantry with adequate collimation. These detectors are connected to on-line computer for data acquisition, processing and display of graphical image of lesion. The patient is injected with SPECT radiopharmaceutical and placed in SPECT system. The gamma rays coming out of the patient are recorded by scintillation detectors to generate 2-Dimiensional image data of distributed activity at lesion site. This 2-D image is used to generate three-dimensional picture of lesion

site by means of computed tomographic (CT) technique. CT is a mathematical algorithm for image reconstruction in 3-D by 2-D images taken at different angles. 3-D reconstructed image is used to take 2-D image slices of the lesion site for planning of treatment. Table 1.5 depicts some of the radioisotopes used in SPECT imaging in the field of nuclear medicine.

Table 1.5 *Radioisotopes used in SPECT*

Radionuclide	$T_{1/2}$	Mode of Decay	Principal γ energy in keV (% abundance)
^{67}Ga	3.26 d	EC	93.31 (38.30)
^{123}I	13.27 h	EC	158.97 (82.80)
^{131}I	8.02 d	β^- & γ	364.48 (81.20)
^{111}In	2.81 d	EC	245.39 (94.17)
^{99m}Tc	6.02 h	IT	140.47 (88.97)
^{201}Tl	72.91h	EC	167.43 (10.00)

1.8.1.2 Positron Emission Tomography (PET)

PET based nuclear diagnostic imaging technique utilizes radiopharmaceuticals labeled with a positron (β^+) emitting radionuclide. These radionuclides emit positron which get annihilated by picking up of electrons nearby the site of radiopharmaceutical accumulation. Annihilated positron emits two 511 keV photons in opposite direction which are coincidentally detected by detectors placed at 180^o angle. Due to coincident detection of photons, collimation is not required for PET system imparts enhanced sensitivity to PET compared to SPECT based system. High sensitivity of PET modality leads to better quality images due to enhanced signal to noise ratio, high temporal resolution, possibility of performing shorter scans, etc. PET imaging modality uses bismuth-germanate (BGO) based detector for efficient detection of high energy (511 keV) gamma rays. Table 1.6 depicts some of the PET radio-pharmaceuticals used in the field of nuclear diagnostic imaging [44, 45].

Table 1.6 *Radioisotopes used in PET*

Radionuclide	$T_{1/2}$ (min)	Mode of Decay	Principal γ energy in keV (% abundance)
^{11}C	20.39	β^+	511.00 (199.5)
^{18}F	109.77	β^+	511.00 (194)
^{68}Ga	68	β^+	511.00 (178)
^{13}N	9.97	β^+	511.00 (199.64)
^{15}O	2.03	β^+	511.00 (199.77)

1.8.2 Therapeutic Radiopharmaceutical

Therapeutic radiopharmaceuticals consist of particulate emitting radionuclides and are intended to deliver the cytotoxic dose of ionizing radiation at target sites. These radionuclides emit particulate such as Alpha (α), beta (β) and conversion electron (e^-) which have high LET value. Therapeutic radiopharmaceutical should have high specificity, extraction efficiency towards target sites and rapid clearance from the non-target organs in order to avoid unwanted damage to the healthy tissue. One of the important factors in development of any new therapeutic pharmaceutical is selection of suitable radionuclide [8, 46, 47]. A list of some of the therapeutic radionuclide is shown in Table 1.7.

Table 1.7 *Some of the commonly available therapeutic radionuclides*

Radio-nuclide	Half-life	Mode of decay	Principal E_γ (keV) [% intensity]	Max. E_β- (keV) [%intensity]	Clinical application
^{32}P	14.26 d	β^-	---	1710	Polycythemia vera, cystic craniopharyngioma, PVNS
^{89}Sr	50.53 d	β^-	910 [0.01]	1496 [100.0]	Painful bone metastasis
^{90}y	64.10 h	β^-	---	2280.1 [100.0]	Hepatic metastasis, PVNS RIT for NHL
^{117m}Sn	13.60 d	IT	158.6 [86]	130 , 150	Bone tumour treatment
^{131}I	8.02 d	β^-	364.5 [81.7]	606 [89.3]	Hyperthyroidism, thyroid cancer, RIT for

					NHL and neuroblastoma
^{153}Sm	46.50 h	β^-	103.2 [29.8]	808.2 [100.0]	Painful bone metastasis, synovitis
^{169}Er	9.40 d	β^-	84 [0.16]	350	Synovitis
^{177}Lu	6.73 d	β^-	208 [11.0]	497.8 [100.0]	Synovitis, RIT for various cancer treatments
^{186}Re	3.72 d	EC, β^-	137 [9.4]	1069.5 [92.5]	Painful bone metastasis, painful arthritis
^{188}Re	17.00 h	β^-	155 [15.1]	2120.4 [100.0]	Painful bone metastasis
^{223}Ra	11.44 d	α	154 [5.59]	5979.2	Bone metastasis

1.9 ^{99m}Tc Based SPECT Imaging Agents

^{99m}Tc is widely used in SPECT imaging of various disorders and diseases due to its favorable nuclear characteristics and ease of availability from ^{99}Mo-^{99m}Tc generators. ^{99m}Tc exhibits multiple oxidation state, and therefore has diverse chemistry. This plays an advantageous role for development of several ^{99m}Tc based radiopharmaceuticals for scanning of several target organs such as thyroid, liver, kidney, bone, brain, myocardium etc. Availability of large number^{99m}Tc based radiopharmaceuticals to cover almost all the organs have made it the 'work horse' of the nuclear diagnostic imaging. Every year approximately 30 million nuclear diagnostic procedures are performed worldwide using ^{99m}Tc labeled radio-pharmaceuticals [5, 43]. Some of these radiopharmaceuticals are shown in Table 1.8.

Table 1.8 *^{99m}Tc-based diagnostic radiopharmaceuticals*[*]

Function	Radiopharmaceutical
Liver scanning	^{99m}Tc - Sulphur Colloid, ^{99m}Tc-Tin Colloid, ^{99m}Tc-Phytate
Kidney function studies	^{99m}Tc-Glucoheptonate, ^{99m}Tc-DTPA, ^{99m}Tc-Dimercaptosuccinate ^{99m}Tc-Mercaptoacetyl triglycine, ^{99m}Tc-Ethylene Dicysteine
Bone scanning	^{99m}Tc-Methylene diphosphonate (MDP)
Hepatobiliary function	^{99m}Tc-Mebrofenin

Lung Scanning	^{99m}Tc-HSA Microspheres / Macroaggregates, ^{99m}Tc-Aerosols
Cardiac studies	^{99m}Tc-Red blood cells; ^{99m}Tc-Pyrophosphate; ^{99m}Tc-glucarate, ^{99m}Tc-Sestamibi, ^{99m}Tc-Tetrofosmin
Brain blood flow	^{99m}Tc-d,l-HMPAO, ^{99m}Tc-L,L-ECD
Infection / Inflammation	^{99m}Tc-Leuocytes; ^{99m}Tc-HIgG; ^{99m}Tc-antigranulocyte antibodies; ^{99m}Tc-ciprofloxacin

*Sood D.D., Reddy A.V.R., Ramamoorthy. N. *Fundamentals of Radiochemistry,* 2004, 298.

1.10 Shaping New Radiopharmaceuticals

A radiopharmaceutical is composed of three basic constituents: a bio-molecule (BM), a bi-functional chelating agent (BFCA) and a radionuclide (RN). Bio-molecules have binding affinity towards a target organ and act as a guiding vehicle for the radio-pharmaceutical. Target affinity depends upon nature of BM and several mechanisms have been reported by which BM can bind with the target cells. A linker acts as spacer between BM and BFCA. It can be an aliphatic chain, a polyamino acid sequence, or a polyether chain. The linker serves twin purpose, firstly the lipophilicity of radiopharmaceutical can be altered by increasing/ decreasing the linker's chain length which improves pharmacokinetics to provide better target to background ratio. Secondly, it protects the bio-affinity of BM by acting as a spacer between BM and radionuclide metal complex. BFCA acts as means to attach radiometal with BM through linker molecule. BFCA contains a chelator group to hold the radiometal by forming complex, and a functional group that covalently binds the linker molecule [42, 46, 48]. Schematic representation of radiopharmaceutical is shown in Fig. 1.5.

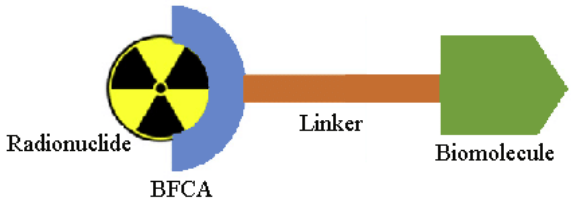

Fig. 1.5 *Schematic representation of a radiopharmaceutical*

Designing of a new radiopharmaceutical starts with synthesizing a target molecule (organic moiety) followed by its radiolabelling with radiometal and biological evaluation in suitable animal model.

1.11 Myocardial Imaging

Myocardial imaging is carried out to evaluate the functioning of heart tissues and to detect any abnormalities. Myocardial imaging of heart patient helps in differentiating the normal myocardium (heart tissues) from the deceased condition, that is, *infarction* and *ischemic*. Normal myocardium has adequate blood flow (perfusion), and hence has sufficient supply of oxygen and nutrients. In case of ischemia, the arteries are partially blocked resulting in reduced perfusion to some part of myocardium. Low perfuse myocardium will have less availability of oxygen in comparison to normal myocardium. However, during stress condition the ischemic portions of myocardium become completely devoid of oxygen supply due to increased whole body demand for oxygen and increase in blood flow. After ending of stress condition, the blood flow is resumed to ischemic myocardial tissues. However, a longer persisting ischemic state may *permanently damage the* affected cells. Once the cells are damaged permanently, then even restoring of blood to them will not restart their myocyte function. This state of myocardium is called infarction. Myocardial imaging agents are those radiopharmaceuticals that help in scanning the three state of myocardium, that is, normal,

ischemic and infarction [7, 45, 46]. The commonly used myocardial imaging agents are listed in Table 1.9.

Table 1.9 *Commonalty used myocardial imaging agents*

Tracer	Type of tracer	Production	Half-life
	SPECT Based		
^{201}Tl	Metal cation	Cyclotron	73 h
^{99m}Tc-sestamibi	Metal complex	Generator	6 h
^{99m}Tc-tetrofosmin	Metal complex	Generator	6 h
^{99m}Tc -teboroxime		Generator	6 h
	PET Based		
^{82}Rubidium	Metal cation	Generator	76 s
^{13}N-ammonia	Inorganic compound	Cyclotron	9.96 min
^{15} O-water	Inorganic compound	Cyclotron	2.04 min
^{18}F-flurpiridaz	Organic compound	Cyclotron	109.8 min

1.12 Industrial Applications of Radioisotopes

Radioisotopes have numerous applications in industry, such as, gamma sterilization of medical equipment, shelf-life enhancement of packed food items, treatment of sewage waste, radiography for non-destructive testing of equipment, gamma scanning of process equipment in refineries, leak detection in liquid stream etc. Gamma rays from ^{60}Co source (in sealed from) are used to deliver cytotoxic doses to eliminate microorganisms present in sealed medical equipment and sealed food items. The disinfection of packed food items enhances its shelf life for long term storage. Radiography testing of mechanical equipment using radioisotope such as ^{192}Ir is helpful in determining presence of any defects such as internal voids, cracks formation, uniformity of material thickness etc., without destroying the specimen, and hence this technique is called 'non destructive testing'. Gamma scanning of large process equipment such as catalytic bed of petroleum refineries helps in finding out any internal abnormality without dismantling it, thereby reducing the time of any maintenance

issue [52-55]. This leads to huge monetary benefits to these industrial plants. Leak testing of liquid stream of crude oil refineries using tracer technique is also one of the applications of radioisotopes. Radioactive tracer in suitable form and using short lived isotope such as, ^{82}Br, is used to detect leakage in buried pipelines, large reactor vessels, heat-exchangers etc. In a nutshell, the use of radioisotopes in industry improves the product quality, process efficiency, reduces the downtime for maintenance and, hence provides huge monetary benefit to the industry [9, 53-55]. Some of the radioisotopes used in industry are shown in the Table 1.10.

Table 1.10 *Some of the radioisotopes used in industry*

Radioisotope	Half-life	Application
Am-241	432 y	Backscatter gauges, smoke detectors, fill height detectors, and in measuring ash content of coal.
Cs-137	30.17 y	Identification of sources of soil erosion and deposition, low-intensity gamma sterilisation.
Cr-51	27.7 yr	Study of coastal erosion, tracer studies in blood.
Co-60	5.27 yr	Gamma sterilisation, industrial radiography, density, and fill height switches.
Au-198	2.7 d	Study of sewage and liquid waste movements, tracing factory waste causing ocean pollution, tracing of sand movement in river beds and ocean floors.
Ir-192	73.8 d	Non destructive testing (NDT) to locate flaws in metal components.
Kr-85	10.756 y	Industrial gauging.
Mn-54	312.5 d	Study of heavy metal components in effluents from mining waste water.
Ni-63	100 y	Light sensors in cameras and plasma display, electronic discharge prevention and in electron capture detectors for thickness gauges.
Se-75	120 d	Used in gamma radiography and non-destructive testing.
Sr-90	28.8.y	Industrial gauging.
Yb-169	32 d	Gamma radiography and non-destructive testing.

1.13 Motivation and Structure of Thesis

From the above discussion, it is evident that radioisotopes play a very significant role for betterment of mankind through their vast application in healthcare, industry and research. Thus continuous explorations of these radioisotopes are required to further improve the quality of mankind. With this motivation, an effort has been put in present thesis to explore ^{99}Mo radioisotope for its novel production method and its novel uses in healthcare and industry.

The present thesis has been divided in to five chapters. The first chapter introduces give brief insight of radioisotopes production and its use in healthcare and industry, with specific attention to ^{99}Mo radionuclide. Subsequent three chapters deals novel production scheme for (n,f)^{99}Mo; its medical application in the form of a novel *myocardial metabolic imaging agent* utilizing daughter radioisotope ^{99m}Tc; and lastly industrial application of ^{99}Mo in the form of organic soluble radiotracer for identification of leakage in heat-exchangers system of crude oil refineries.

In the second chapter, a novel separation and purification methodology has been described to obtain high specific activity ^{99}Mo from thermal neutron irradiated U-Al alloy. The purity of obtained (n,f)^{99}Mo was assayed its utility for medical application through ^{99}Mo-^{99m}Tc radioisotope generators.

The third chapter is related to medical application of ^{99}Mo through using its short-lived daughter radioisotope, that is, ^{99m}Tc.Two fatty acid based small organic molecules were synthesized. Further, synthesized molecules were radiolabeled with ^{99m}Tc and using tricine/ EDDA and tricine/ TPPTS as coligands to form stable complexes with radio-metal. Total four radiolabeled compounds were prepared which are: (1) 11C-FA-HYNIC-^{99m}Tc-EDDA complex, (2) 12C-FA-HYNIC-^{99m}Tc-EDDA complex, (3) 11C-FA-HYNIC-^{99m}Tc-TPPTS/tricine complex, and (4) 12C-FA-HYNIC-^{99m}Tc-TPPTS/tricine complex.

Subsequently, efficacies of these radiocomplexes as myocardial metabolic imaging agent in an animal model were evaluated. Obtained bio-distribution pattern in target organs of selected animal model, which were injected with the prepared radio-formulations, have been described. Also, their uptake/ retention in non-target organs (liver, lungs, kidney, spleen etc.) have been analyzed. Out of all these above mentioned radio-complexes, 12C-FA-HYNIC-^{99m}Tc-EDDA has shown promising result, and was further examined for its potential in myocardial imaging using dynamic SPECT imaging.

The fourth chapter is pertaining to the industrial application of ^{99}Mo. A novel methodology was described for the preparation of ^{99}Mo based organic soluble radiotracer. Starting from the aqueous alkaline solution of ^{99}Mo, its daughter ^{99m}Tc was separated by solvent extraction with MEK. The leftover ^{99}Mo activity was then converted into organic soluble ^{99}Mo-α-benzoinoxime complex use as industrial radiotracer. The prepared radiotracer was evaluated for their potential to detect leakage in serially connected *heat-exchangers* unit of a leading crude oil refinery. The similar leak detection is also carried out using ^{99m}Tc-MEK, as another radiotracer. The results obtained from these two radiotracers were compared.

1.14 Scope of the Present Work

In the present work a radiochemical separation method has been developed to separate and purify (n,f)^{99}Mo, suitable for medical application, from thermal neutron irradiated U-Al alloy target. Towards medical application of ^{99}Mo, through its daughter radioisotope i.e. ^{99m}Tc, a novel ^{99m}Tc labeled myocardial metabolic agent was prepared and its efficacy was tested in Swiss-mice. Towards industrial application of ^{99}Mo, an organic soluble ^{99}Mo-alfa-benzoin- oxime radiotracer was prepared and tested in identification of leaky heat exchanger system of a crude oil refinery.

Chapter 2

Separation and purification of (n,f)^{99}Mo from neutron irradiated uranium aluminum alloy

In this chapter a novel radiochemical processing methodology has been developed for separation and purification of fission ^{99}Mo from thermal neutron activated U-Al alloy target. Starting with simulation studies using non-irradiated U-Al alloy target and ^{99}Mo tracer, process steps such as dissolution, precipitation and purification on ion-exchange column were optimized for Mo recovery. Further studies were done using irradiated U-Al alloy target. Alkaline dissolution of the target (100 mg) leads to complete dissolution of aluminum matrix of the target, whereas uranium remains undissolved.^{99}Mo activity in the target leached into solution alongwith a few fission products impurities, while most of the fission products, activation products did not get dissolved. Filtrate which contains ^{99}Mo alongwith some dissolved fission products impurities such as ^{131}I, ^{103}Ru, ^{95}Zr, ^{95}Nb, ^{132}Te, ^{239}Np etc., was further purified by sequential steps comprising of precipitations, boiling and ion-exchange method. Aluminum present in the filtrate was precipitated as $Al(OH)_3$, iodine as $AgI/AgIO_3$ precipitate. Subsequently, molybdenum was selectively precipitated as Mo-α-benzoin oxime, leaving behind impurities in filtrate. Ruthenium was separated by boiling it off as RuO_4. Final purification was carried out using anion exchange method using AG resin to desired purity level of ^{99}Mo. The radiochemical yield of the (n, f)^{99}Mo in the final purified fraction was found to be >80% and the purity of the product was in conformity with the international pharmacopoeia standards.

2.1 Introduction

^{99}Mo is the parent radioisotope of ^{99m}Tc, which has favorable nuclear properties of short half-life (6.02 h), low gamma energy (140 keV) and suitable chemical properties. All of these favorable features make ^{99m}Tc a suitable radionuclide for preparation of vast majority of radio-pharmaceuticals for nuclear diagnostic imaging. Currently, about thirty million SPECT based medical examinations are carried out world-wide annually using ^{99m}Tc labeled compounds. The conventional ^{99}Mo/^{99m}Tc generator consists of a chromatographic column with ^{99}Mo–^{99m}Tc pair in transient equilibrium and from which ^{99m}Tc is eluted with high degree of purity [68]. ^{99}Mo, in turn, is produced either by ^{98}Mo(n,γ)^{99}Mo reaction or by ^{235}U(n,f)^{99}Mo. In the former route the low thermal neutron capture cross section (0.14 b) and low abundance of ^{98}Mo (24.1%) results in low specific activity of ^{99}Mo (<3.7 x 10^{10}Bq/g) thereby requiring large alumina column for ^{99m}Tc generators and resulting in large elution volumes for ^{99m}Tc [66]. On the other hand, the latter reaction, due to high fission cross section of ^{235}U(n_{th},f), coupled with the high fission yield of ^{99}Mo (6.1%), results in high specific activity of ^{99}Mo (> 7.4 x 10^{14}Bq/g) [73]. However, in addition to specific activity the medically used radio-isotopes must satisfy the stringent pharmacopoeia specifications of the radiochemical and radionucleidic purity for safe in-vivo studies in patients [59]. Irradiation of uranium target cause the generation of large number of fission products spanning elements with atomic number (Z) from 35 (Br) to 64 (Gd) along with bulk uranium. Some transuranium elements, namely Np and Pu also get generated during neutron activation of ^{238}U, present in target, followed by β^- decay of ^{239}U. In view of above, the radiochemical separation of ^{99}Mo from irradiated uranium target requires careful separation procedures to achieve the desired decontamination factors with regard to the other impurities. At the same time the yield of purified ^{99}Mo should be reasonably high for economic viability of the process.

Radionuclides constituting significant gamma activity in the irradiated target are shown in Table 2.1along with their nuclear data.

Researchers have been used different target designs such as uranium metal, alloy or uranium oxide for fission ^{99}Mo production. Several approaches have been followed all over the world for purification of fission ^{99}Mo which usually involve multiple steps comprising dissolution, solvent extraction, precipitation, ion exchange and sometimes sublimation. However, the radiochemical purification flowsheet to obtain fission molybdenum invariably starts with dissolution of the irradiated target either with alkali or acid.

The first ^{99m}Tc generator based on fission ^{99}Mo was developed at Brookhaven National Laboratory and was based on acid dissolution of target followed by purification of molybdenum using acidic alumina column [69]. The produced ^{99}Mo, however, could not be put to medical use as the product did not comply with pharmacopoeia standards. The above mentioned process was further improved by Union Carbide Co. Ltd. [56] and thus resulted in the development of the well known CINTICHEM process for (n,f)^{99}Mo production. The first step in this process was acidic dissolution of uranium oxide layer in a mixture of 1.25 mol L^{-1} H_2SO_4 and concentrated HNO_3. Iodine impurity in the resulting solution was precipitated as AgI and removed by filtration. Molybdenum in the filtrate was precipitated by forming Mo-ABO complex with α-benzoin oxime (ABO) while keeping Ru and Rh impurities in the solution using the help of hold back carriers. The obtained Mo-ABO precipitate was then dissolved in alkali. Subsequent purification was done by column chromatography. ^{99}Mo yield for the CINTICHEM process was more than 90%. Another group of researchers at Chalk River, Canada carried out Nitric acid dissolution of UAl_3 target assisted by $Hg(NO_3)_2$ followed by subsequent purification employing acidic alumina column [58]. The CINTICHEM process for production of

fission ^{99}Mo was modified at Argonne National Laboratory to use low enriched uranium (LEU) metal foil as target for irradiation [70]. Sandia National Laboratory also followed the same process for the production of medical grade (n,f)^{99}Mo [62].

Recently a modified form of CINTICHEM process was developed at Pakistan Institute of Nuclear Science and Technology [64], where the LEU target was enveloped in 15 μm thick Ni foil sandwiched between two Al plates for irradiation. After irradiation, the target wrapped in Ni foil was completely dissolved in HNO_3 and the ^{131}I impurity was precipitated as AgI by the addition of $AgNO_3$. Filtrate containing ^{99}Mo was added with α-benzoin oxime to precipitate Mo-ABO complex, which was further dissolved in NaOH solution. Final purification of ^{99}Mo in the solution was carried out with a series of columns filled with silver coated charcoal and activated charcoal.

Oak Ridge National Laboratory has developed a process based on alkaline dissolution of irradiated uranium–aluminum alloy target, followed by filtration and solvent extraction of molybdenum from the aqueous filtrate using bis(2-ethyl-hexyl)phosphoric acid as extractant [62]. At Karlsruhe [67] the uranium target used was in the form of UAl_3 alloy plates sandwiched in aluminum clad. The target was first dissolved in NaOH solution followed by filtration.Subsequently,^{99}Moin filtrate was purified by series of anion exchangers, viz. AG1x8 and Chelex-100.Similar method has been followed in Argentina for (n,f)^{99}Mo production [63]. Likewise alkaline dissolution of irradiated UAl_3 alloy target followed by different purification approaches involving ion exchange columns was followed at iThemba Laboratory, South Africa [71]. The yield of the final purified fraction of^{99}Mo product was 85%.

At Bhabha Atomic Research Centre [65] laboratory scale purification of ^{99}Mo was carried out by solvent extraction of molybdenum from an aqueous solution of irradiated

^{233}U target with α-benzoin oxime in ethyl acetate followed by anion exchange separation. However, the chemical recovery of ^{99}Mo in this process was 65%.

In this present work, a new methodology for separation and purification of (n,f)^{99}Mo from irradiated UAl_3 alloy target has been developed. The process starts with the dissolving the irradiated UAl_3 alloy target in NaOH. ^{99}Mo, ^{131}I and ^{103}Ru, were found to be leached into the solution along with Al and traces of ^{95}Zr, and ^{95}Nb. However, bulk of the fission products remained in the undissolved uranium residue. ^{99}Mo was further separated from other impurities with α-benzoin oxime thereby exploiting the twin advantage of alkaline dissolution and α-benzoin oxime precipitation. The demonstration experiment has been carried out using 100 mg of natural uranium based UAl_3 alloy.

Table 2.1 *Nuclear data of radionuclides and detection efficiency.*

Radio-nuclide	Energy (keV)	Half-life (h)	Branching intensity (%)	Detection efficiency* (HPGe) (%)
^{99}Mo	740	66	12.1	0.0119
^{132}Te	228	76.8	142	0.0228
^{239}Np	278	56.6	81.2	0.0195
^{131}I	364	192	89.5	0.0159
^{103}Ru	497	942	44.1	0.0121
^{95}Zr	724	1536	99.8	0.0116
^{95}Nb	766	840	88.2	0.0254
^{141}Ce	145	768	48.4	0.0314
^{140}Ba	162	306	62	0.0299

**Distance between source and detector was kept at 5 cm*

2.2 Experimental

2.2.1 Chemicals

All the reagents used in the experiments were of analytical reagent grade. α-Benzoin oxime (ABO) and Amberlyst A-26 (MP) resin were obtained from SD Fine Chemicals Ltd., Mumbai. Uranium aluminum alloy (UAl_3) was obtained from Atomic Fuel Division (AFD), silver coated activated charcoal was obtained from Sigma Aldrich.

2.2.2 Preparation of carriers

Individual carrier solutions (2 mg mL^{-1} with respect to metal concerned) for Zr, Sr, Fe, Te and Ru elements were prepared in 1 M HNO_3.

2.2.2.1 Preparation of ,Sr Fe and Ru carrier solution

Carrier for Sr, Fe and Ru were prepared by dissolving their nitrate salts viz. $Sr(NO_3)_2$, $Fe(NO_3)_3$ and $Ru(NO_3)_3$ in 1 mol L^{-1}solution of HNO_3.

2.2.2.2 Preparation of Te carrier solution

Te carrier solution was prepared by using its oxide salt (TeO_2).The salt was dissolved by heating in concentrated HNO_3which containing a few drops of 0.2 mol L^{-1} HF. Obtained solution was evaporated to dryness and reformulated with 1 mol L^{-1} HNO_3.

2.2.2.3 Preparation of Zr carrier solution

Zr carrier solution was prepared by using oxychloride salts ($ZrOCl_2.8H_2O$).The calculated amount of salt was dissolved in concentrated HNO_3 heating, followed by evaporation. The solid residue was reformulated in 1 mol L^{-1} HNO_3.

2.2.3 Preparation of ^{99}Mo tracer solution

^{99}Mo tracer, prepared by dilution of the (n, γ)^{99}Mo solution, in the form of $^{99}MoO_4^{2-}$, was obtained from Radio Pharmaceuticals Division (RPhD), BARC. Dilution with double distilled water (DDW) was done to obtained 2 μCi / ml radioactive concentration of ^{99}Mo.

2.2.4 Preparation of α-benzoinoxime (ABO) solution

2 % (w/ v) solution of ABO in ethanol was prepared by dissolving the calculated amount of ABO powder into absolute ethanol.

2.2.5 Simulation study with cold Uranium-Aluminum alloy target

Simulation study was carried out by digesting nearly 100 mg uranium aluminum alloy powder in 6 mol L^{-1} NaOH. The digestion assembly consists of a hot plate with temperature regulator, glass hood for covering the quartz beaker and alkali trap. Whole digestion assembly was kept inside a well ventilated fume-hood. The dissolution was carried out for 10 min at about 150^0C temperature. After the dissolution, the mixture was transferred into a 50 mL capacity glass centrifuge tube and centrifugationwas done at 1000 rpm for 10 min. The supernatant solutionwas separated from undissolved uranium residue. The solution was further added with 10 mg Mo carrier, in the form of ammonium molybdate, and ^{99}Mo tracer (7.4 x 10^4 Bq). The solution was acidified with 10 M HNO_3 solution with the final acidity of 3.5 mol L^{-1}. To this solution α-Benzoinoxime solution (2% in ethanol) was added to precipitated Mo. Subsequently the precipitate was dissolved in conc. HNO_3 and dilute with DDW to get a suitable acidity of solution for its further loading on ion-exchange column. Solution was subjected to anion exchange separation employing a glass column filled with Amberlyst-A26 resin. Ion-exchange process was optimized for the retention and recovery of Mo from the column.

2.2.6 Study with irradiated uranium–aluminum alloy

2.2.6.1 Target preparation

The natural uranium–aluminum alloysample weighing 100 mg was taken in quartz tube and sealed. This quartz tube containing target material was put inside an alumina can

(Fig. 2.1) and its lid was cold welded.Leak tightness of this containment was checked by submerging the cold welded aluminum can in water.

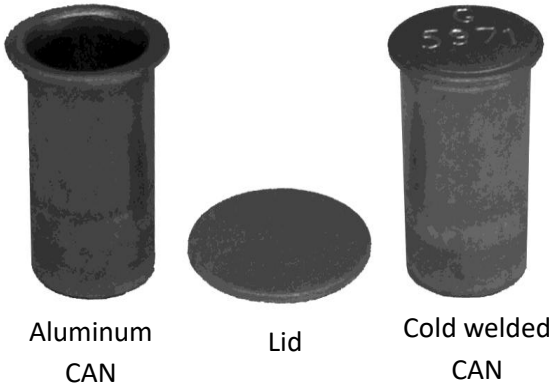

Fig. 2.1 *Aluminium CAN for target containment*

2.2.6.2 Target Irradiation

The sealed sample was irradiated at DHRUVA reactor for seven days at average neutron flux (ϕ) of 5 x 10^{13} ns^{-1} cm^{-2}. DHRUVA reactor is 100 MW(Th) tank type reactor with vertical placing of fuel element assemblies (Fig. 2.2). Heavy water is used as moderator, coolant and reflector. Natural uranium in metal form is used as fuel. DHRUVA reactor has dedicated channels for production of radioisotopes inside reactor core called tray rod locations. The aluminum can, containing target material, was kepton a special irradiation assembly called *tray rod* (Fig. 2.3). *Tray Rod* was then placed inside reactor core for irradiation. After completion of irradiation period, the target was cooled for two days and thenthe aluminum can (containing irradiated target) was placed inside a lead shielded cask for transportation to radioactive laboratory.

2.2.6.3 Recovery of quartz tube containing irradiated target

The alumina can inside the shielded cask was transferred into a hot-cell, where its lid was cut-off using specially designed gadget. The quartz tube was taken out from the

aluminum can and placed inside a lead container and transported to a glove-box for further processing.

Fig. 2.2 *Picture showing tray-rod assembly containing Aluminum CAN*

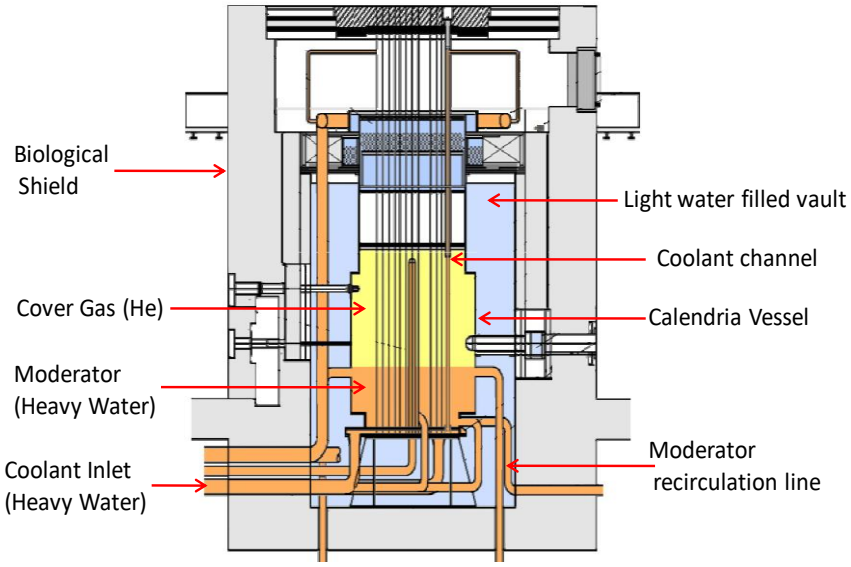

Fig. 2.3 *Schematic diagram of DHRUVA reactor for irradiation of target*

2.2.6.4 Radiochemical processing of irradiated target

2.2.6.4.1 Dissolution of irradiated target

The quartz tube containing the irradiated UAl_3 sample was transferred from the lead container to the glove-box. The quartz tube was broken and the fission gases (Kr, Xe) were allowed to pass through High Efficiency Particulate Aerosol (HEPA) filters. The sample was digested in 10 mL of 6 mol L^{-1} NaOH for 20 min at 150^{o}C in a quartz beaker kept on a heating mantle. After complete digestion of alloy, the beaker was sealed and bagged out of the glove-box to a fume hood. The solution along with the residue was

transferred into a centrifuge tube and was centrifuged at 1000 rpm for 10 min. The residue and filtrate were separated. The washings of residue (2 mL) were added to the original filtrate and made up to 10 mL in a flask (alkaline stock containing Mo) while the residue was dissolved in 10 ml of 2 mol L^{-1} HNO_3 (acidic stock solution) for quantification purpose. Appropriate aliquots from the alkaline stock and the acidic stock solution were taken for assaying the radioactivity in solution and residue. The counting was carried out on HPGe detector based γ-spectrometry system.

2.2.6.4.2 Removal of aluminum, iodine and ruthenium impurities

One mL of alkaline stock solution was taken for ^{99}Mo separation study. To this solution, 12 mg of aluminum as $Al(NO_3)_3$ was added as carrier. Aluminum matrix was removed by precipitation of $Al(OH)_3$. For precipitation, the pH of the solution was adjusted between 8–9 by the addition of dilute HNO_3. The resulting mixture was centrifuged for 10 min at 1000 rpm.The solution was decanted into a beaker and the remaining precipitate was further washed with 5 mL of 0.5 mol L^{-1} NH_4OH. The washing was added to the solution and final volume was made up to 20 mL.

For removal of iodine, the 20 mL of the above mentioned solution was added with 15 mg of KI and 20 mg KIO_3 as carrier for iodine. The solution was heated for 10 min at temperature of ~110^{o}C. Iodine present in the solution was precipitated by additionof 2 mL of $AgNO_3$ solution (50 mg $AgNO_3$ in 2 mL 0.1 mol L^{-1} HNO_3). The precipitate thus obtained was filtered through a 1″ diameter Whatmann 541 filter paper and washed with 2 mol L^{-1} NaOH. The washing was added to the filtrate solution and total volume was made 25 mL. Addition of KIO_3 was required to precipitate some of the iodine which was observed to be present as IO_3^- .

For removal of ruthenium impurity, the filtrate (25 mL) was evaporated to dryness followed by adding 6 mL of concentrated HNO_3 and 40 mg of $NaBiO_3$. The resultant solution was boiled-off to remove Ru as volatile RuO_4. The residue obtained was made up to 28 mL with 3–4 mol L^{-1} HNO_3.

2.2.6.4.3 Separation of molybdenum

The obtained solution (sec. 2.2.6.4.2) was digested for 30 min and was allowed to cool to room temperature. To this solution was added Zr, Ru, Sr, Te, Fe carriers (1 mL each of concentration 2 mg mL^{-1} solution). Molybdenum was precipitated from this solution by drop wise addition of 6 mL of ABO solution (20 mg mL^{-1} in ethyl alcohol). The precipitate was separated from mother liquor by centrifuging for 10 min at 1000 rpm. The remaining precipitate was washed thoroughly with 3 mol L^{-1} HNO_3 and centrifuged. This process was repeated three times. The above precipitate was dissolved in 15 mL of 2 mol L^{-1}NaOH. The solution was boiled off. The residue was reformulated with 0.4 mol L^{-1}NaOH, which was again centrifuged to get a clear solution. The solution was passed through a glass column filled with *silver activated charcoal* (AgC), and effluent was collected. The AgC column was further washed with 10 mL 0.4 mol L^{-1} NaOH and the washing effluent was added to the previously collected effluent.

2.2.6.4.4 Purification of ^{99}Mo by anion exchange column

A glass column of dimension (15 cm length x 1 cm dia.) with a reservoir of 15 mL capacity was filled with 10 mL bed of Amberlyst A-26 (MP) 50–100 mesh resin (Fig. 2.4).The resin was converted from chloride form to nitrate form by passing 1 mol L^{-1} HNO_3 through it. The acidity of the Mo solution (Section 2.2.6.4.3) was adjusted to 0.1 mol L^{-1} HNO_3 before its loading on the ion-exchange column. Total loading solution

volume was 25 mL, which was loaded on the column at the rate of 2 bed volume per hour and effluent was collected for quantification. The column was washed by passing 2 bed volumes of 0.1 mol L^{-1} HNO_3 at the same rate and the washing effluent was collected. After washing, the Mo loaded on the column was eluted with 6 mol L^{-1} HNO_3 at the rate of one bed volume per hour and continued up to 5 bed volumes.

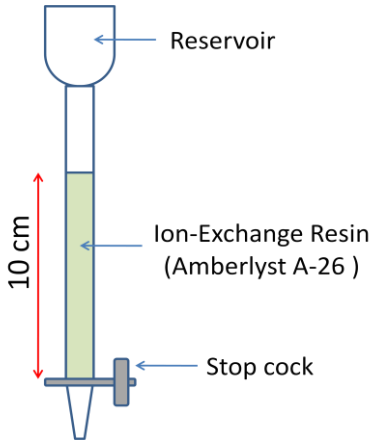

Fig. 2.4 *Ion-exchange column for purification of* ^{99}Mo

2.2.6.5 Estimation of ^{99}Mo and fission products

Gamma spectrometric assay of ^{99}Mo and other fission and activation products in solutions obtained at various stages of the separation process was carried out on a lead shielded 30% HPGe coupled with 4096 channel analyzer in standard geometry. All the samples were made up to 5 mL for gamma counting. Uncertainty involved in the measurements is 5%. The efficiency calibration of the detector was carried out using a standard ^{152}Eu source in 5 mL solution. The graph between log of efficiency (ε) versus log of energy (E_γ) was fitted using second degree polynomial, viz.,

$$\ln(\varepsilon) = a + b \ln(E_\gamma) + c (\ln E_\gamma)^2 \quad (1)$$

The activity (A) of the radionuclide was calculated from the measured count rate (cps) using the formula:

$$A = cps/ (\varepsilon a_\gamma) \quad (2)$$

Where a_γ is the branching intensity of the γ-ray.

2.2.6.6 Determination of the radionuclides left in solid residue

500 mL from the acidic stock solution (Section 2.2.6.4.1) was assayed for activity of various radionuclides formed. The nuclides estimated were ^{141}Ce, ^{140}Ba, ^{132}Te, ^{239}Np, ^{131}I, ^{103}Ru, ^{95}Zr, ^{99}Mo and ^{95}Nb. Similarly the radioactivity of nuclides in alkaline stock solution was estimated. From the activity ratio, percentage of nuclides leached into NaOH and that remaining in the residue was calculated. The total activity of individual fission product formed was also calculated.

2.2.4.6 Estimation of the alpha activity in ^{99}Mo solution

10 mL from the Mo solution obtained after elution anion exchange purification was placed in a glass beaker. The solution was heated under IR lamp to reduce the its volume to 100 μL. The solution was transferred to a S.S. planchette with 0.1 mol L^{-1} HNO_3 and evaporated to dryness. The planchette was counted for alpha activity for a duration of 10,000 s in ZnS(Ag) counter.

2.3 Results and Discussion

2.3.1 Simulation study

Initial experiments were carried out using ^{99}Mo tracer in order to optimize the conditions for separation and purification of ^{99}Mo. Uranium–aluminum alloy was digested in 6 mol L^{-1}NaOH solution and, to this solution Mo carrier and tracer were added. Molybdenum was selectively precipitated as Mo-ABO complex with α-benzoin oxime (ABO) in acidic medium. The precipitation with ABO is very selective for Mo and therefore could be exploited for its separation from other metal ions [60]. In the present study, conditions were optimized for Mo–ABO precipitation. It was observed that about 30 min of digestion in 3.5 mol L^{-1} nitric acid and Mo:ABO weight ratio of 1:10 was

necessary to obtain more than 95% yield of Mo–ABO precipitate. Addition of H_2O_2 did not improve the yield of precipitation. More than 95% precipitation yield of Mo was obtained under these optimum conditions.

Vigorous boiling was observed during the dissolution of Mo– ABO precipitate in concentrated nitric acid, which resulted in large Mo losses. Hence the Mo–ABO complex was decomposed by boiling with 2 mol L^{-1} NaOH, which was found to be simple with no loss of Mo. Further purification of Mo was carried out using anion exchange (Amberlyst A-26 (MP)) resin. Initial attempts to load Mo on the anion exchanger in 0.1 mol L^{-1} NaOH medium were not successful. Hence, Mo loading was carried out in 0.1 mol L^{-1} HNO_3 and elution was carried out with 6 M HNO_3. Molybdenum was eluted within five bed volumes.

2.3.2 Studies with irradiated uranium–aluminum alloy

A wide range of radionuclides that were produced either by fission or by activation during the irradiation uranium–aluminum alloy target are easily measurable by gamma counting as depicted in Table 2.1. The nuclear data these radionuclides, namely, half-life, γ-ray energy, branching intensity and efficiency at the respective γ-ray energy in the standard geometry are also given in the same table.

While acid dissolution of target was preferred for metal/ oxide targets [56, 57, 62, 64, 70], $Hg(NO_3)_2$ assisted dissolution of alloy target was carried out at CRNL [58]. However, dissolution step required 1 h. In the present work, the first step for separation and purification of fission molybdenum involved digestion of the irradiated target in 6 mol L^{-1}NaOH which could be achieved in 20 min. The residue thus obtained was dissolved in nitric acid. The activity of the various fission and activation products in the residual uranium oxide (acidic solution) and the alkaline solution are given in Table 2.2.

The Table 2.2 shows the effectiveness of the alkaline dissolution step for the separation of ^{99}Mo from the majority of fission and activation products along with bulk uranium.^{99}Mo and ^{131}I were quantitatively dissolved in NaOH along with a significant fraction of ^{103}Ru and ^{95}Zr, while small fraction of ^{95}Nb, ^{141}Ce, ^{132}Te and ^{239}Np were also present with it. On the other hand bulk of the ^{239}Np, ^{132}Te, ^{103}Ru, ^{95}Zr, ^{95}Nb and ^{141}Ce were retained in the hydrated uranium oxide. The total activities of the radionuclides produced at the end of two days processing are also shown in Table 2.2.

Table 2.2 *Percentage of various radio-nuclides leached into NaOH solution and those remaining in the residue (after 2 days of processing).*

Radio-nuclide	Energy (keV)	Activity leached into alkali (%)	Activity remaining in solid residue (%)	Total activity (10^7 Bq)
^{99}Mo	740	100.0	0	7.7
^{132}Te	228	2.8	97.2	12.7
^{239}Np	278	0.2	99.8	26.5
^{131}I	364	100.0	0	60.5
^{103}Ru	497	17.9	82.1	599.6
^{95}Zr	724	7.3	92.7	4.6
^{95}Nb	766	1.8	98.2	3.7
^{141}Ce	145	1.1	98.9	6.7
^{140}Ba	162	0	100	1.9

After alkaline digestion of the target, different groups have opted for anion exchange and chelation column based processes for further purification of fission molybdenum [67, 63, 71]. However, column based processes involve loading and washing steps prior to elution which contribute to a lot of radioactive liquid waste and spent resins contribute to solid waste. On the other hand, the commercially successful CINTICHEM process [56, 57] largely depended on precipitation steps. A radiochemical processing flow sheet has been developed for the present study (Fig. 2.5) to get purified (n, f)^{99}Mo.This flow-sheet has been validated for its reproducibility. Initial purification

steps consist of precipitation and the final purification was carried out by using anion exchange resin. Percentage of various nuclides present after different steps of separation process are given in Table 2.3.

The alkaline solution contained aluminum and traces of some fission products along with Mo. In an innovative approach for efficient separation of ^{99}Mo, removal of major matrix (aluminum) was carried out by $Al(OH)_3$ precipitation in alkaline solution. This step proved advantageous as along with Al, 90% ^{95}Zr, 80% ^{132}Te and 99% ^{95}Nb also got removed, while ^{131}I (90%), ^{103}Ru (80%) were retained in the solution.

Precipitation of ^{131}I by AgI route revealed that about of ^{131}I 30% activity was still left in the supernatant. Considering the alkaline dissolution route, it was surmised that some fraction of the ^{131}I might be present as IO_3^- . Hence iodine separation was done using KI and KIO_3 carriers. About 2% iodine was left in the solution at this stage. Interestingly, during this step Zr and Nb were also significantly removed and less than 1% Zr, 10% Ru and Te were left in the solution. In the $NaBiO_3$ boiling off step, Ru was completely removed as RuO_4. To get rid of the remaining fission products, Mo–ABO precipitation was carried out after adding the carriers. Organic matter and trace quantity of iodine were removed by silver coated charcoal column. Fig. 2.6 and Fig. 2.7show the gamma ray spectra of initial alkaline solution and final purified ^{99}Mo solution. It is clear that the ^{99}Mo fraction obtained after the series of separation steps was highly pure with radionuclidic purity of nearly 100%. The radiochemical yield of ^{99}Mo fraction was better than 80%.

The activity of the major contaminants with respect to ^{99}Mo in the final purified fraction is given in Table 2.4. The beta activity in the irradiated target was contributed by ^{147}Pm, ^{89,90}Sr and ^{99}Tc. Taking into consideration the low activity of ^{141}Ce (analog of Pm) and ^{140}Ba (analog of Sr) in the alkali leached solution and their easy removal in the

subsequent purification steps and also the long half-life of ^{99}Tc, it was concluded that the concentration of pure active radionuclides in the final purified ^{99}Mo is below the specification limit. Therefore, beta activity was not measured. Alpha activity present in the final purified fraction of ^{99}Mo is also shown in Table 2.4.

The trace amount of uranium present in the ^{99}Mo fraction was estimated by total reflection X-ray fluorescence measurement on the decayed purified ^{99}Mo solution. It was found to be below the detection limit of the instrument (15 ng mL^{-1}). The specifications for ^{99}Mo derived from different pharmacopoeia [72] are also shown in the Table 2.4 for comparison of purity of obtained (n,f)^{99}Mo.

Table 2.3 *Activity of radio-nuclides remaining in Mo-fraction after various steps of separation with respect to the alkaline feed solution.*

Radio-nuclide	$Al(OH)_3$ filtrate (%)	AgI filtrate (%)	$NaBiO_3$ boiled off solution (%)	ABO dissolved solution (%)	AgC eluted solution (%)	Anion exchange eluted solution (%)
^{132}Te	20.8	13.1	10.9	0	0	0
^{131}I	89.7	1.9	1.5	0.1	0.06	0
^{103}Ru	81.9	9.9	0.00	0	0	0
^{95}Zr	11.5	0.8	0.6	0	0	0
^{99}Mo	96.6	93 2	93.8	85.1	83.4	81.1
^{95}Nb	0.8	-	0.8	0.7	0	0
^{141}Ce	0	0	0	0	0	0

2.3.3 Radioactive waste

In the plant level operation of the scheme, the hydrated uranium oxide will constitute the solid waste. Accordingly the solid waste contained all the fission products which were retained in the uranium metal residue. The fractions generated in steps 2.2.4.1–2.2.4.3 contributed to liquid and solid waste. For processing of 100 mg of irradiated uranium aluminum alloy, activity in the solid waste was 7.1 x 10^9 Bq and activity in the liquid waste was 9.3 x 10^6 Bq. The solid waste obtained in representative

processing of 1 mL of NaOH solution, the NaOH dissolution, $Al(OH)_3$ precipitation, $AgI/AgIO_3$ precipitation steps was estimated to be < 0.5 g. The liquid waste volume obtained by ABO precipitation and anion exchange step was 200 mL. The waste volumes are expected to be same when the enriched uranium aluminum target will be used.

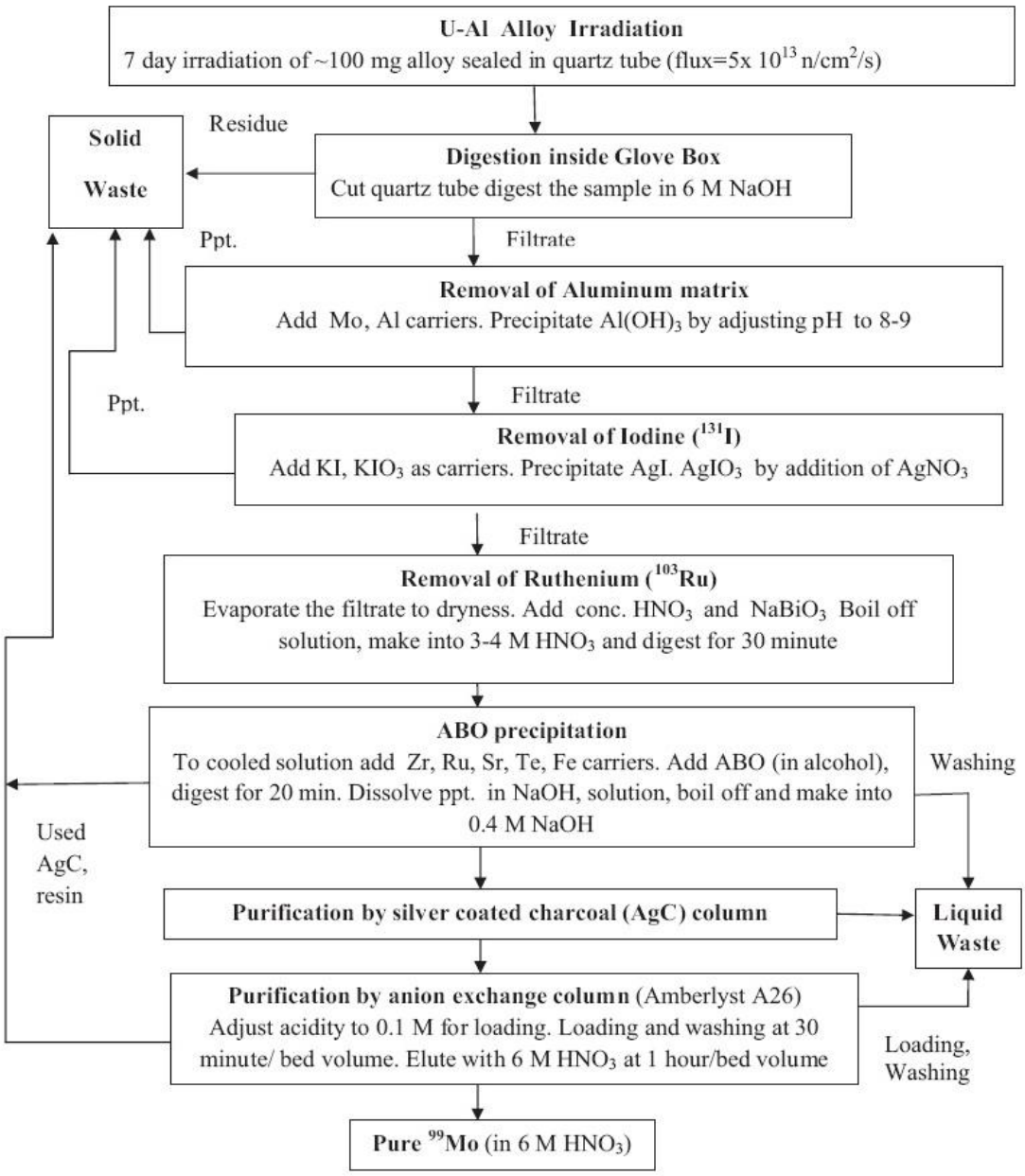

Fig. 2.5 *Detailed methodology for the purification of* ^{99}Mo

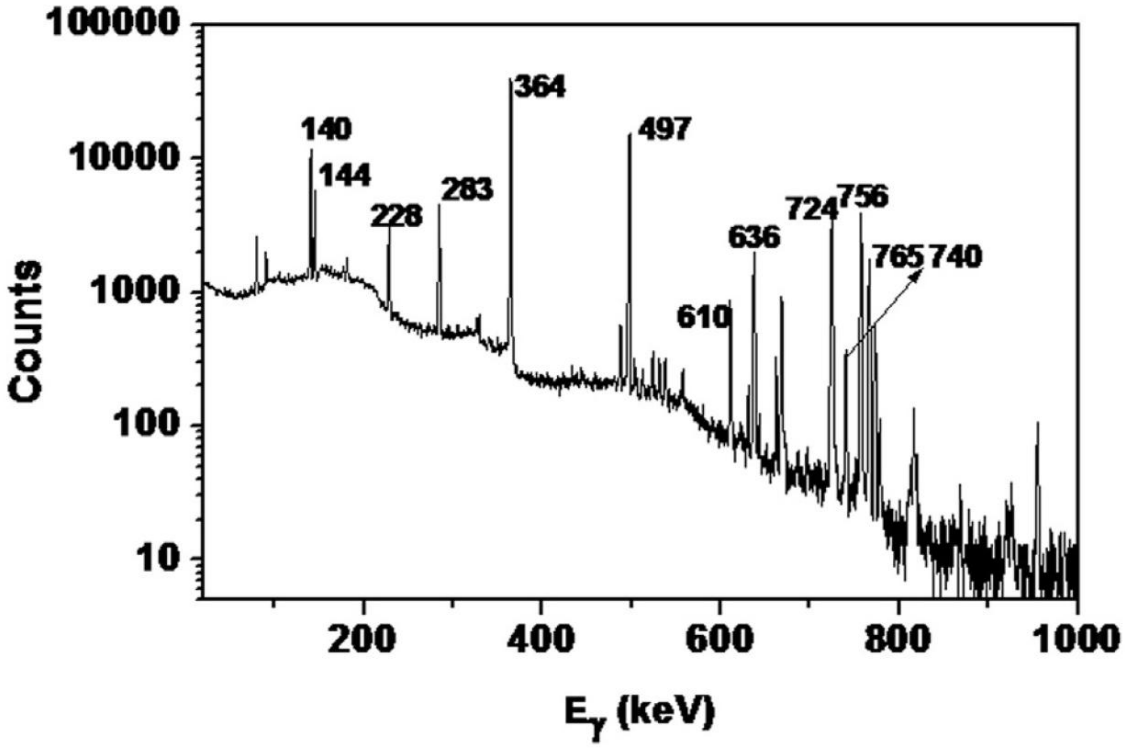

Fig. 2.6 *Gamma Spectrum of alkaline solution*

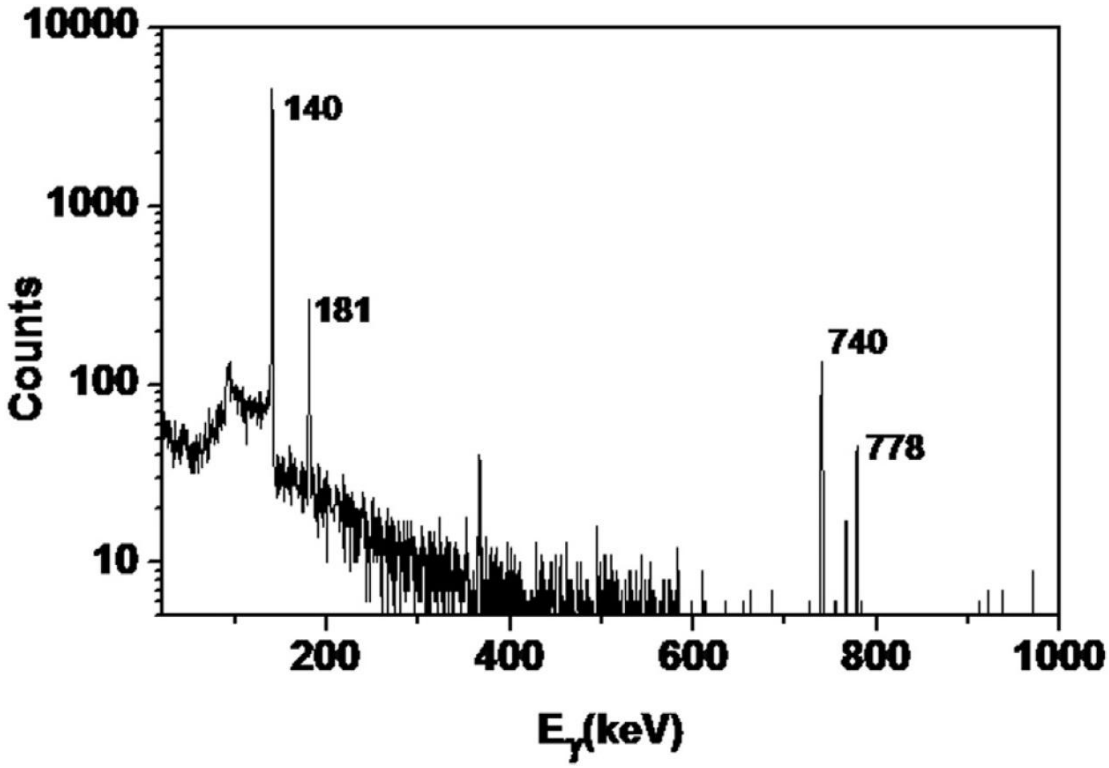

Fig. 2.7 *Gamma Spectrum of purified ^{99}Mo*

Table 2.4 *Radionuclidic purity of the separated ^{99}Mo.*

Nuclide	A(radionuclide)/A(^{99}Mo)	
	Present work	Specification (Villiers, 2003)
^{131}I	$< 2 \times 10^{-6}$	$< 5 \times 10^{-5}$
^{103}RU	$< 7 \times 10^{-5}$	$< 5 \times 10^{-4}$
^{95}Zr	$< 1 \times 10^{-5}$	Not specified
^{95}Nb	$< 2 \times 10^{-5}$	Not specified
Uranium	< DL (15 ng mL^{-1})	Not specified
$\sum\beta$	Not measured	$< 2 \times 10^{-4}$
$\sum\alpha$	$< 6 \times 10^{-10}$	$< 1 \times 10^{-9}$

2.4 Conclusion

A new radiochemical method has been developed for separation and purification of fission produced ^{99}Mo. The irradiated UAl_3 alloy (100 mg) was dissolved in NaOH to get rid of the majority of fission products and alpha activity which were contained in the form of compact solid waste. This was followed by $Al(OH)_3$ precipitation to remove major Al matrix. Following the specific steps for removal of impurities, such as, iodine and ruthenium, pure ^{99}Mo was obtained with an overall radiochemical yield > 80% with required radionuclidic purity for medical applications.

Chapter 3

Syntheses, and biological evaluation of ^{99m}Tc-HYNIC-fatty acid complexes for myocardial imaging

This chapter aims towards development of ^{99m}Tcbased radiopharmaceuticals for their possible use in cardiac imaging as myocardial metabolic marker. These radiotracers were designed and tested as a possible alternative for medically used ^{123}I-radiolabelled fatty acid based myocardial imaging agents. The significance of the present study emerges from the fact that ^{123}I ($T_{1/2}$: 13.2 hrs) is a cyclotron produced radioisotope which limits its availability due to limited footprint of cyclotrons across all nuclear medicine centers. On the other hand, ^{99m}Tc is readily available at these radiopharmacies through ^{99m}Tc-^{99}Mo radioisotope centers. In the present study, two fatty acid (FA)-hydrazinopyridine-3-carboxylic acid (HYNIC) conjugates (11C-FA-HYNIC and 12C-FA-HYNIC) were synthesized using HYNIC as bi-fucntional chelating agent (BFCA).Further, the synthesized compounds were radiolabeled with ^{99m}Tc using two different co-ligands system viz. tricine/ethylenediaminediacetic acid (EDDA), and tricine/trisodium triphenylphosphine-3,3',3''-trisulfonate (TPPTS).Total four ^{99m}Tc-HYNIC-FA complexes were prepared. While all four radiolabeled complexes showed uptake in the myocardium, 12C-FA-HYNIC-^{99m}Tc-EDDA complex showed higher uptake and retention in myocardium compared to other complexes. Bio-distribution pattern obtained from the prepared ^{99m}Tc-HYNIC-FA complexes was compared with ^{125}I-iodophenyl pentadecanoic acid (IPPA). In general, uptake of the ^{99m}Tc-complexes in non-target organs was found to be than that of ^{125}I-iodophenyl pentadecanoic acid (IPPA). Additionally, the 12C-FA-HYNIC-^{99m}Tc-EDDA complex, exhibited lower liver

accumulation compared to that of ^{125}I-IPPA. All these features were favorable for cardiac imaging, however the heart-to-blood ratio of the complexes were low (<1). Dynamic SPECT imagingSwiss mouse with 12C-FA-HYNIC-^{99m}Tc-EDDA complex showed delineation of its myocardium from nearby non-target organs. The results obtained from these studies encourages for further screening of synthetically modified ^{99m}Tc-HYNIC fatty acids for their possible use as myocardial metabolic imaging agent in cardiac patients.

3.1 Introduction

Ischemia and infarction are the diseased state of cardiac caused by the reduced perfusion of blood in the myocardium tissues. Ischemic portion of cardiac tissues have low blood supply but are still viable and can regain their myocyte functioning after restoration of normal blood. However, myocyte cells became dead in infracted portion of myocardium and therefore are not viable. Diagnosis of ischemic/ infracted portion of myocardium is needed for the treatment planning of heart patient. Fatty acids molecules are the major source of energy for normoxic (normally perfused) myocardial tissues. Naturally occurring long chain fatty acids such as palmitic acid , stearic acid etc., can enter inside the myocardial cells by CD-36 transport protein present on the cell membrane (Fig. 3.1). Once fatty acid entered inside the myocyte, it get activated by the an enzyme Acyl-CoA and remain inside the cell till it gets metabolize in mitochondria.

Due to reason mentioned above, radiolabeled fatty acid based compounds can act as potential diagnostic agent for detecting alterations in cardiac metabolism.Also, these can be considered as sensitive markers for myocardial ischemia and infarction [74,75, 76]. Several fatty acid analogues have been radiolabeled with PET or SPECT isotopes and

clinically evaluated for their potential in metabolic myocardial imaging [76-82]. Fig 3.3 depicts some of these radiotracers.

PET radiopharmaceuticals allow dynamic imaging of the myocardial metabolism. However, currently used clinical radiotracers based on ^{11}C radioisotope ($t_{1/2}$:20 min) viz. ^{11}C-palmitic acid and ^{11}C-acetate, poses severe limitation due to their short half-life.This in turn necessitates for in-house production and handling of large quanta of initial activity to yield substantial amount of the radiopharmaceutical for clinical use.

Several SPECT radiotracers based on ^{123}I have also been used to probe myocardial metabolism in vivo. Among them, ^{123}I-iodophenylpentadecanoic acid (IPPA) and ^{123}I-beta-methyl-p-iodophenylpentadecanoic acid (BMIPP) (Fig. 3.2) have shown promising result as a radiopharmaceutical for non-invasive imaging of myocardial metabolism. Despite the availability of these radiopharmaceuticals for myocardial metabolic imaging, considering the attractive features of ^{99m}Tc radioisotope, such as optimal half-life, easy availability of the isotope from $^{99}Mo/^{99m}Tc$ generator, significantly low cost, possibility of formulation of a lyophilized kit etc., a ^{99m}Tc-agent for this purpose may be more desirable.

Several researchers have made efforts to develop ^{99m}Tc-labeled fatty acid based radiotracers to image myocardiumabnormalities [83-93]. Although ^{99m}Tc-radiotracers based on fatty acids have proved their efficacy to target myocardium in animal models, low myocardial uptake and significant non-target uptake limited their further evaluation for clinical use. Continuous efforts are being made to design a ^{99m}Tc-fatty acid radiotracer with better myocardial uptake and rapid clearance from non-target organs to obtain clinically acceptable heart-to-non-target ratios.

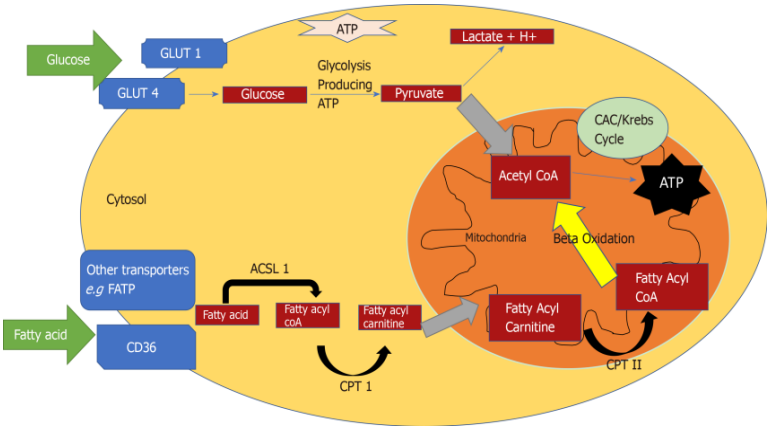

Fig. 3.1 *General depiction of transport of fatty acid molecules into myocytes*

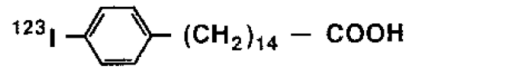

(^{123}I-IPPA)

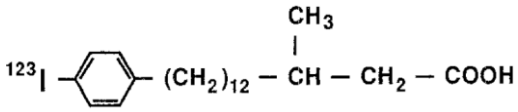

(^{123}I-BMIPP)

Fig. 3.2 *^{123}I Radiolabeled IPPA and BMIPP*

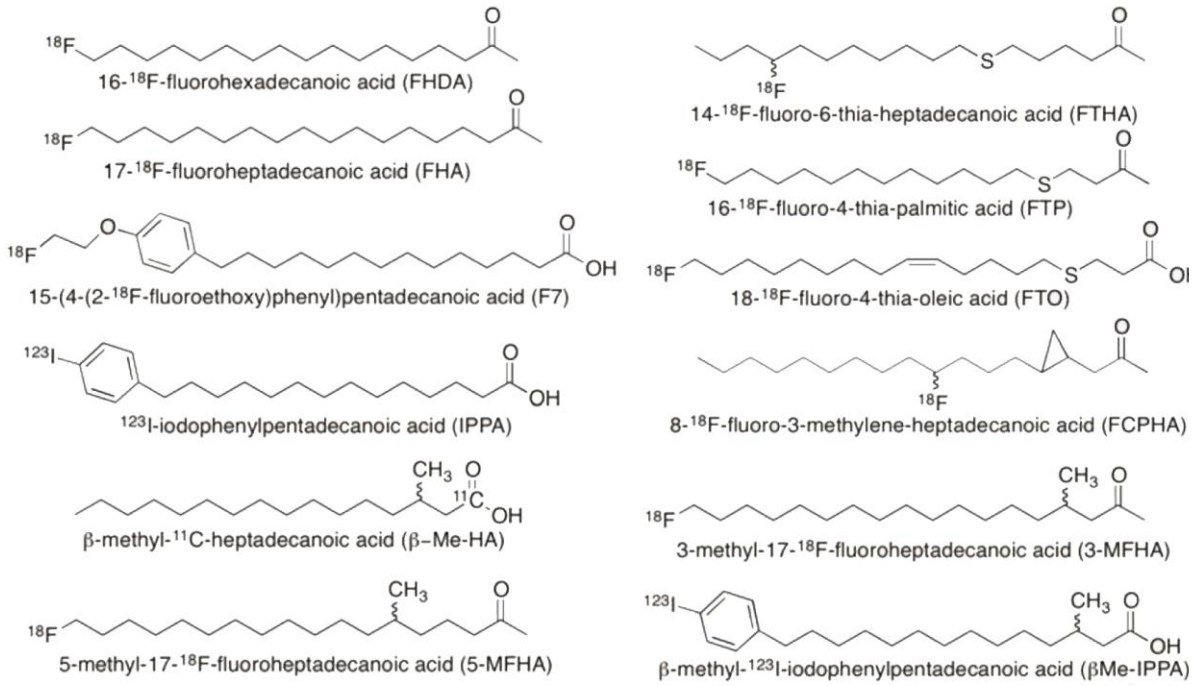

Fig. 3.3 *Fatty acid based PET/ SPECT myocardial metabolic tracers*

Usually, a ^{99m}Tc labeled fatty-acid based radiopharmaceuticals have a fatty-acid molecule covalently bonded with a linker molecule, which in turn bonded with a bifunctional chelator (BFCA) in complexation with ^{99m}Tc metal (Fig. 3.4). Alterations to the radiotracer to achieve the required pharmaco-kinetics are generally achieved by modifying the linker or by the groups through which the fatty acid is radiolabeled with ^{99m}Tc. Similarly, the nature of ^{99m}Tc-core is also found to affect the in- vivo distribution and clearance of the radiotracer, and offers an additional route to achieve desirable pharmacokinetics. In this regard, several fatty acid complexes with different ^{99m}Tc-cores such as $[^{99m}TcN(PNP)]^{2+}$ [83, 84], ^{99m}Tc-4+1 [85-87], $^{99m}Tc(CO)_3$-cyclopentadienyl [88], $[^{99m}Tc(CO)_3(H_2O)_3]^{+}$ [86], $[^{99m}TcO]^{3+}$ [90–93] have been prepared and evaluated. However, fatty acid molecules labeled with ^{99m}Tc through HYNIC BFCA have not been evaluated so for. Some of the commonly used ^{99m}Tc-cores are shown in Fig. 3.5.

Fig. 3.4 *Schematic of ^{99m}Tc labelled fatty acid based myocardial imaging agent*

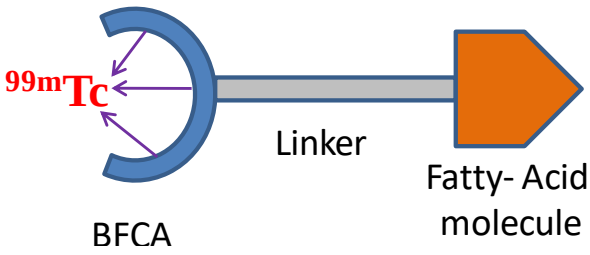

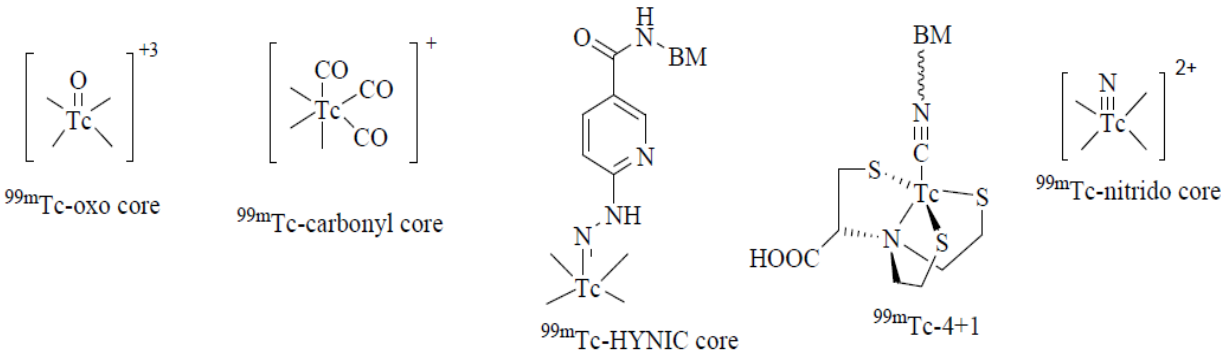

Fig. 3.5 *Commonly used ^{99m}Tc-core for labelling of target molecule*

In the recent past, several ^{99m}Tc-HYNIC complexes of small peptides, antibodyfragments and other biomolecules for imaging processes at cellular level has been reported [94–112]. Among these radiotracers, ^{99m}Tc-HYNIC-TOC, ^{99m}Tc-HYNIC-TATE, ^{99m}Tc-HYNIC-annexin V and ^{99m}Tc-HYNIC-RGD have shown considerable promise and have been translated to the clinics. The HYNIC BFCA in some of these studies has proved to be superior than ^{99m}Tc-radiotracers prepared using other labeling strategies, from the perspective of imaging [113]. The HYNIC moiety acts as a mono-dentate chelator in complexation with ^{99m}Tc radiometal wherein the co-ordination sphere is completed by use of other co-ligands. By careful choice of the co-ligands in the complexation, sizeable difference in the lipophilicity of the resultant radiotracer can be achieved. This advantage of the HYNIC BFCA over that of the other ^{99m}Tc-labeling methodologies stems from the possibility to be able to fine-tune the *in vivo* pharmacokinetic behavior of the radio-tracers by use of different co-ligands for ^{99m}Tc complexation with the HYNIC BFCA [114].

These possibilities provided an impetus for the present study wherein the ^{99m}Tc-HYNIC complexes of long chain fatty acids have been evaluated with respect to their potential as myocardial tracers. The development of fatty acid radiotracer demands high target uptake and rapid clearance from background non-target organs such as blood, liver, lungs. Though, fatty acids of 15–21 carbon chain lengths have been documented to exhibit highest myocardial extraction [115]. However, in the present study, fatty acids with chain lengths of 11 and 12 carbon [11C-FA (1a)] and [12C-FA (2a)] (Fig. 3.6) are chosen, considering the fact that among the ^{99m}Tc-labeled metabolic myocardial imaging agents reported so far, highest myocardial uptake was shown by 11 and 12 carbon fatty-acids [83, 86, 87]. Use of the HYNIC-BFCA and different co-ligands such as tricine, EDDA and TPPTS allows modulation of the lipophilicities of the ^{99m}Tc-HYNIC

complexes and also tailoring the in vivo pharmacokinetic behavior of the complexes. The two fatty acids (**1a**, **2a**) were synthetically modified at the ω-carbon to yield HYNIC-fatty acid conjugates [11C-FA-HYNIC (**1c**) and 12C-FA-HYNIC (**2c**)] (Fig. 3.7). These derivatives upon complexation with ^{99m}Tc with tricine/ EDDA or tricine/ TPPTS as co-ligands yielded four complexes viz. 11C-FA-HYNIC-^{99m}Tc-EDDA (**1e**), 12C-FA-HYNIC-^{99m}Tc-EDDA (**2e**), 11C-FA-HYNIC-^{99m}Tc-TPPTS/tricine (**1f**) and 12C-FA-HYNIC-^{99m}Tc-TPPTS/tricine (**2f**) (Fig. 3.8). All four ^{99m}Tc-complexes were then evaluated, *in vitro* as well as *in vivo*, for their potential in imaging cardiac metabolism. The results obtained with the four complexes were compared with the ^{125}I-IPPA an analogue of clinically used metabolic marker ^{123}I-IPPA [84].

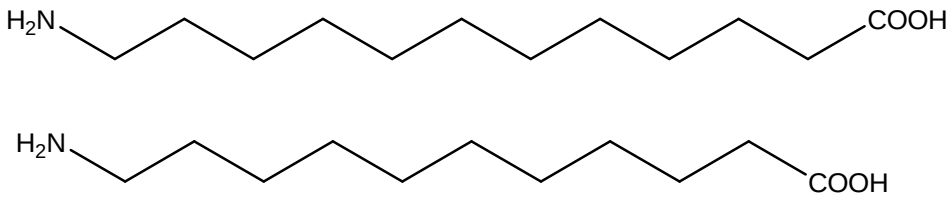

Fig. 3.6 *11C-Fatty Acid and 12C-Fatty acid compounds*

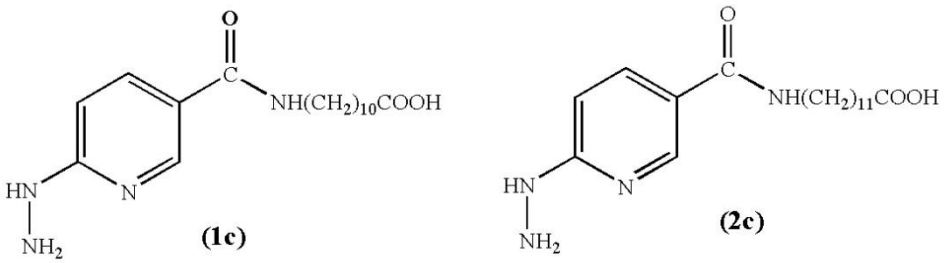

Fig. 3.7 *Synthesized 11C-FA-HYNIC (1c) and 12C-FA-HYNIC (2c) compounds*

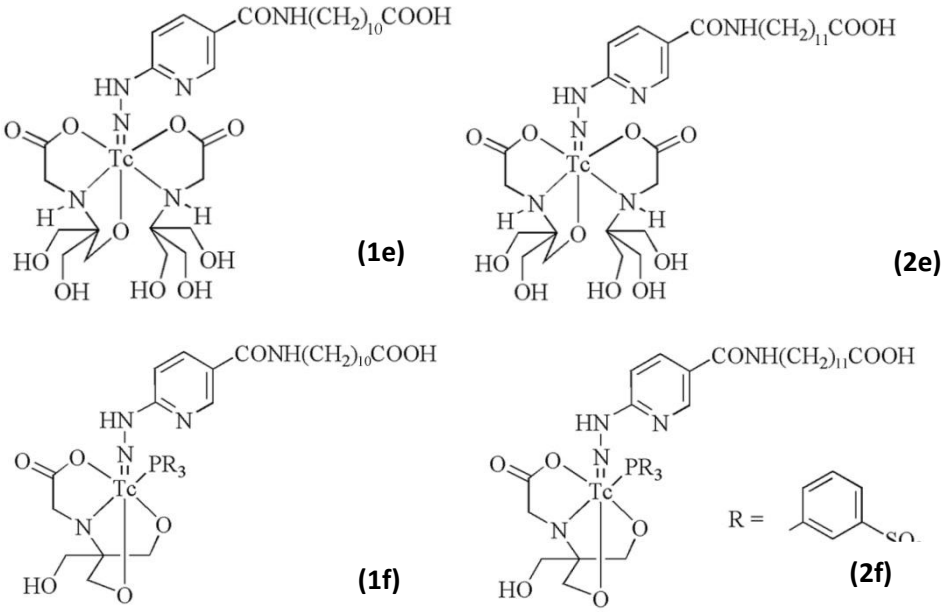

Fig.3.8 *^{99m}Tcradiolabeled complexes of 11C-FA-HYNIC (1c) and 12C-FA-HYNIC (2c)*

3.2 Experimental

3.2.1 General consideration

The compounds 11-amino undecanoic acid, 6-chloronicotinic acid, hydrazine hydrate (80%), N-hydroxysuccinimide, EDDA and stannous chloride were obtained from Aldrich, USA. The compounds 12-aminododecanoic acid, di-*tert*-butyldicarbonate (Boc anhydride) and *N-ethyl*, *N'*-(3-dimethylamino)carbodiimide hydrochloride (EDCI) were purchased from Fluka, Germany. Tricine was purchased from Sigma, Germany. TPPTS was obtained from Alfa Aesar, U.K. All other reagents used were of analytical grade. Sodium pertechnetate ($Na^{99m}TcO_4$) was eluted with normal saline prior to use from a $^{99}Mo/^{99m}Tc$ generator, supplied by Board of Radiation and Isotope Technology, India. ^{125}I-IPPA was prepared according to the procedure described previously [84]. Silica gel plates (silica gel 60 F_{254}) were obtained from Merck, India. The HPLC was carried out on a JASCO PU 2080 Plus dual pump HPLC system, Japan, with a JASCO 2075 Plus tunable absorption detector and Gina Star Gabi radiometric detector system, using a C-18 reversed phase HiQSil (5 μm, 4x250 mm) column. Different loops having internal

diameters (ID) of 0.5 mm and 0.8 mm with an in cell flow volume of 20 µL and 500 µL respectively in Gina Star radiometric detector system were used for radioactivity detection. A small loop was used for complex characterization (high radioactive concentrations) whereas a bigger loop with an additional guard C-18 column (5 µm, 4.6 x 10 mm) was used for acyl-CoA activation experiment and metabolite analyses experiment (low radioactivity content). The IR spectra were recorded on a JASCO FT-IT/420 spectrophotometer, Japan. The NMR spectra were recorded on a 300 MHz or 500 MHz Varian spectrophotometer, USA. Mass spectra were recorded on aexpression^{L} CMS Mass Spectrometer, Advion, USA using electron spray ionization (ESI) in positive mode. The SPECT studies were carried out using a microSPECT scanner FLEX Triumph™ LabSPECT4 (Trifoil Imaging Inc, Northridge, CA).

3.2.2 Synthesis

Using *6-Chloronicotinic acid* as starting material, *Succinimidyl 6-Boc-hydrazinopyridine-3-carboxylic acid* (HYNIC-Boc-NHS)was first synthesized following a reported procedure [94]. Subsequently, synthesis of*11C-FA-HYNIC-Boc, 12C-FA-HYNIC-Boc, 11C-FA-HYNIC and 12C-FA-HYNIC was carried out.* Synthesis schemes for these compounds are shown in Fig. 3.9 – Fig. 3.13. Following are the details of synthesis procedure carried out for the above mentioned compounds.

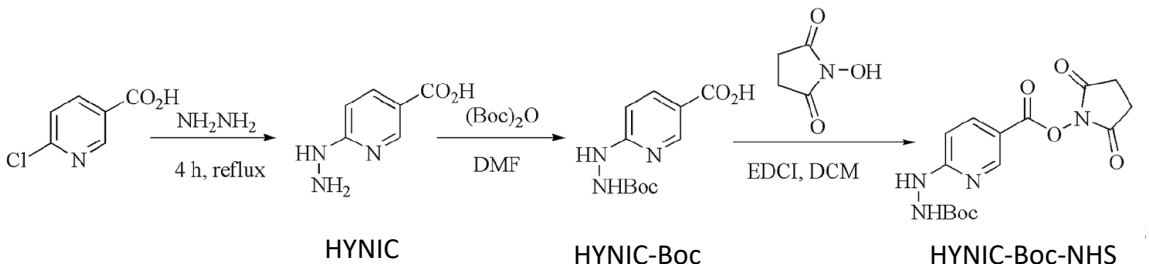

Fig. 3.9 *Synthesis scheme for HYNIC-Boc-NHS*

3.2.2.1 Synthesis of 6-Hydrazinopyridine-3-carboxylic acid (HYNIC)

6-Chloronicotinic acid (4.0 g; 25.38 mmol) was added to 80% hydrazine hydrate (17.5 ml; 465.0 mmol) in a round bottom flask. The mixture was placed in a 100°C oil bath for 4 hr. The obtained reaction mixture was cooled to ambient temperature followed by concentrated to dryness to give a white solid. The solid was further dissolved in water and subsequently acidify to pH 5.5 with concentrated hydrochloric acid. A precipitate was formed after acidification. The precipitate was filtered and the solid obtained was washed with 95% ethanol and ether and dried in *vacuo*.

Yield 77% (3 g); m.p. 292-293^{o}C; ^{1}H NMR δ_H: 6.69 (d, J = 8 Hz, 1 H), 7.84 (dd, J = 2.4, 8.8 Hz, 1 H), 8.5 1 (d, J = 2.4 Hz, 1 H).

3.2.2.2 Synthesis of 6-Boc-hydrazinopyridine-3-carboxylic acid (HYNIC-Boc)

A solutioncontaining*6-hydrazinopyridine-3-carboxylic acid* (HYNIC) (0.7 g; 4.9 mmol) and *triethyl amine* (0.6 ml; 5.9mmol) in DMF (10 ml) was added with di-tert-butydicarbonate (1.07 g; 4.9mmol) and stirred at room temperature. The reaction mixture became homogeneous after 1 hr. Stirring was continued for 16 hr at room temperature. Subsequently, the reaction mixture was concentrated to dryness under vacuum to give a brown colour solid. This residue was dissolved in a minimum amount of ethyl acetate and passed through glass column filled with silica gel 60 (230-400 mesh) using ethyl acetate as eluant to remove colored impurities. The eluate was concentrated to dryness to give the desired product (HYNIC-Boc). The obtained product was used without further purification. Yield: 94% (2.33g). ^{1}H NMR δ_H: 1.40 (s, 9 H), 6.52 (d, J = 8.8 Hz, 1 H), 7.97 (dd, J = 2.4, 8.8 Hz, 1 H), 8.58 (d, J = 2.4, l H).

3.2.2.3 Synthesis of Succinimidyl 6-BOC-hydrazinopyridine-3-carboxylic acid (HYNIC-Boc-NHS)

A solution containing *6-BOC-hydrazinopyridine-3-carboxylic acid* (HYNIC-Boc) (0.73 g; 2.88 mmol) and N-hydroxysuccinimide (0.33 g; 2.88 mmol) in DMF (10 ml) was added with a solution of dicyclohexylcarbodiimide (0.59 g; 2.88 mmol) in DMF (5 ml) and stirred at room temperature. This reaction mixturebecame cloudy after 1 hr and stirring was continued for 16 hr at roomtemperature. The reaction mixture was filtered and the filtrate was concentrated todryness to give a brown residue. The residue was dissolved in a minimum amount of ethyl acetate and purified by a column silica gel 60 (230-400 mesh) and using ethyl acetate as an eluant. The obtained eluate was concentrated to dryness to give 0.6 g of a yellow solid.The obtained solid was further purified by recrystallization in ethyl acetate/ hexanes. Yield 60%; m.p. 169 -172°C; ^{1}H NMR δ_H: 1.41 (s, 9 H), 2.87 (s, 4 H), 6.64 (d, J = 8.8 Hz, 1 H), 8.08 (dd, 2.4, 8.8 Hz, 1 H), 8.73 (d, J = 2.4 Hz, l H).

3.2.2.4 Synthesis 11-(6-Boc-hydrazinopyridine-3-amido) undecanoic acid (1b)

A mixture of ω-amino acid (1a) (100 mg, 0.5 mmol), triethylamine (150 mg, 1.5 mmol) and succinimidyl 6-Boc-hydrazinopyridine-3-carboxylic acid (126 mg, 0.5 mmol) in DMF (5 mL) was stirred overnight at room temperature. Upon completion of the reaction (cf. TLC), the reaction mixture was concentrated *in vacuo* and the crude product obtained was further purified by silica gel column chromatography eluting with ethyl acetate. The chemical purity of the compound was estimated by ^{1}H-NMR.

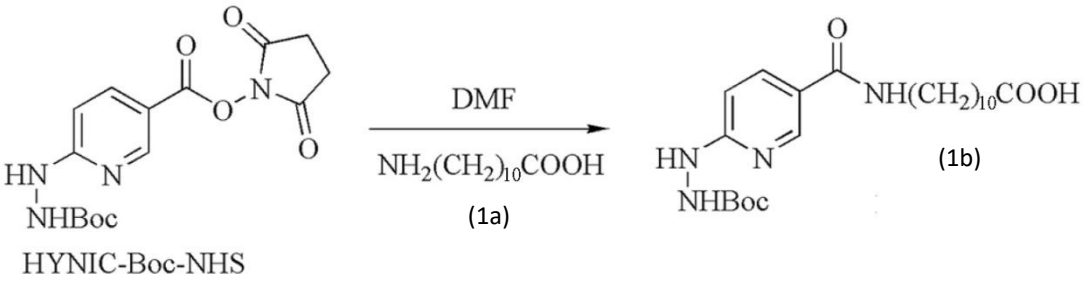

Fig. 3.10 *Synthesis of 11C-FA-HYNIC-Boc*

Yield: 80% (174 mg), R_f (ethyl acetate) = 0.4, purity > 95%.

IR (neat, cm^{-1}): 3295 (b); 2926 (s); 2854 (s); 1704 (b); 1635 (s); 1537 (s); 1474 (m); 1368 (w); 1276 (w); 1163 (s).

δ_H (300 MHz; CD_3OD; Me_4Si) 8.53 (1H, s, pyridine 2-H); 7.99 (1H, d, pyridine 4-H, $J_{4,5}$ = 9 Hz); 6.70 (1H, d, pyridine 5-H, $J_{4,5}$= 9 Hz); 3.3–3.4 (2H, m, –$CH_2C\underline{H}_2NHCO$–); 2.02–2.36 (2H, m,–$CH_2C\underline{H}_2COOH$); 1.54–1.70 (4H, m, –$C\underline{H}_2CH_2NHCO$– & –$C\underline{H}_2$-CH_2COOH); 1.48 (9H, s, $(C\underline{H}_3)_3C$–); 1.2–1.42 (12H, m, $(C\underline{H}_2)_6$).

δ_C (500 MHz; DMSO-D_6; Me_4Si) 165.25 (CONH); 161.986(NH–C–N); 156.26 (NH–COO); 148.15(N]$\underline{C}$2–C); 136.98 (C]$\underline{C}$ 4–C); 121.14 ($\underline{C}$–CONH); 104.99 (C=$\underline{C}$5–C); 79.57 ($(CH_3)_3\underline{C}$–); 49.05 (–$CH_2\underline{C}H_2NHCO$–); 29.65, 29.47, 29.41, 29.26, 28.56,27.76, 26.96, 25.78 ($(CH_2)_8$ and $(\underline{C}H_3)_3C$).

ESI-MS (+ve mode): mass (calculated) 11C-HYNIC-Boc conjugate [$C_{22}H_{36}N_4O_5$] 436.3; m/z (observed) 437.1.

3.2.2.5 Synthesis 12-(6-Boc-hydrazinopyridine-3-amido) undecanoic acid (2b)

Synthesis of 12-(6-Boc-hydrazinopyridine-3-amido)undecanoic acid was carried out in similar fashion as shown in section 3.2.2.2 and taking108 mg (0.5 mmol) of ω-amino acid (1b). The chemical purity of the final compound was estimated by ^{1}H-NMR.

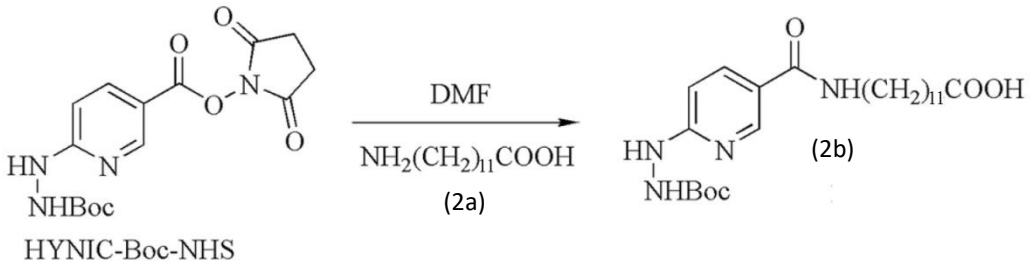

Fig. 3.11 *Synthesis scheme of 12C-FA-HYNIC-Boc*

Yield: 75% (168 mg), R_f (ethyl acetate) = 0.4, purity > 95%.

IR (neat, cm ^{1}): 3290 (b); 2913 (s); 2849 (s); 1696 (b); 1633 (s); 1539 (w); 1462 (m); 1260 (w); 1150 (w).

δ_H (300 MHz; CD_3OD; Me_4Si) 8.53 (1H, s, pyridine 2-H); 7.99 (1H, d, pyridine 4-H, $J_{4,5}$ = 8.4 Hz); 6.70 (1H, d, pyridine 5H, $J_{4,5}$= 8.4 Hz); 3.32–3.44 (2H, m, $–CH_2C\underline{H}_2NHCO–$); 2.01–2.35 (2H, m, $–CH_2C\underline{H}_2COOH$); 1.52–1.70 (4H, m, $–C\underline{H}_2CH_2NHCO–$ & $–C\underline{H}_2CH_2COOH$); 1.48 (9H, s, $(C\underline{H}_3)_3C–$); 1.16–1.42 (14H, m,$(C\underline{H}_2)_7$).

δ_C (500 MHz; DMSO-D_6; Me_4Si) 165.25 (CONH); 161.986 (NH–C–N); 156.26 (NH–COO); 148.15(N]C2–C); 136.98 (C]C 4–C); 121.14 (C–CONH); 104.99 (C]C5–C); 79.57 ($(CH_3)_3C–$); 49.05 ($–CH_2CH_2NHCO–$); 29.65, 29.47, 29.41, 29.26, 28.56,27.76, 26.96, 25.78 ($(CH_2)_9$ and $(CH_3)_3C$).

ESI-MS (+ve mode): mass (calculated) 12C-HYNIC-Boc conjugate [$C_{23}H_{38}N_4O_5$] 450.2; m/z (observed) 451.1.

3.2.2.6 Synthesis of11-(6-Hydrazinopyridine-3-amido)undecanoic acid (1c)

Compound 1b/2b (0.1 mmol) was stirred with TFA (2 mL) for 2 h at room temperature. The solvent was removed *in vacuo* to give the desired product 1c/2c. The product was used as such without further purification. The chemical purity of the compound was estimated by ^{1}H-NMR.

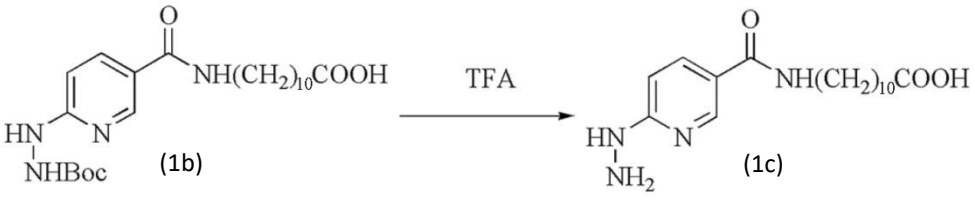

Fig. 3.12*Synthesis scheme of 11C-FA-HYNIC*

Yield: quantitative (33 mg), purity > 90%.

δ_H (300 MHz; CD_3OD; Me_4Si) 8.52 (1H, d, pyridine 2-H, $J_{1,4}$ = 1.8 Hz); 8.09 (1H, dd, pyridine 4-H, $J_{4,5}$ = 9 Hz & $J_{1,4}$ = 1.8 Hz);6.84 (1H, d, pyridine 5-H, $J_{4,5}$ = 9 Hz); 3.3–3.42 (2H, m, –CH_2-C$\underline{H}_2$NHCO–); 2.27 (2H, t, –$CH_2C\underline{H}_2$COOH, J = 7.2 Hz); 1.5–1.72 (4H, m, –$C\underline{H}_2CH_2\bar{N}H$CO– & –$C\underline{H}_2CH_2$COOH); 1.18–1.44 (12H, m, $(C\underline{H}_2)_6$).

δ_C (300 MHz; DMSO-D_6; Me_4Si) 174.45 (COOH); 164.88 (CONH); 159 (NH–C–N); 156.57 (NH–COO); 146.73 (N=$\underline{C}$2–C); 137.02 (C=$\underline{C}$4–C); 122.09 ($\underline{C}$–CONH); 106.35 (C=$\underline{C}$5–C); 51.73 (–$CH_2\underline{C}H_2$NHCO–); 29.98, 29.43, 29.38, 29.25, 29.21, 29.01, 26.95, 24.49 $(\underline{C}H_2)_8$.

ESI-MS (+ve mode): mass (calculated) 11C-HYNIC conjugate [$C_{17}H_{28}N_4O_3$] 336.2; m/z (observed) 337.8.

3.2.2.7 Synthesis of 12-(6-Hydrazinopyridine-3-amido)undecanoic acid (2c)

Similar procedure was carried out for the synthesis of 12C-FA-HYNIC as mentioned in section 3.2.2.4.The chemical purity of the final compound was estimated by ^{1}H-NMR.

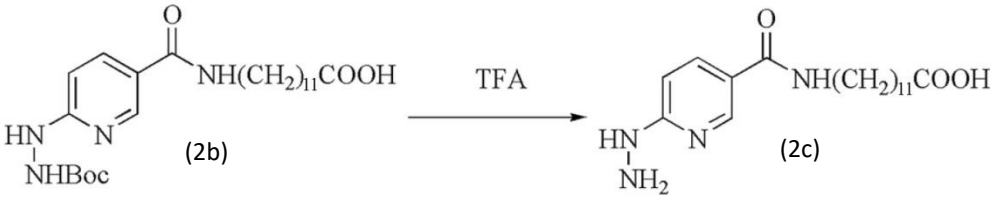

Fig. 3.13 *Synthesis scheme of 12C-FA-HYNIC*

Yield: quantitative (47 mg), purity > 92%.

δ_H (300 MHz; CD_3OD; Me_4Si) 8.40 (1H, d, pyridine 2-H, $J_{1,4}$ = 1.5 Hz); 8.18 (1H, dd, pyridine 4-H, $J_{4,5}$ = 9.3 Hz & J = 1.5 Hz);6.96 (1H, d, pyridine 5-H, $J_{4,5}$ = 9.3 Hz); 3.32–3.42 (2H, m, –$CH_2C\underline{H}_2$NHCO–); 2.27 (2H, t, –$CH_2C\underline{H}_2$COOH, J = 7.2 Hz); 1.50–1.68 (4H, m, –$C\underline{H}_2CH_2$NHCO– & –$C\underline{H}_2CH_2$COOH); 1.22–1.44 (14H, m, $(C\underline{H}_2)_7$).

δ_C (300 MHz; DMSO-D_6; Me_4Si) 174.95 (COOH); 164.88 (CONH); 159 (NH–C–N); 156.57 (NH–COO); 147.30(N=$\underline{C}$2–C); 137.44 (C=$\underline{C}$4–C); 122.09 ($\underline{C}$–CONH); 106.79

(C=C5–C); 51.73 (–CH_2CH_2NHCO–); 30.42, 29.60, 29.43, 29.38, 29.25, 29.21, 29.01, 26.95, 24.49 $(CH_2)_9$.

ESI-MS (+ve mode): mass (calculated) 12C–HYNIC conjugate [$C_{18}H_{29}N_4O_3Na$] 372.2; m/z (observed) 373.7.

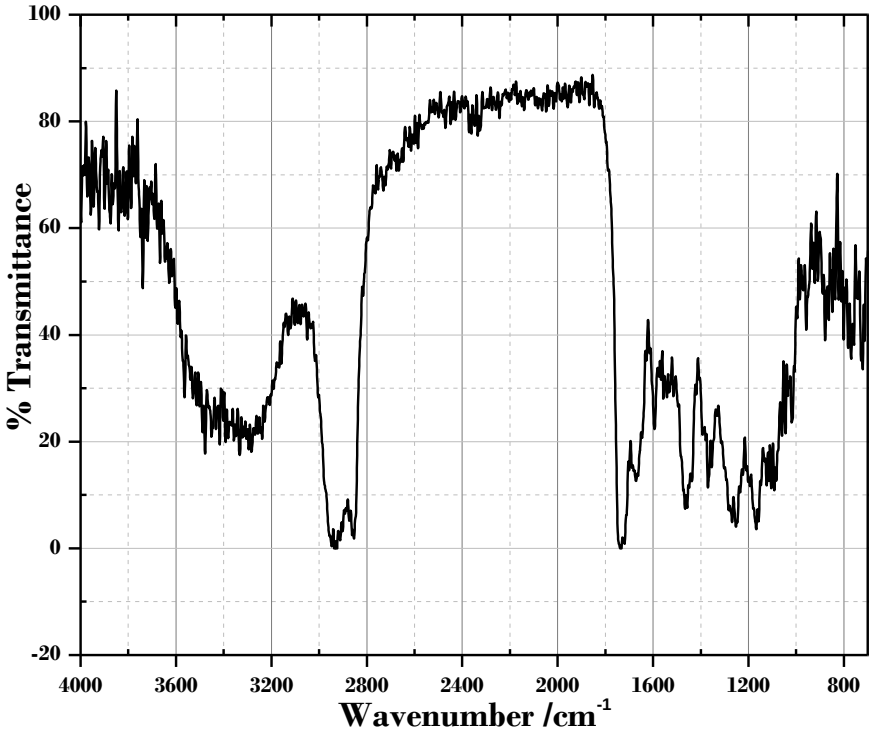

Fig. 3.14(a) *IR Spectrum of 11C-FA-HYNIC-Boc*

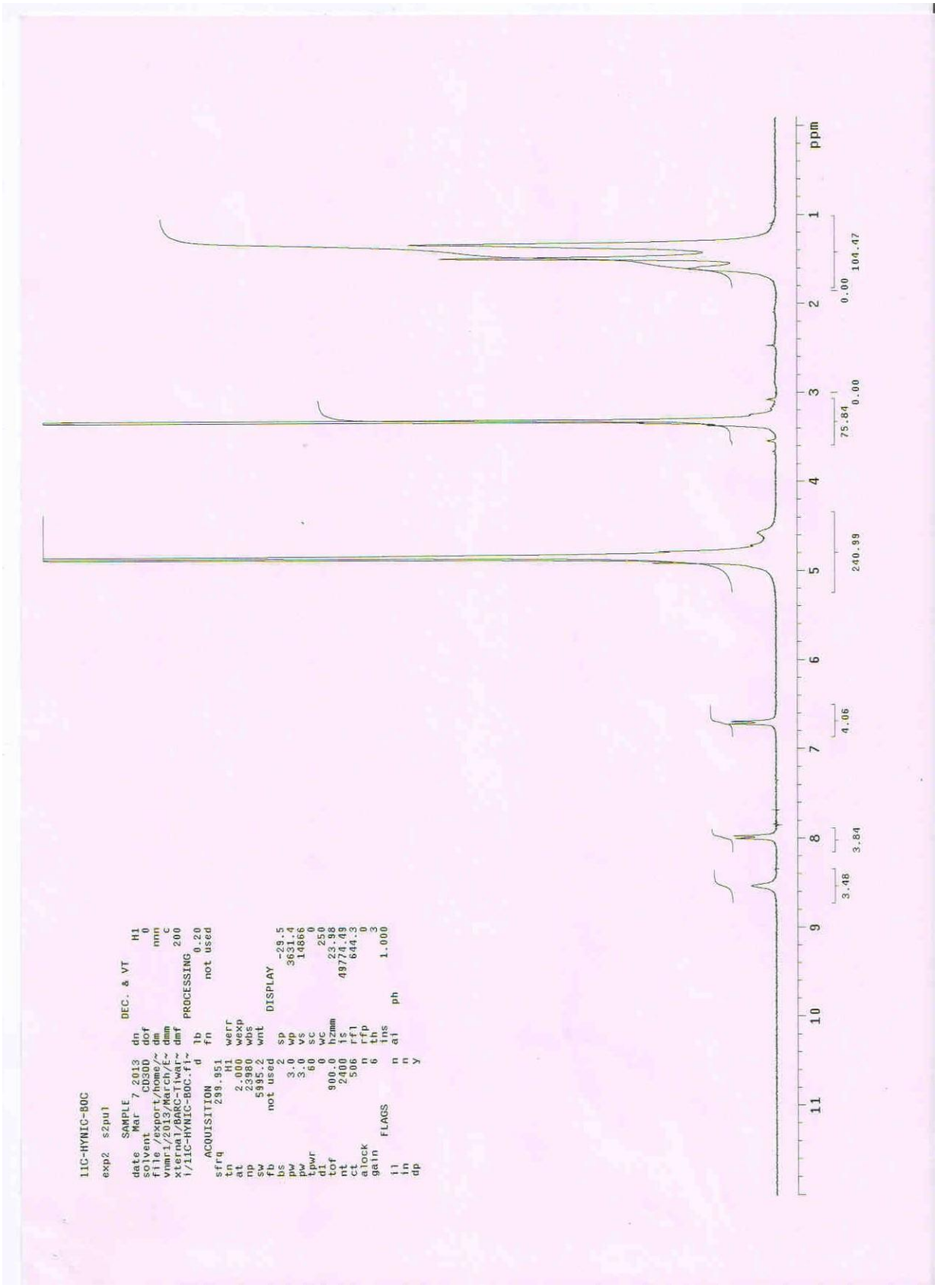

Fig. 3.14 (b) *^{1}H NMR Spectrum of 11C-FA-HYNIC-Boc*

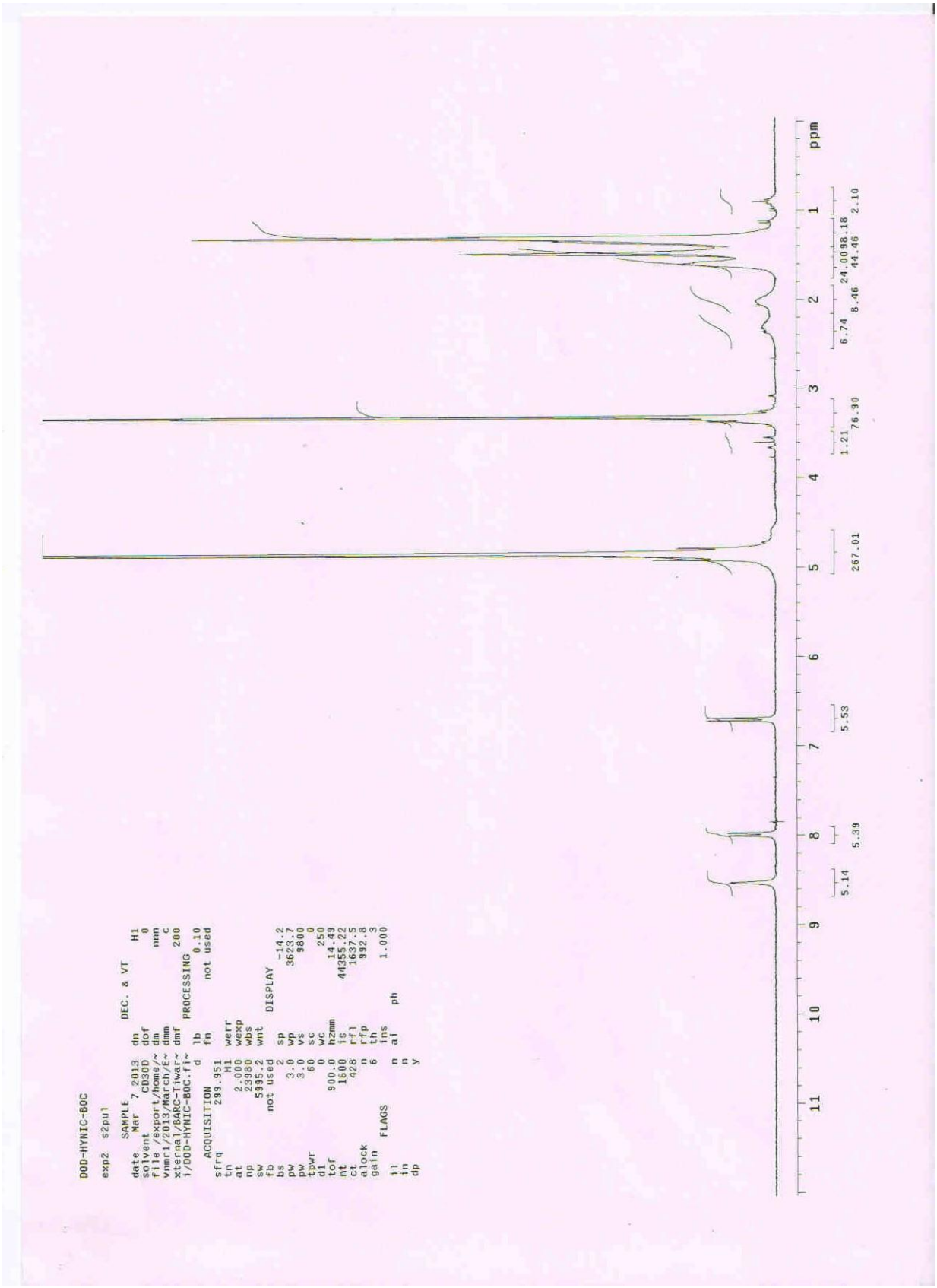

Fig. 3.15 *^{1}H NMR Spectrum of 12C-FA-HYNIC-Boc*

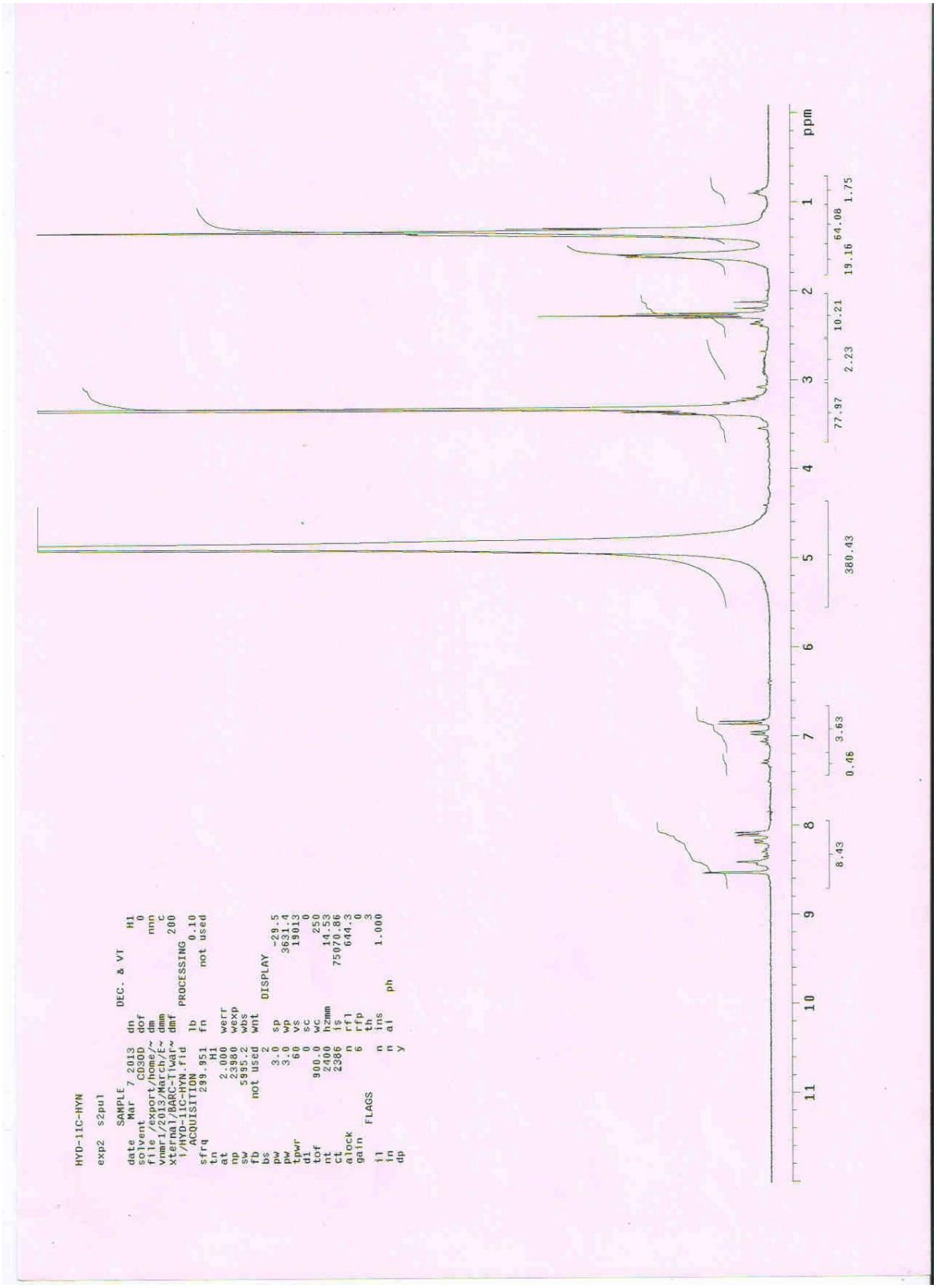

Fig. 3.16 *^{1}H NMR Spectrum of 11C-FA-HYNIC*

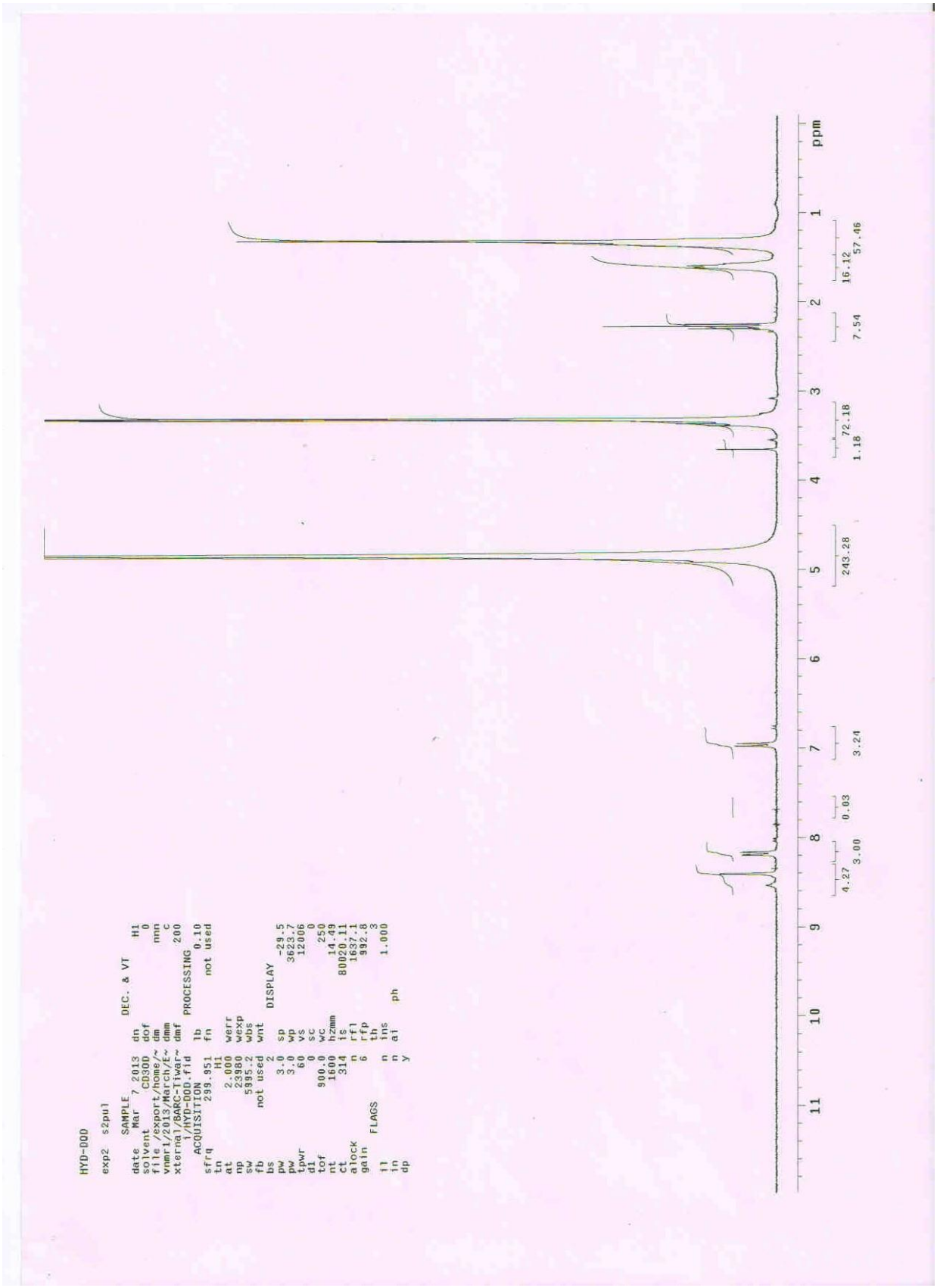

Fig. 3.17 *^{1}H NMR Spectrum of 12C-FA-HYNIC*

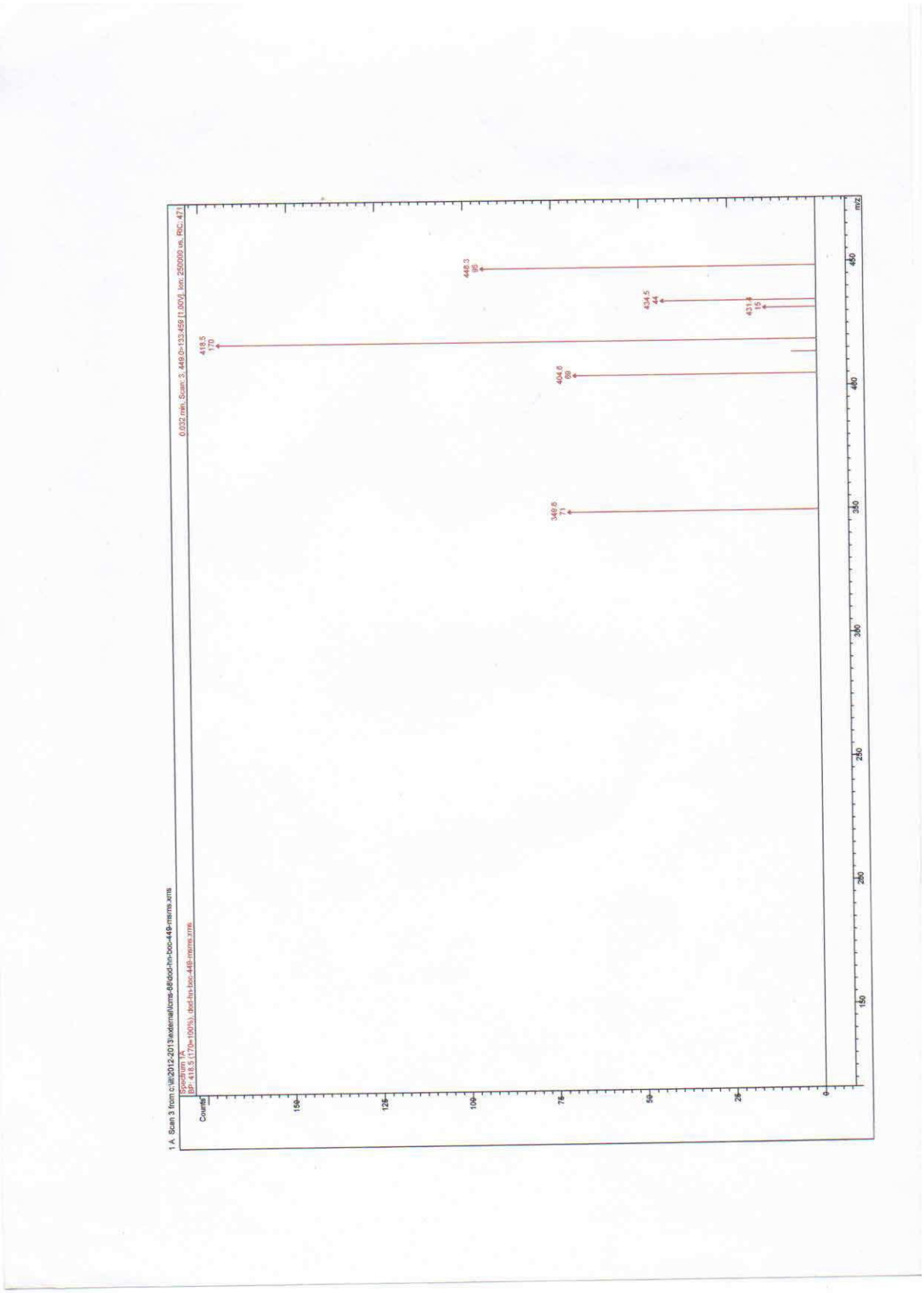

Fig. 3.18 *Mass Spectrum of 12C-FA-HYNIC-Boc*

3.2.3 Radiolabeling

Radiolabeling of 11C-FA-HYNIC and 12C-FA-HYNIC with ^{99m}Tc was carried out using tricine, EDDA and TPPTS as co-ligands. Radiolabeling schemes are depicted in Fig. 3.19 to Fig. 3.21. Details of procedure followed are as following.

3.2.3.1 Preparation of11C/12C-FA-HYNIC-^{99m}Tc-tricine complex (1d/2d)

Freshly eluted $^{99m}TcO_4$ (10–25 mCi, 0.5 mL) was added to a vial containing fatty acid-HYNIC conjugate (**1c** or **2c**, 3–5 mg) in methanol (200 μL), $SnCl_2{\cdot}2H_2O$ (100 mg) in 0.1 N HCl (100 μL) and tricine (40 mg) in water (0.5 mL). The sealed vial was heated in a boiling water bath for 30 min. The vial was then cooled to room temperature and the complex formed was analyzed by HPLC.

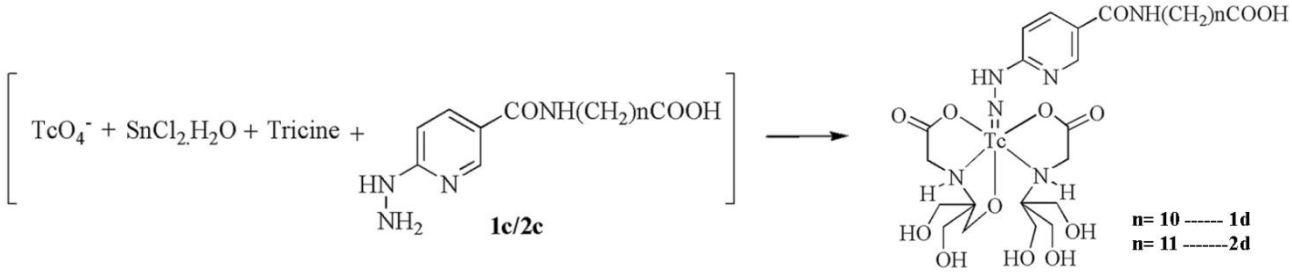

Fig. 3.19*Radiolabelingscheme with ^{99m}TcusingTricine ligand*

3.2.3.2 Preparation 11C/12C-FA-HYNIC-^{99m}Tc-EDDA complex (1e/2e)

Freshly eluted $^{99m}TcO_4$ (10–25 mCi, 0.5 mL) was added to a vial containing a mixture of fatty acid-HYNIC conjugate (**1c** or **2c**, 3–5 mg) in methanol (500 μL), $SnCl_2{\cdot}2H_2O$ (100 mg) in 0.1 N HCl (100 μL), tricine (40 mg) dissolved in water (0.3 mL) and EDDA (10 mg) dissolved in water (0.3 mL) for preparing complexes **1e/2e**. After cooling the vial to room temperature, the complexes 1e/2e were analyzed by HPLC.

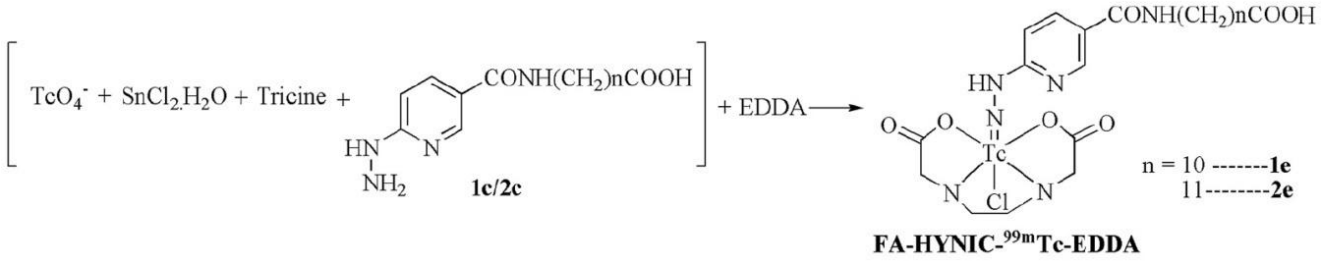

Fig. 3.20 *Radiolabelingwith ^{99m}Tc using Tricine/ EDDA as ligands*

3.2.3.3 Preparation 11C/12C-FA-HYNIC-^{99m}Tc-TPPTS/tricine complex (1f/2f)

Freshly eluted $^{99m}TcO_4$ (10–25 mCi, 0.5 mL) was added to a vial containing a mixture of fatty acid-HYNIC conjugate (**1c** or **2c**, 3–5 mg) in methanol (500 μL), $SnCl_2 \cdot 2H_2O$ (100 mg) in 0.1 N HCl (100 μL), tricine (40 mg) dissolved in water (0.3 mL) and TPPTS (2–3 mg) dissolved in water (0.3 mL). The vial was sealed and the reaction mixture was heated in a boiling water bath for 30 min. After cooling the vial to room temperature, the complexes **1f/2f** were analyzed by HPLC.

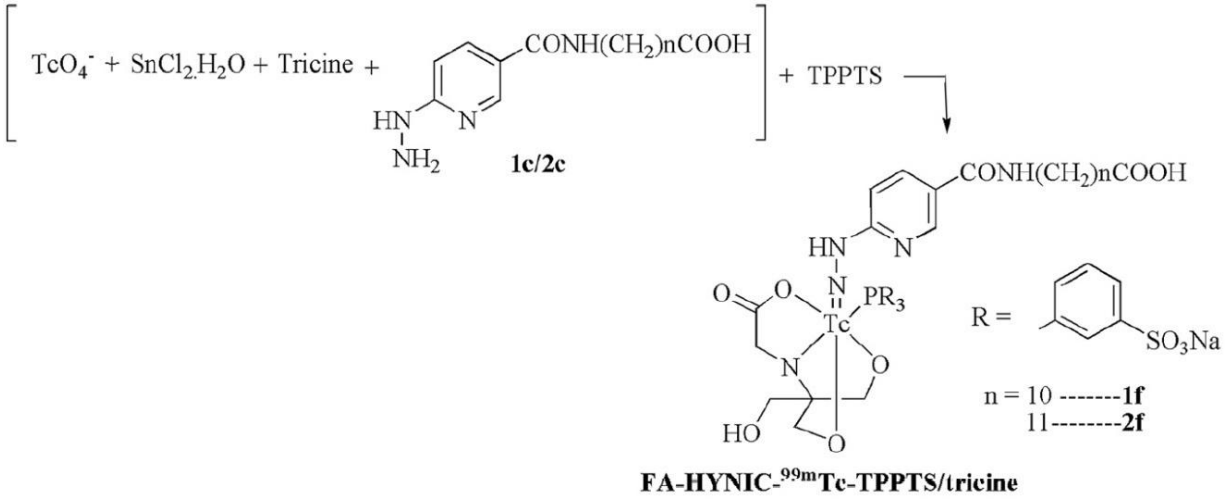

Fig. 3.21 *Radiolabeling with ^{99m}Tcusing TPPTS/ Tricine as ligands*

3.2.4 Quality control

3.2.4.1 HPLC Analysis

The radiochemical purity (RCP) of the ^{99m}Tc-fatty acid complexes (**1e/2e** and **1f/2f**) was determined by reversed phase HPLC. Two gradient elution solvent systems were used for unambiguous analysis of the reaction mixture. The first solvent system involved ammonium acetate buffer (0.38%, solvent A) and methanol (solvent B) as the mobile phase. Gradient elution program followed with this solvent system was, 0 min 50% A, 10 min 0% A, 30 min 0% A. All four complexes were analyzed using this solvent system. The second solvent system involved, water (0.1% TFA) (A) and methanol (0.1% TFA) (B) with the following gradient elution program; 0 min 90% A, 30 min 0% A, 50 min 0% A. Flow rate of the solvent was maintained at 1 mL min^{-1}. Test solution (20 μL) was injected into the column using a micro-syringe and elution was monitored by radioactivity profile.

The same C-18 reversed phase analytical column was used for the purification of the complexes (**1e/2e** and **1f/2f**). Fraction containing the required fatty acid complex was collected in a clean vial and after removing the solvent, residue was reconstituted in 10% aqueous ethanol. About 18.5 MBq (500 μCi) of pure radiolabeled fatty acid complex was obtained by this method that was used for subsequent *in vitro* and *in vivo* studies. For imaging studies, however, the HPLC purified fatty acid complex was reconstituted in minimum volume of 6% HSA instead of 10% aqueous ethanol.

3.2.4.2 Partition coefficient (log $P_{o/w}$)

The HPLC purified complex (0.1 mL, 185 KBq/5 μCi) was mixed with double distilled water (0.9 mL) and n-octanol (1 mL) and vortexed for 3 min. The mixture was then centrifuged at 3500g for 5 min to effect clear separation of the two layers. Equal aliquots

from the two layers were withdrawn in triplicates and measured for associated radioactivity. The readings thus obtained were used to calculate the log $P_{o/w}$ value (octanol–water partition) of the complex.

3.2.4.3 Determination of serum stability and protein association

The purified fatty acid complex (50 μL, 370 KBq/10 μCi) was incubated in human serum (450 μL) at 37^{o}C for 30 min. Thereafter, the serum proteins were precipitated by addition of ethanol (500 μL). The solution was centrifuged and the supernatant was analyzed by HPLC to ascertain the stability of the complex in serum. The precipitate was washed twice with ethanol and the activity associated with precipitate was expressed as a percent of the initial activity (370 KBq/ 10 μCi).

3.2.4.4 Enzymatic activation of fatty acid complexes

The activation of a representative ^{99m}Tc-fatty acid complex, **2e**, by acyl-CoA synthetase was carried out using liver cell extracts obtained from normal Swiss mouse. Normal Swiss mice (2 nos.) were sacrificed and the liver was perfused with phosphate buffered saline (pH 7.4, 20 mL). Thereafter, the liver was excised, frozen in liquid nitrogen and homogenized using Tris– HCl. The cell extracts thus obtained was used for the activation of radiolabeled fatty acid. Activation reaction mixture consisted of HPLC purified complex **2e** (7.4 MBq/200 μCi in 10% aqueous ethanol), 200 mM Tris–HCl (pH 7.5), 8 mM $MgCl_2$, 2 mM EDTA, 20 mM sodium chloride, 0.2 mM dithiothreitol, 1.0 mM ATP and 1.0 mM CoA. Total volume of the reaction mixture was 1 mL. The reaction was carried out at 37^{o}C for 30 min and ceased by addition of a mixture containing 2-propanol, hexane and 1 N H_2SO_4 (40:10:1; 1 mL). Subsequently, the reaction mixture was

centrifuged and the supernatant was transferred into a separate vial. The supernatant was evaporated to dryness, reconstituted in water (0.5 mL) and analyzed by HPLC.

3.2.5 Bio-distribution studies on Swiss mice

All procedures performed herein were in accordance with the national laws pertaining to the conduct of animal experiments. Normal female Swiss mice (20– 25 g body weight) were used for the in vivo distribution studies. The mice were kept fasting for 6–7 h prior to the experiment. Water was given *ad libitum*. The HPLC purified radiolabeled preparation (100 μL, 740 KBq/20 μCi) was administered intravenously through tail vein of each mouse. Individual sets of animals (n = 3) were utilized for studying distribution at different time points (2 min, 5 min, 10 min and 30 min). At the end of each time point, respective set of animals were sacrificed and the relevant organs and tissue were excised for the measurement of associated activity. The organs were weighed and the activity associated with each organ was measured in a flat-bed type NaI(Tl) counter with suitable energy window for ^{99m}Tc (140 keV$\pm$10%). The activity associated with each organ/ tissue was expressed as a percent injected dose per gram (% ID per g).

3.2.6 Liver metabolite analysis

One hour after intravenous administration of the radiolabeled fatty acid (**2e**, 200 μL, 74 MBq/2 mCi) into normal mice (2 animals), the animals were sacrificed and liver tissue perfused using phosphate buffered saline (20 mL). Thereafter liver was excised, frozen in liquid nitrogen and homogenized using ethanol. The ethanol slurry was centrifuged at 10000g for 20 min and the supernatant obtained was analyzed using HPLC.

3.2.7 SPECT imaging using 12C-FA-HYNIC-^{99m}Tc-EDDA complex

Normal female Swiss mice (n = 2, 20–25 g body weight) were used for the *in vivo* imaging with fatty acid complex **2e**. The animals were fasted for 4–6 h prior to the experiment. Just before the experiment, the animals were anaesthetized by inhalation of isoflurane/oxygen mixture [3% isoflurane/97% oxygen (v/v) for induction of anesthesia (2–4 min), 2% isoflurane/ 98% oxygen (v/v) for maintaining anesthesia] maintained at a flow rate of 1L min^{-1}. A catheter with 34G needle was inserted into the tail vein of the animal and the animal was appropriately positioned in the SPECT camera. About 100–150 μL(11MBq/300 μCi) of the radiolabeled preparation (**2e**) was administered intravenously and whole body images were acquired till 15 min post-injection (p.i.) using Low Energy General Purpose (LEGP) collimator. Dynamic images were acquired at a rate of one frame every 30 s. The SPECT images were reconstructed using 2D MLEM reconstruction option using 30 iterations. The data was viewed and analyzed in PMOD data analysis and quantization software (PMOD Technologies). The washout dynamics of the tracer from the myocardium and background organs was obtained by marking a region of interest (ROI) and observing the clearance pattern in the marked ROI over the complete period of study.

3.5 Results and discussion

3.5.1 Synthesis and spectroscopy

Two fatty acids of intermediate chain lengths (11 and 12 carbon) were synthetically modified with HYNIC bifunctional chelator at the ω-position to facilitate radiolabeling with ^{99m}Tc. Overall scheme for the synthesis of fatty acid-HYNIC conjugates (1 and 2) is shown in Fig. 3.22. Succinimidyl 6-Boc-hydrazinopyridine-3-carboxylic acid (HYNIC-Boc-NHS) synthesized in the first step, following a reported procedure [94], was coupled

to the amine group at ω-position of the fatty acid (**1a/2a**) to yield the Boc-protected fatty acid-HYNIC conjugates (**1b/2b**). Subsequently, by removing the Boc-protection, target ligands (1/2) were obtained. All the intermediates and final conjugates were characterized by FT-IR, ^{1}H-NMR and ESI-MS. ^{1}H-NMR of the intermediates as well as the target ligand was consistent with the expected structure and ESI-MS provided additional confirmatory evidence for the formation of the expected ligand.

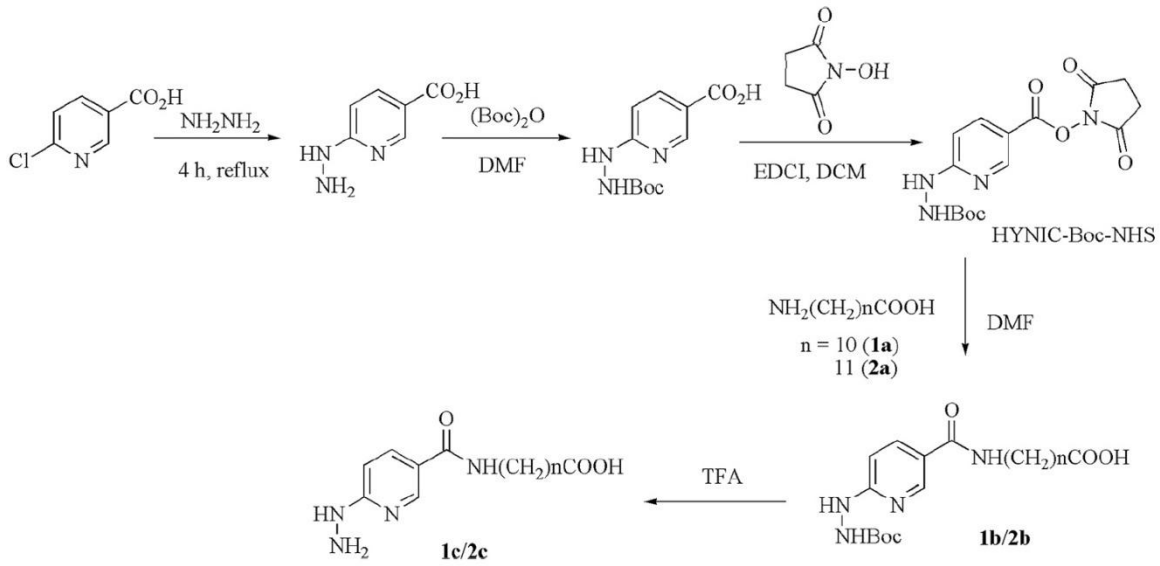

Fig. 3.22 *Synthesis scheme of HYNIC-fatty acid conjugates (1c/2c)*

3.5.2 Radiolabeling with ^{99m}Tc and HPLC analysis

Fatty acid-HYNIC conjugates (**1/2**) were subsequently radiolabeled with ^{99m}Tc, following the protocol mentioned in the experimental section. Since HYNIC ligand coordinates to ^{99m}Tc in a mono-dentate fashion, presence of co-ligands are necessary to complete the co-ordination sphere of the metal to achieve stability. Though a number of co-ligands have been identified for stabilizing the HYNIC complex [114], in the present study tricine, EDDA and TPPTS were used as co-ligands. The overall scheme for the preparation of fatty acid-HYNIC-^{99m}Tc complexes is shown in Fig. 3.23. With the set of two fatty acid-

HYNIC conjugates and the above co-ligands, a total of six ^{99m}Tc-fatty acid complexes are prepared (**1d/2d, 1e/2e and 1f/2f**). The complexes were subsequently analyzed by HPLC (Fig. 3.25). The only tricine complex is known to exhibit low stability in solution [114], and was therefore not evaluated for its biological behavior [116]. Nevertheless, HPLC characterization of **1d/2d** confirmed the separate identity of these intermediate tricine complexes, which was different from that of the final complexes **1e/2e** and **1f/2f**. This characterization is essential as formation of EDDA/TPPTS complexes is via the tricine intermediate complex. It was observed that using ammonium acetate buffer and methanol as mobile phase, TPPTS complexes (**1f/2f**) eluted out early, nearlymatching with the elution profile of ^{99m}Tc-pertechnetate (Fig. 3.25). To differentiate **1f/2f** from $^{99m}TcO_4^-$, a second solventsystem involving water and methanol was used. Though, the HPLC pattern observed using latter solvent system conclusively differentiated between $^{99m}TcO_4^-$ and the complexes **1f/2f**, the complexes appeared as multiple peaks which otherwise eluted as a single sharp peak in ammonium acetate buffer–methanol system (Fig.3.24). However, similar effects of solvent on elution profile have been observed earlier [111]. The radiochemical purity of the four complexes, determined from the peak area measurements of the HPLC elution profile were found to be **1e** (76%, Sp. Act. 6.3 mCi mg^{-1})/**2e** (83%, Sp. Act. 5.2 mCi mg^{-1}) and **1f** (78%, Sp. Act. 2.6 mCi mg^{-1})/**2f** (88%, Sp. Act. 3.5 mCi mg^{-1}). All the four ^{99m}Tc-HYNIC-fatty acid complexes (**1e/2e** and **1f/2f**) were purified by analytical HPLC using ammonium acetate buffer-methanol system before using for further biological studies.

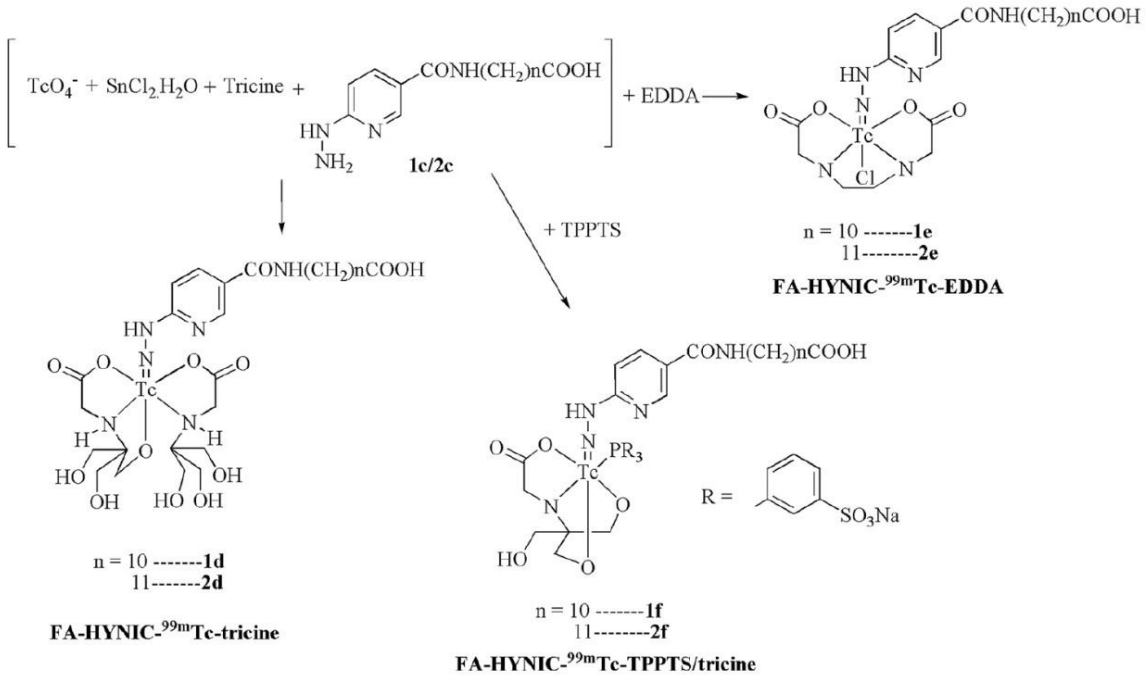

Fig. 3.23 *Radiolabeling scheme of HYNIC-fatty acid conjugates (1c/2c) with* ^{99m}Tc

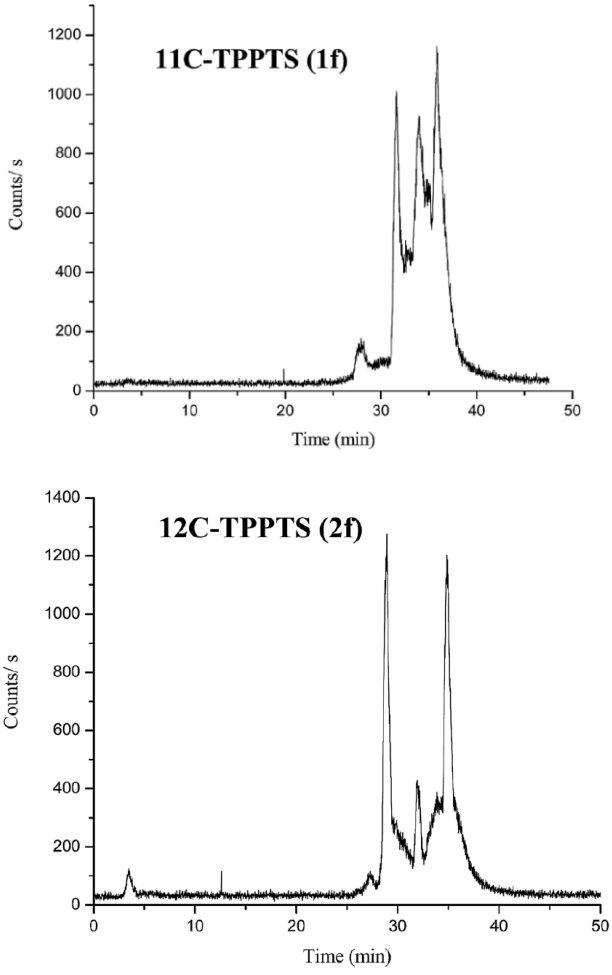

Fig. 3.24 *HPLC chromatograms of* ^{99m}Tc*-HYNIC-fatty acid-TPPTS complexes (1f/2f) in water: methanol*

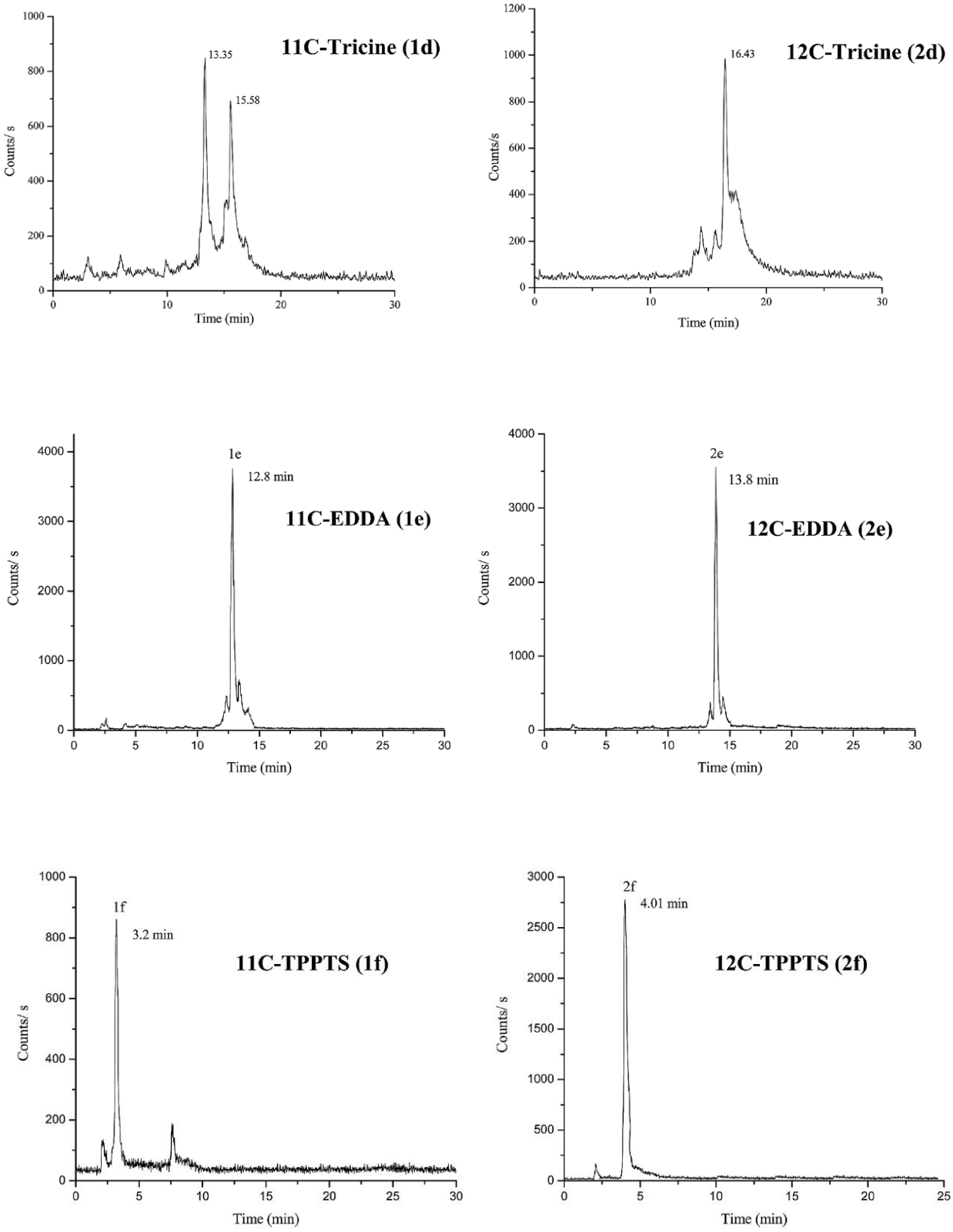

Fig. 3.25 *HPLC chromatograms of* ^{99m}*Tc-HYNIC-fatty acid complexes (1d/2d, 1e/2e and 1f/2f).*

3.5.3 Partition coefficient (Log $P_{O/W}$)

Fatty acids enter myocytes through passive diffusion or CD36 protein mediated active transport [87]. Fatty acid transport by passive diffusion depends on its lipophilicity. To obtain a measure of lipophilicity of the complexes (**1e/2e**, **1f/2f**) their partition coefficient, log $P_{o/w}$, was determined using octanol-water system and following a reported procedure [117]. The log $P_{o/w}$ obtained for the four complexes is shown in Table 3.1. It is not surprising to observethat there is strong correlation between the fatty acid chain length and lipophilicity (log $P_{o/w}$) of the ^{99m}Tc-complexes.

Table 3.1 *Partition coefficient of the FA-HYNIC-^{99m}Tc Complexesalong with their retention time in HPLC*

^{99m}Tc complexes	log $P_{O/W}$	t_R (min)
11C-EDDA (le)	1.85	12.8
11C-TPPTS/tricine (1f)	-0.31	3.2
12C-EDDA (2e)	2.05	13.8
12C-TPPTS/tricine (2f)	-0.12	4.1

3.5.4 Comparison of serum stability of radiolabeled complexes

The stability of HPLC purified ^{99m}Tc-fatty acid complexes (**1e/2e** and **1f/2f**) in human serum was tested by incubating the complexes in serum for 30 min. The HPLC chromatogram of the supernatant obtained after the precipitation of serum proteins showed no signs of degradation of the complex (RCP of all four complexes was >90%, Fig. 3.26). About 20% of the activity was found associated with the serum proteins. Weak interaction between fatty acids and serum proteins are known and considered responsible for its solubility and transport *in vivo*.

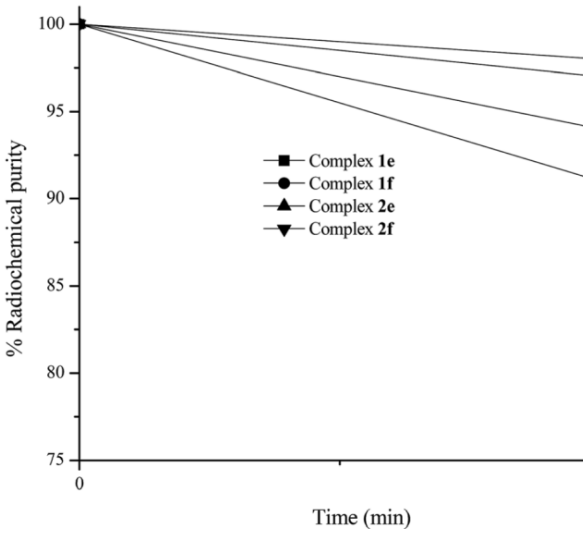

Fig. 3.26 *Serum stability of ^{99m}Tc-HYNIC-fatty acid complexes (1e/2e and 1f/2f)*

3.5.5 Activation by acyl-CoA synthetase enzyme

Fatty acids once transported inside the myocytes get activated by acyl-CoA synthetase to FA-CoA ester in presence of ATP. Fig. 3.27 and Fig. 3.28 are showing the HPLC chromatograms of pure ^{99m}Tc-complex and activity in aqueous extract obtained after protein precipitation respectively. The HPLC chromatograms clearly indicate transformation of the parent ^{99m}Tc-FA complex (**2e**) in cell extracts containing acyl-CoA synthetase, whichconfirms the activation of the fatty acid complex by acyl-CoA synthetase.

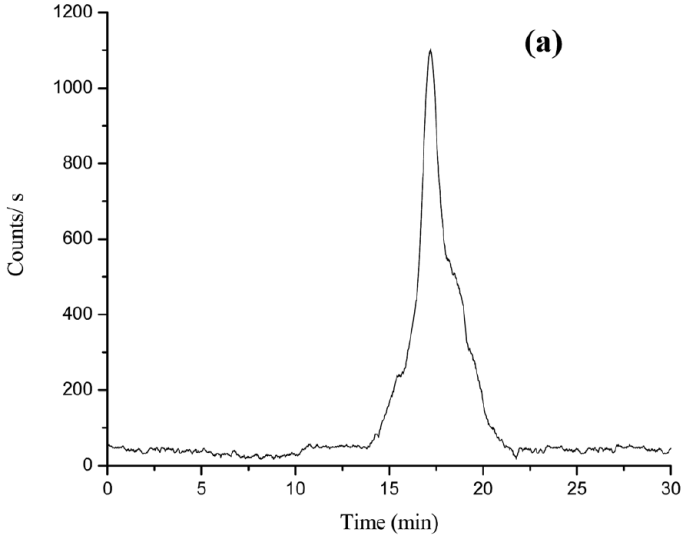

Fig. 3.27 *HPLC chromatogram original ^{99m}Tc-12C-FA-EDDA complex (2e)*

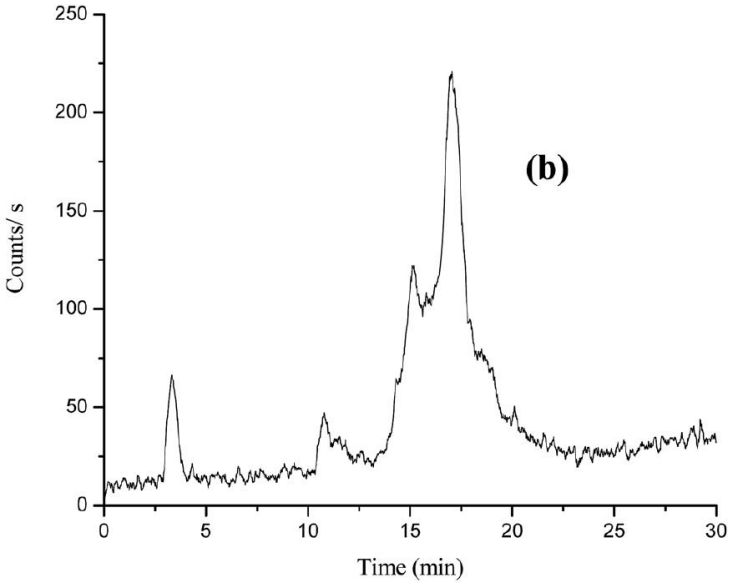

Fig. 3.28 *HPLC chromatogram of aqueous extract of ^{99m}Tc-12C-FA-EDDA complex (2e) and enzyme activation reaction mixture*

3.5.6 Biodistribution

3.5.6.1 Myocardial Uptake

Biodistribution studies of HPLC purified complexes (**1e/2e** and **1f/2f**) reconstituted in 10% ethanol were carried in normal female Swiss mice (Table 3.2 to Table 3.5). For comparison of biodistribution purified complexes with a reference compound ^{125}I-IPPA, literature reported values were taken of the later have been taken (Table 3.6). Myocardial uptake of the four^{99m}Tc-fatty acid complexes and the reference compound, ^{125}I-IPPA, is shown in Fig. 3.29. Both fatty acid complexes with EDDA as co-ligand (**1e/2e**) showed better uptake in the myocardium compared to their TPPTS counterparts (**1f/2f**). This may be attributed to the lower lipophilicity of the TPPTS complexes which resulted in lower uptake in the myocardium. Among the four ^{99m}Tc-fatty acid complexes, complex **2e** showed the highestmyocardial uptake [5.95 (0.74) %ID per g] at 2 min p.i. However, this is significantly lower than that of the myocardial uptakeshown by ^{125}I-IPPA [9.51 (1.61) %ID per g]. As expected with longchain fatty acids, all ^{99m}Tc-fatty acid complexes (**1e/2e** and **1f/2f**) exhibited bi-phasic clearance from the myocardium, with initial rapid clearance

phase till 10 min p.i. followed by slow clearance phase thereafter. Though all four complexes showed significant activity in myocardium even at 30 min p.i., it was lower than that observed for ^{125}I-IPPA [7.10 (1.79) % ID per g, Fig. 3.29].

Table 3.2 *Bio-distribution pattern of* 11C-FA-HYNIC-^{99m}Tc-EDDA *complexes (1e)*

Complex **1e**								
	2 min		***5 min***		***10 min***		***30 min***	
	%ID/g	S.D.	%ID/g	S.D.	%ID/g	S.D.	%ID/g	S.D.
Liver	32.94	7.55	30.51	3.96	24.17	1.25	12.60	1.13
Int + GB	2.27	0.61	4.13	0.89	12.92	1.40	20.90	3.19
Kidney	7.74	2.70	4.35	0.24	3.50	0.46	1.95	0.19
Heart	5.10	0.92	2.07	0.45	2.22	0.21	1.19	0.17
Lungs	9.11	3.39	4.13	0.56	4.12	0.67	2.35	0.45
Spleen	10.19	10.45	1.45	0.25	2.62	0.48	1.60	0.62
Muscle	0.80	0.08	0.62	0.14	0.63	0.20	0.46	0.02
Blood	15.81	1.28	5.81	1.58	6.41	0.97	3.41	0.32

Table 3.3 *Bio-distribution pattern of 11C-FA-HYNIC-^{99m}Tc-TPPTS/tricine complex (1f)*

	2 min		***5 min***		***10 min***		***30 min***	
	%ID/g	S.D.	%ID/g	S.D.	%ID/g	S.D.	%ID/g	S.D.
Liver	59.99	10.6	47.8	10.5.3	39.57	10.34	24.52	4.84
Int + GB	5.8.3	0.67	20.81	5.96	27.22	9.94	25.45	4.3
Kidney	7.06	1.10	3.64	0.47	3.50	0.46	2.08	0.1
Heart	4.87	0.26	2.52	1.24	1.76	0.53	0.8.3	0.31
Lungs	10.65	1.78	4.53	1.04	5.08	3.02	2.02	0.32
Spleen	6.02	2.0	5.98	5.7	4.0	1.16	4.6	1.03
Muscle	0.01	0.00	0.6	0.1	0.68	0.2	0.01	0.00
Blood	16.08	2.36	7.03	2.75	6.47	2.29	3.1	0.35

Table 3.4 *Bio-distribution pattern of 12C-FA-HYNIC-^{99m}Tc-EDDA complex (2e)*

	2 min		***5 min***		***10 min***		***30 min***	
	%ID/g	S.D.	%ID/g	S.D.	%ID/g	S.D.	%ID/g	S.D.
Liver	10.57	0.45	10.29	0.48	8.26	0.18	7.33	1.48
Int + GB	3.23	0.31	3.51	0.13	3.21	0.17	4.01	0.29
Kidney	7.01	0.33	6.79	0.52	5.11	0.33	3.30	0.60
Heart	5.95	0.74	4.97	0.56	3.37	0.28	2.19	0.21
Lungs	13.01	0.36	12.74	0.85	10.54	1.05	5.91	1.34
Spleen	4.27	0.46	5.64	0.85	4.83	0.56	3.34	0.26
Muscle	1.72	0.13	1.84	0.22	1.74	0.11	0.88	0.24
Blood	15.67	1.68	13.39	0.61	9.01	0.5.3	6.94	0.81

Table 3.5 *Bio-distribution pattern of 12C-FA-HYNIC-^{99m}Tc-TPPTS/tricinecomplex (2f)*

	2 min		***5 min***		***10 min***		***30 min***	
	%ID/g	S.D.	%ID/g	S.D.	%ID/g	S.D.	%ID/g	S.D.
Liver	54.37	19.83	46.39	3.00	36.5.3	2.35	8.44	0.39
Int + GB	3.10	0.11	9.70	4.01	20.80	1.89	26.07	5.45
Kidney	4.08	1.10	2.20	0.55	1.53	0.30	0.65	0.18
Heart	2.79	0.40	1.08	0.14	0.81	0.23	0.32	0.06
Lungs	4.43	0.68	1.98	0.41	1.97	0.35	1.13	0.02
Spleen	1.58	0.29	0.42	0.08	0.61	0.12	2.25	2.56
Muscle	1.39	0.71	0.80	0.22	0.67	0.09	0.19	0.06
Blood	5.19	1.50	2.52	0.64	2.01	0.30	0.98	0.03

Table 3.6 *Biodistribution of* ^{125}*I-IPPA*

^{125}I-IPPA								
	2 min		***5 min***		***10 min***		***30 min***	
	%ID/g	S.D.	%ID/g	S.D.	%ID/g	S.D.	%ID/g	S.D.
Liver	49.39	6.67	34.03	3.45	47.94	10.04	30.40	6.82
Int + GB	2.09	0.62	2.65	0.46	2.73	0.24	4.81	1.52
Kidney	9.96	2.58	11.02	0.10	15.11	0.04	11.25	1.18
Heart	9.51	1.61	7.84	0.93	9.16	0.17	7.10	1.79
Lungs	23.9.3	5.26	14.47	3.34	12.2.3	2.39	11.39	2.55
Spleen	13.47	2.35	8.31	1.54	15.97	1.13	10.23	1.91
Muscle	1.57	0.23	1.91	0.16	2.06	0.01	1.94	0.34
Blood	5.12	0.52	5.53	0.57	6.36	1.12	6.42	1.59

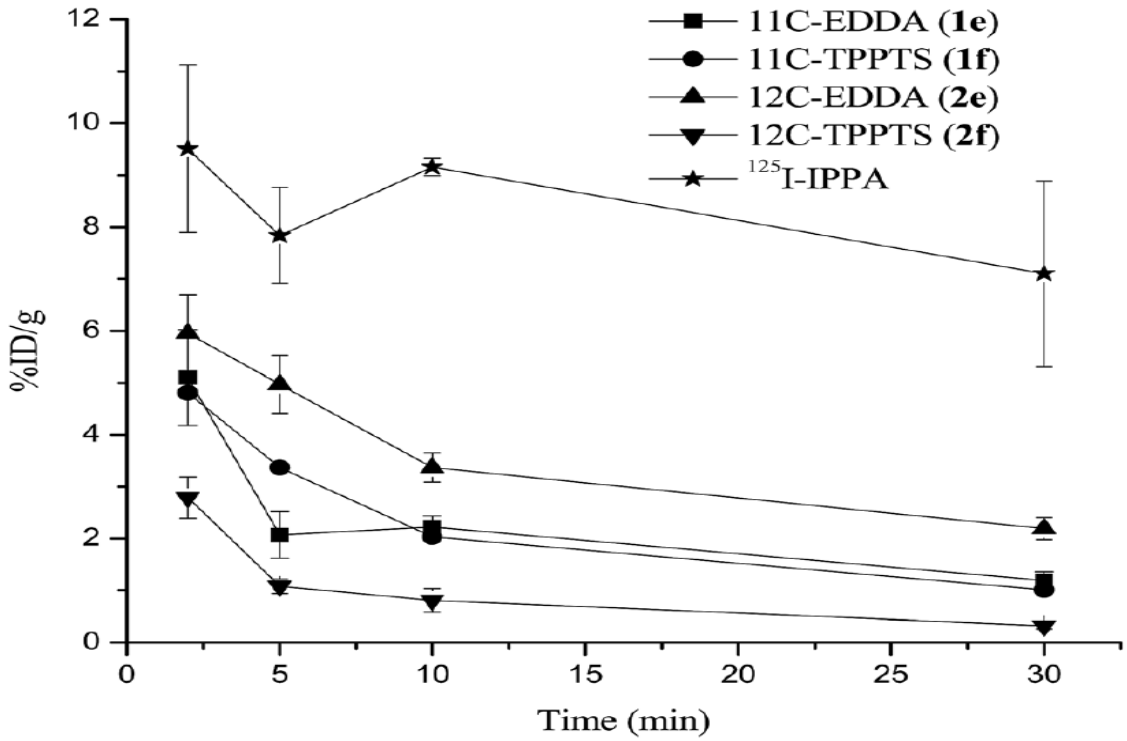

Fig. 3.29 *Uptake and retention characteristics of* ^{99m}*Tc-HYNIC-fatty acid complexes (1e/2e and 1f/2f) and* ^{125}*I-IPPA in the myocardium of Swiss mice.*

3.5.6.2 Washout kinetics of radiolabeled complexes from non-target organs

High uptake and retention of the radiotracer is essential for myocardial SPECT imaging. However, if not more, clearance of the radiotracer from the background tissue/organs such as blood, liver and lungs, is equally important to obtain high contrast images. Time dependent clearance pattern of injected activity from non-target organs are shown in figures from Fig. 3.30 - Fig. 3.32. Critical ratios for heart imaging (heart/blood, heart/lungs and heart/liver) are also shown in the figures from Fig. 3.33 to Fig. 3.35. It could be noted that the clearance of ^{99m}Tc-HYNIC-fatty acid tracers (**1e/2e** and **1f/2f**) from non-target organs such as liver and lungs was better compared to ^{125}I-IPPA. Especially the complex **2e**, among all the other complexes, showed significantly lower liver uptake [10.57 (0.45) % ID per g] at 2 min p.i. The latter biological behavior is desirable in IPPA analogues, since early imaging could differentiate between normal/ischemic myocardium and infarct. Consequently, heart to liver ratio of this complex (Fig. 3.35) is better than ^{125}I-IPPA. All ^{99m}Tc-HYNIC-fatty acid complexes (**1e**/**2e** and **1f/2f**) cleared rapidly from liver compared to ^{125}I-IPPA, with TPPTS complexes (**1f/2f**) showing very sharper fall in liver activity, possibly due to the hydrophilic nature of TPPTS ligand. Uptake of TPPTS complexes (**1f/2f**) in lungs was also observed to be lower than that of EDDA analogues (**1e/2e**).

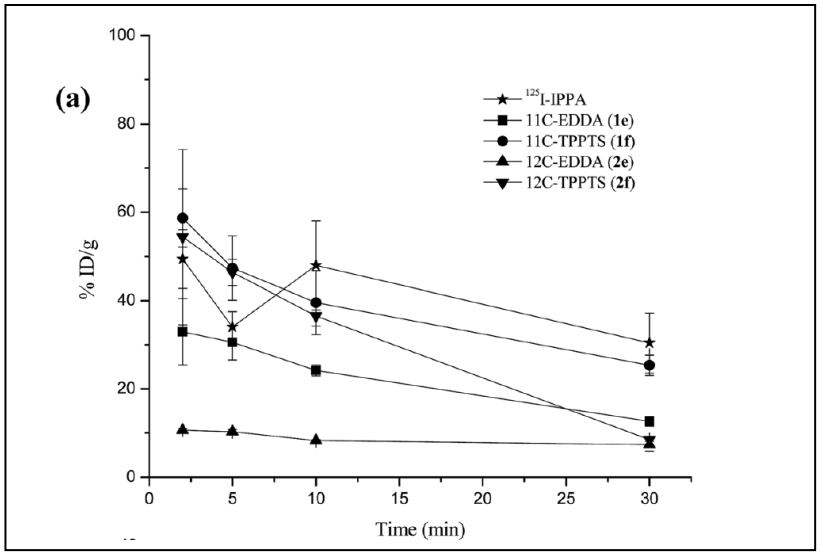

Fig. 3.30 *Washout kinetics of four complexes (1e/2e and 1f/2f) from liver in comparison with ^{125}I-IPPA.*

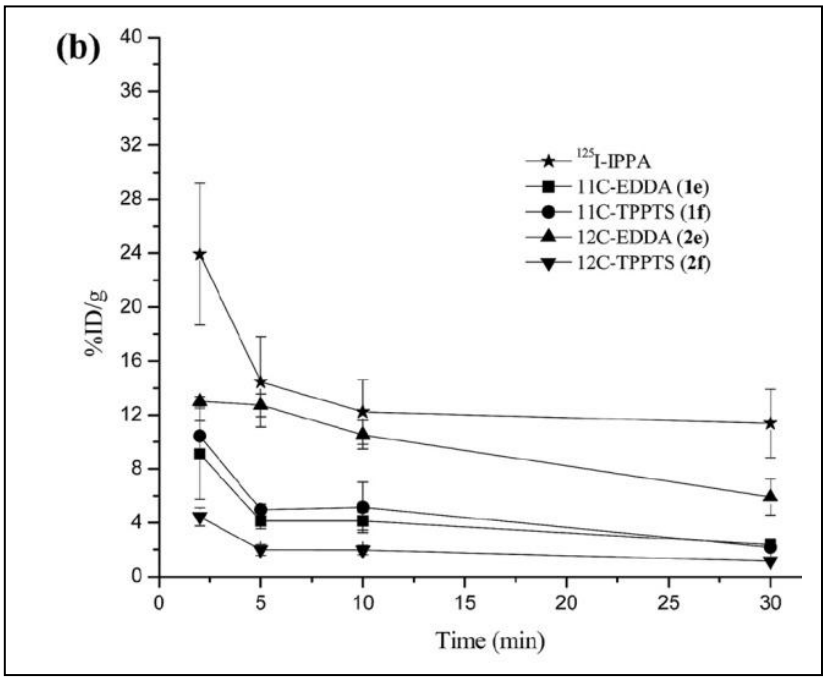

Fig. 3.31 *Washout kinetics of four complexes (1e/2e and 1f/2f) from lungs in comparison with* ^{125}*I-IPPA.*

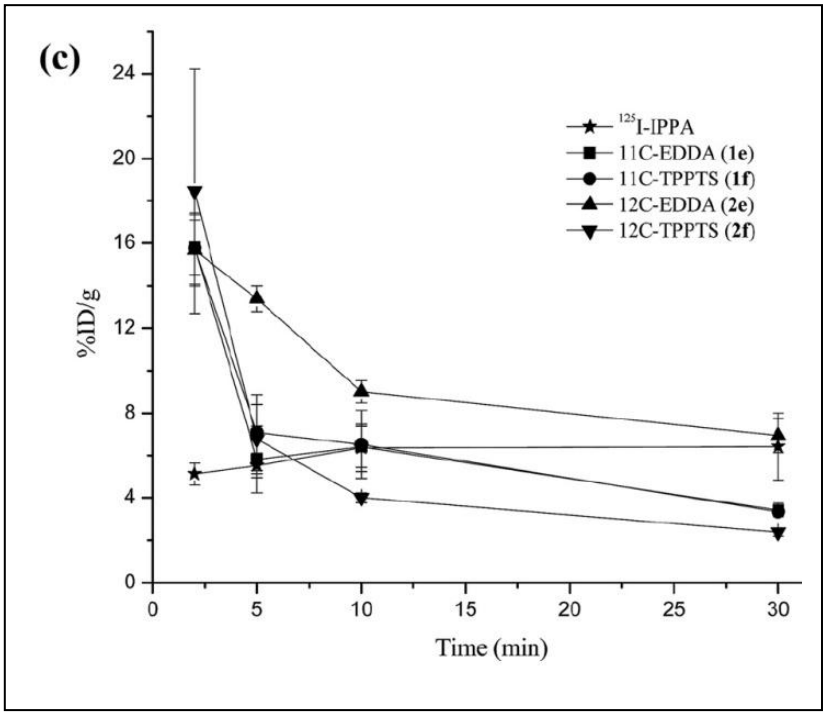

Fig. 3.32 *Washout kinetics of four complexes (1e/2e and 1f/2f) from blood in comparison with* ^{125}*I-IPPA.*

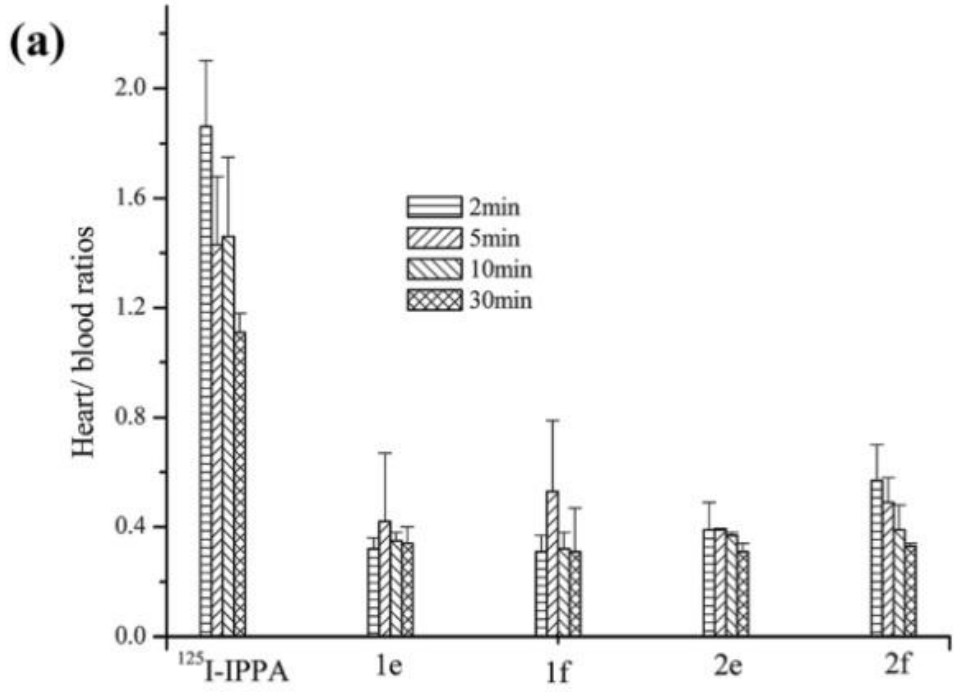

Fig. 3.33 *Time dependent changes in the heart/blood ratios of different ^{99m}Tc-labeled fatty acids (1e/2e and 1f/2f) in Swiss mice.*

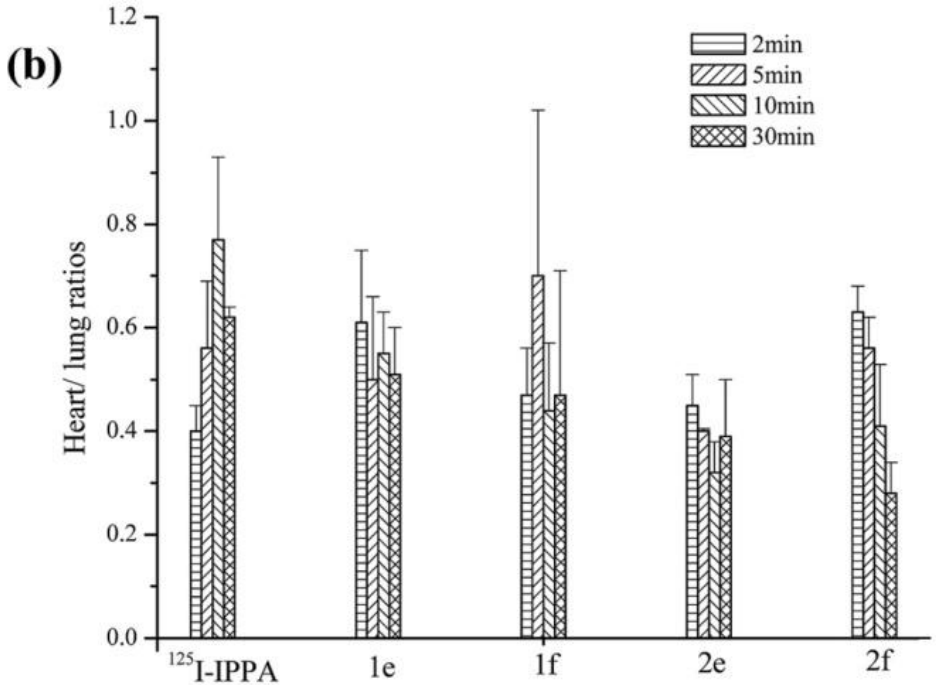

Fig. 3.34 *Time dependent changes in the heart/lung ratios of different ^{99m}Tc-labeled fatty acids (1e/2e and 1f/2f) in Swiss mice.*

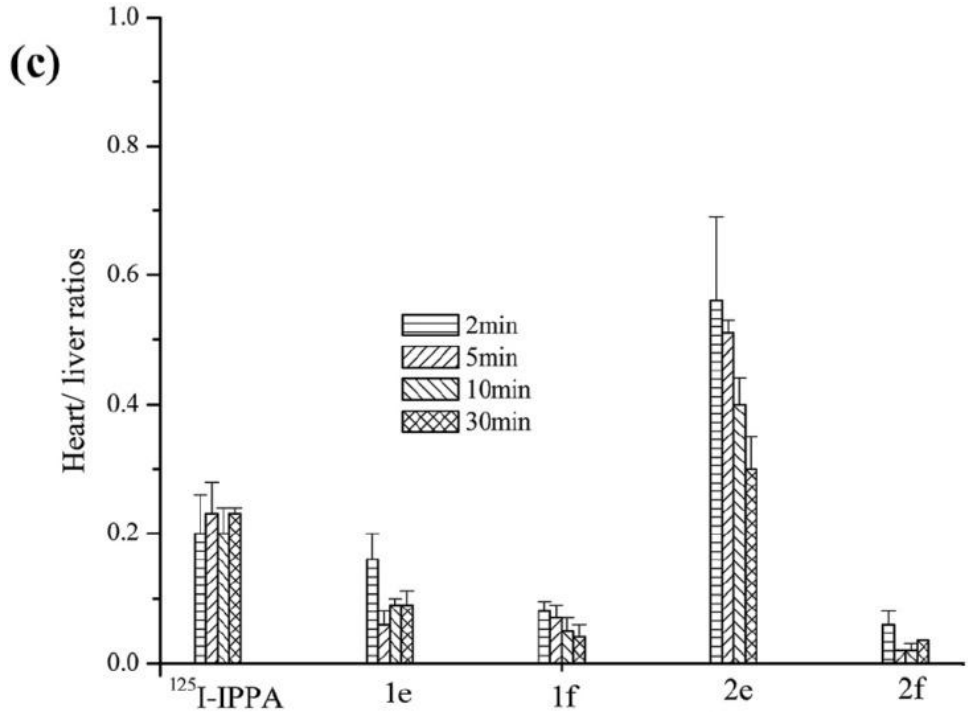

Fig. 3.35 *Time dependent changes in the heart/liver ratios of different ^{99m}Tc-labeled fatty acids (1e/2e and 1f/2f) in Swiss mice.*

All the ^{99m}Tc-complexes (**1e/2e** and **1f/2f**) showed significant blood pool activity initially compared to ^{125}I-IPPA. Though the blood pool activity cleared rapidly, with mean values observed 10 min p.i. being similar to or better than ^{125}I-IPPA, heart/bloodratio of all the complexes (Fig. 3.33) remained suboptimal throughout the period of study. It could be easily ruled out that activity observed in the myocardium is due to residual blood in the myocardium, because, considering average weight of heart to be about 0.1 g, activity observed in the myocardium for all the ^{99m}Tc-complexes at all the time points is higher than the activity corresponding to 0.1 g of blood.

3.5.6.3 Comparison of Biodistribution pattern with [^{99m}Tc]MAMA-HDA

The direct comparison of the biological potential of the ^{99m}Tc-HYNIC-radiotracers used in the present study with that of some promising ^{99m}Tc-labeled-fatty acids [85, 86, 88] is not possible because of the use of different species of animals (mice versus rats) used in the biodistribution studies. In comparison with the results of most promising ^{99m}Tc-fatty acid tracer i.e. [^{99m}Tc] MAMA-HAD [90] evaluated in the same species, only compound **2e** showed a similar myocardial uptake [5.46 (1.15) % ID per g]. However, the heart/liver ratio at 2 min p.i. was clearly more promising for **2e** (0.6 vs. 0.2). [^{99m}Tc]MAMA-HDA showed better characteristics in terms of both a significant uptake in heart and also a rapid blood clearance leading to high heart/blood ratios (1.5 vs. 0.39 at 2 min p.i.).

3.5.6.4 Analysis of metabolites in liver homogenates

Since the ^{99m}Tc-HYNIC-fatty acids (**1e/2e** and **1f/2f**) excrete mainly via the hepatobiliary pathway and significant activity was found to be associated with the liver, it was felt pertinent to carry out analyses of the metabolites in liver homogenates. HPLC analysis of representative ^{99m}Tc-fatty acid complex (**2e**) in liver homogenate, collected at 1 h p.i., showed fractional metabolic transformation of the tracer (Fig. 3.36). Fatty acids are known to metabolize through β-oxidation leading to formation of short chain residues which in the HPLC gradient elution system (ammonium acetate buffer/methanol) used in the present study, will be eluted early from C-18 column. Though, an additionalpeak at lower retention times (3 min) was observed (Fig. 3.36), no effort was made to characterize the polar metabolite formed. An interesting finding with respect to difference in peak shape of complex **2e** in liver homogenate was observed to that in Fig. 3.27. However, the identical peak broadness and position (retention time) for both ensured no contribution due to metabolic trans-formation of the radiotracer.

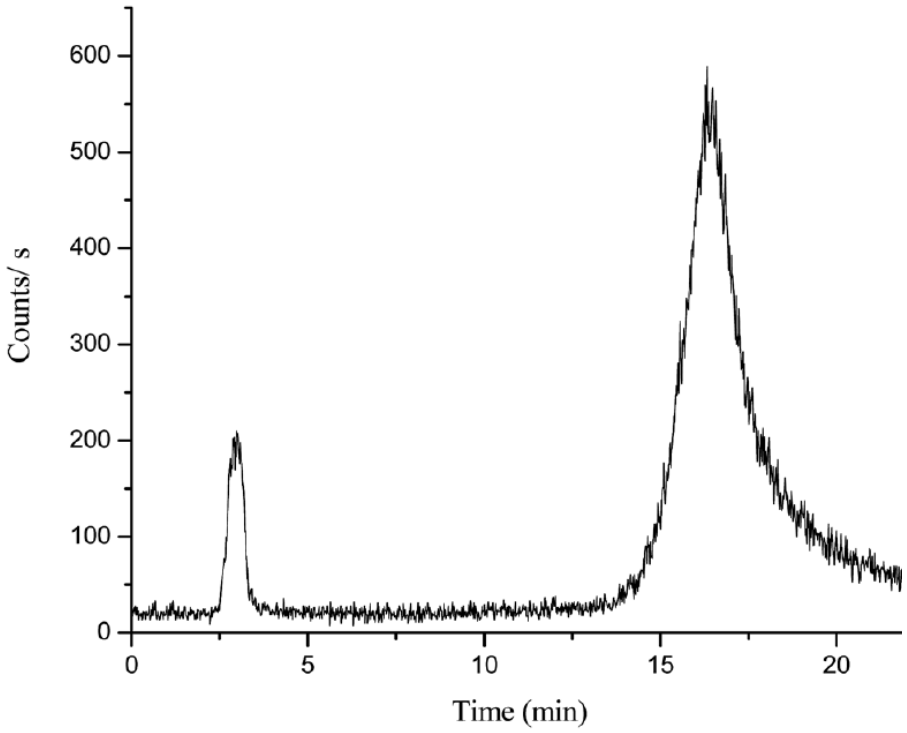

Fig. 3.36 *Time HPLC analyses of 12C-EDDA complex (2e) observed in liver homogenates in Swiss mice at 60 min p.i.*

3.5.6.5 Myocardial imaging in Mouse

Myocardial imaging in mouse was carried out to validate the uptake and washout pattern observed in bio-distribution results and to assess the imaging potential of 12C-EDDA complex (**2e**). Fig. 3.37 shows a representative planar image frame of the 12C-EDDA complex (**2e**) obtained at 2 min p.i. which represented high resolution and sensitivity. Though bio-distribution experiments showed sub-optimal heart/blood ratios, delineation of the myocardium from the non-target organs, liver and blood, could be observed.

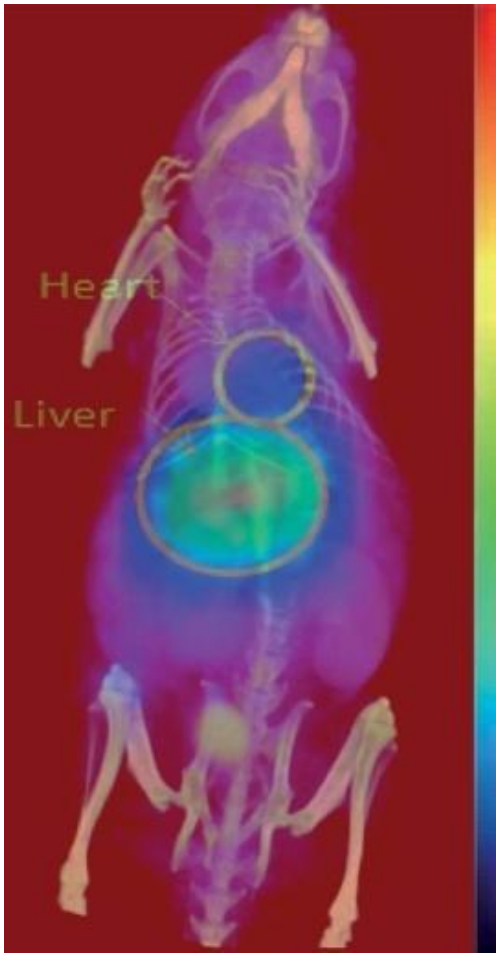

Fig. 3.37 *Whole body planar image of 12C-EDDA complex (2e) in Swiss mice*

3.5.6.6 Dynamic SPECT Imaging

Dynamic SPECT scans of the mouse myocardium were acquired upto 15 min p.i. Fig. 3.38 shows the time vs. activity kinetics curve obtained after selecting an ROI which indicated a net positive uptake of the tracer (**2e**) in the myocardium above the background i.e. blood pool activity. The clearance kinetics observed in the myocardium in SPECT is in agreement with the biodistribution results (Fig. 3.29). A bi-phasic clearance pattern was observed, with initial rapid clearance phase up to 3 min, when 50% decrease in initial myocardial activity was observed, followed by slow clearance upto 15 min. An inverse kinetics was observed in the case of non-target organ, liver, where initial rise in liver activity is followed by retention in the uptake values upto 15 min.

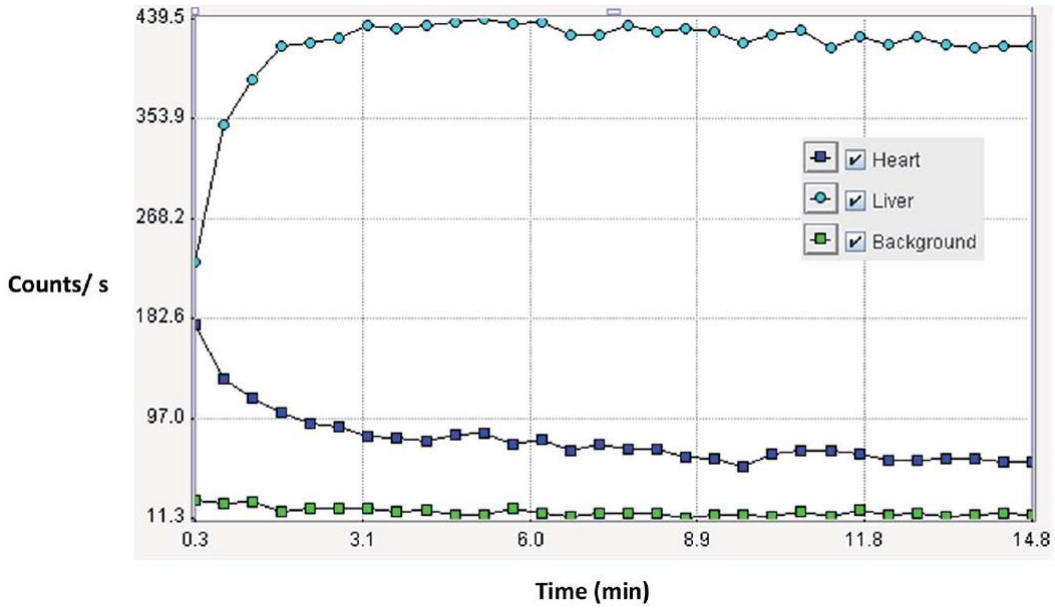

Fig. 3.38 *Time-activity distribution kinetics of 12C-EDDA complex (2e) in Swiss mice.*

3.6 Conclusion

Two fatty acid-HYNIC conjugates (11C and 12C) were synthesized in good yield and labeled with ^{99m}Tc, using EDDA and TPPTS as co-ligands. The biodistribution studies of radio-labeled complexes in female Swiss mice showed reasonable initial myocardial uptake for all four ^{99m}Tc tracers with 12C-EDDA complex exhibiting maximum uptake and retention in the myocardium. Further, low liver uptake values and distinct myocardial delineation in micro-SPECT image, obtained with the 12C-EDDA complex, proves conducive for early cardiac imaging. However, significant association of the tracer with blood pool diminished its imaging potential for the aforementioned application. The present study documents the advantages of the HYNIC BFCA in designing fatty-acid based radiotracers for metabolic cardiac imaging. The pharmacokinetic data obtained also provides insights towards the relevance of screening other ^{99m}Tc-HYNIC-fatty acids with chain lengths of 15C and 16C, with a view to improving the myocardial uptake/retention and achieving high heart/blood ratios.

Chapter 4

Development of ^{99}Mo-alfa-benzoin oxime complex as industrial radiotracer for leak detection studies in petroleum refinery

In this chapter the studies carried out to demonstrate industrial application of ^{99}Mo radioisotope as radiotracer have been described. ^{99}Mo activity was converted into an organic soluble metal complex of ^{99}Mo-alfa-benzoin oxime (^{99}Mo-ABO), suitable for its use as industrial radiotracer for leak detection studies in organic carrying stream of petroleum refinery. Performance of the developed organic soluble ^{99}Mo-ABO based radiotracer was tested in a diesel hydro-treater (DHDT) unit of a crude oil refinery. DHDT unit was made of serially connected heat exchangers and some of them were suspected for leakage. The developed ^{99}Mo-ABO complex was used to study its effectiveness for detection of leakage in heat-exchangers units which were carrying hydrocarbon stream at high temperature and high-pressure.

Starting with the aqueous alkaline solution of (n, f)^{99}Mo activity, a radiochemical methodology was developed to obtain ^{99}Mo as ^{99}Mo-ABO form suitable for mixing with organic phase. Prepared ^{99}Mo-ABO radio-complex was used to carry out radiotracer study in organic phase to identify the leaky heat exchangers from a series of four heat exchangers. In order to verify the reproducibility of the results obtained from the ^{99}Mo-ABO radiotracer injection, ^{99m}Tc in organic phase was used as another radiotracer for leak detection in the same setting. The developed radiotracer '^{99}Mo-ABO complex' was

found to be a suitable industrial radiotracer for its application in high temperature and high-pressure hydrocarbon stream carrying components of petroleum refinery.

4.1 Introduction

Petroleum refineries producing diesel product are required to limit the concentration of sulfur in the final product before sending it to retail outlet due to the strict pollution control norms issued by the government. The established norms make it mandatory to reduce sulfur content below 10 ppm in diesel product and thereby complying with EURO-V standard. Therefore, hydro-treating process is carried out to remove sulfur from the crude diesel and thus make it compliant with the above mentioned EURO-V standard. In order to ensure good quality of the diesel product from the petroleum refinery, early detection of any leakage in the stream of the hydro-treating unit is required. Hence, ensuring a better production efficiency, occupational safety and to control environmental pollution [118-120]. Generally, any observed deviation from the normal operating parameters of hydro-treating unit such as product contamination, pressure loss and reduction in process efficiency indicates the presence of leak in the system [120, 121].

Diesel hydrotreater (DHDT) units are the essential component of various petroleum refineries, whose primary function is to remove sulfur from the crude diesel stream. These are designed for treatment of high sulphur distillates and cracked feed streams using a suitable catalyst and a hydrogen rich gas stream. The catalyst is packed inside a large vessel column and crude diesel is fed into this column for hydrodesulfurization (HDS) or hydrotreating process. Generally, cobalt-modified molybdenum disulfide (MoS_2) based catalyst are used for hydrodesulfurization reaction. The catalytic reaction taking inside the DHDT unit removes the organic sulphur, oxygen and nitrogen

compounds present in the feed. It also improves the cetane number of the diesel product. The catalytic process results in the generation of large amount of heat. The recovery of this heat is desired for the efficient and economical operation of the refinery. The heat energy is recovered from the hot diesel product coming out from the catalytic bed and transferred to the crude diesel going into the catalyst bed by means of heat-exchangers. [119, 120]. Heat exchangers are specially designed vessel which allow for the exchange of heat energy between the two liquid streams without any mixing of mass. They are widely used in petroleum refineries, chemical and petrochemical plants, natural gas processing, refrigeration, power plants, air conditioning and room heating [119-121]. Fig. 4.1 depicts a typical diagram of a heat-exchanger. It comprises of two distinct regions, namely, shell and tube. Two different liquid streams can flow through shell and tube without getting mixed into one another, however exchange of heat can take place between them. There are several types of heat exchangers depending upon process requirement and the most common type of heat exchangers employed in DHDT units of petroleum refineries are serially connected shell and tube type of breech-lock heat exchangers.

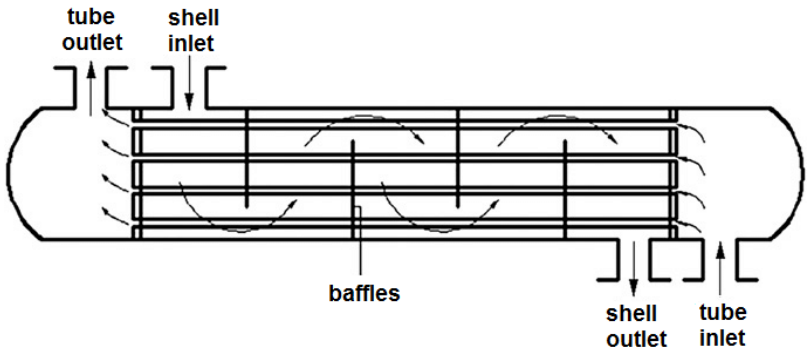

Fig 4.1 *Typical heat-exchanger*

Conventional techniques used for the identification of leaks in heat exchanger systems are visual inspection, pressure change method, chemical reagent test, dye penetrant test, acoustic leak detection and mass spectrometry [121]. However, the high operating temperature and pressure of the process rules out online mode with these

techniques. These conventional tests can be employed only after shutting down the refinery to carry out leak detection investigation. Hence, conventional techniques are not commercially viable [118, 120].

During the operation the typical pressure and typical temperatures inside the breech lock heat exchangers are 10-17.6 MPa and 350-600^{o}C respectively. Due to these extreme operating conditions, heat exchangers do not have sampling ports to avoid any fire hazards, which rules out the use of the use of conventional tracers (non-radioactive tracers) leak detection during online operating conditions. However, use of radio-tracers avoid the requirement for any sampling port due to penetrating nature of gamma rays which can be detected from outer surface of the heat exchanger system, and hence enable online measurement [118, 122, 123, 124].

Bromine-82 [$T_{1/2}$: 36 h; Eγ: 1.32 MeV (26.8%), 0.55 MeV (70%)] in organic form is a commonly used radiotracer for leakage investigation in hydrocarbon stream as mentioned above [119, 125, 126]. However, ^{82}Br decays by emission of high energy gamma photons which may result in cross peak detection by the closely placed detectors in vicinity of heat exchangers. Hence, it may lead to misinterpretations of the data acquired from the detectors. On the other hand, comparatively lower gamma energy and longer half-life of molybdenum-99 [$T_{1/2}$: 66 h; Eγ: 740 keV (12.8%), 181 keV (6.2 %)] makes it a promising alternative to ^{82}Br.

NaI(Tl) based scintillation detectors of very high sensitivity are used for the detection of radiotracer present in the organic stream of heat-exchangers system. They can detect the presence of the radiotracer in the diesel stream in minimum possible time and with high accuracy. These detectors are placed at strategic location surrounding the serially connected heat-exchangers and their output is collectively stored through an electronic device called MIDAS (multi input data acquisition system). A typical placing

arrangement of detectors around heat-exchangers for radiotracer investigation is shown in Fig. 4.2 and the typical real time out-put data from MIDAS in shown in Fig. 4.3. The data is recorded online after radiotracer injection to the heat-exchanger system, and can be analyzed quickly to identify the leaky heat exchanger [122, 124, 127]. These features of radiotracers investigation technique minimize the downtime of the large capacity petroleum refineries rendering huge economic benefits.

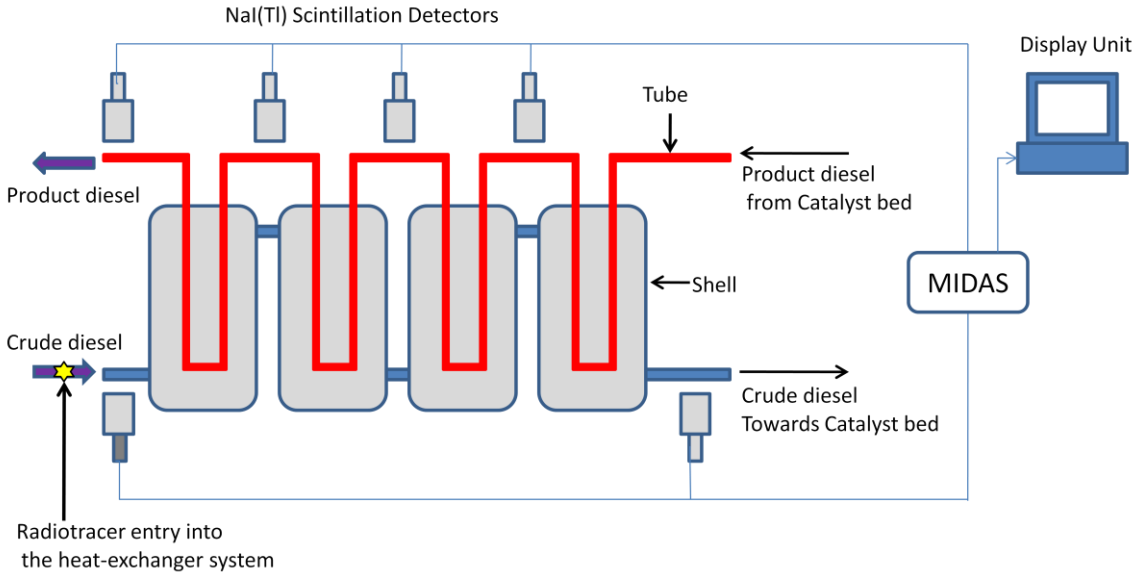

Fig. 4.2 *Typical arrangement of radiation detectors for radiotracer investigation*

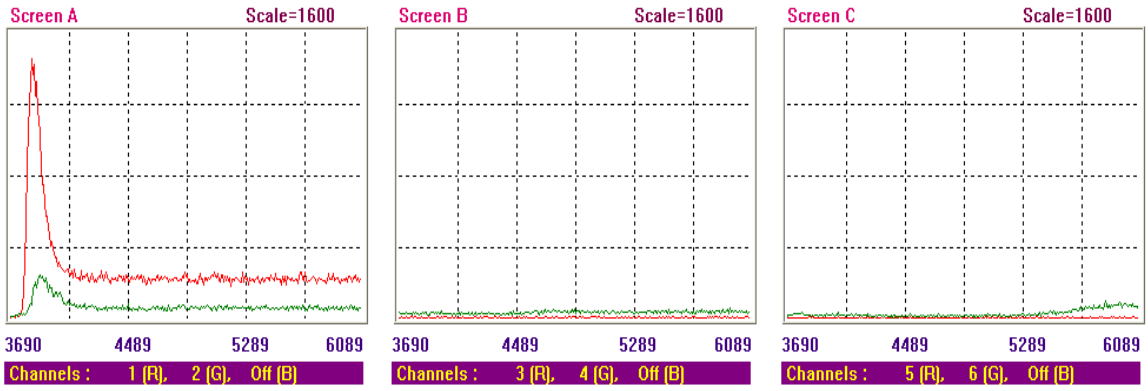

Fig. 4.3 *Picture showing online output from MIDAS*

A pre-calculated activity radiotracer is injected as a sharp pulse into the high pressure side of the heat exchanger system using a specially designed injection system. The liquid flowing through shell side and tube side of the heat exchanger in DHDT unit have pressure difference and its typical value falls in the range of 1.18-1.47 MPa. Presence of any leakage in the heat-exchanger will cause the fractional amount of injected radiotracer to enter into the low pressure side from the high pressure side though the leak. Therefore detection of any radiation at low pressure side is an indication of leakage [120, 121]. The location and collimation of the radiation detectors are strategically chosen to avoid cross peak detection and to record statistically sufficient counts. In a typical arrangement of detectors for radiotracer investigation, detectors are placed in following fashion: one detector at high pressure side inlet, one at high pressure side outlet and at all low pressure side outlets of the serially connected heat exchangers with one detector at each place. Rise in the count-rate above background in the lower pressure side outlets of the heat exchangers indicates presence of the leakage.

In the present work a radiotracer investigation has been carried out at DHDT unit of a petroleum refinery, identification of leaky heat exchangers was carried out using a newly developed industrial radiotracer ^{99}Mo-ABO complex in the organic phase. Reproducibility of the result was verified by a proven industrial radiotracer, ^{99m}Tc [$T_{1/2}$: 6 h; Eγ: 140 keV] in organic phase [128-130].

4.2 Experimental

4.2.1 General Consideration

All the reagents used in the experiments like alfa-benzoinoxime (ABO), chloroform, methyl ethyl ketone (MEK), etc., were of analytical reagent grade.

4.2.2 Preparation of technetium-99m radiotracer dissolved in diesel

A glass vial containing 10 ml of aqueous alkaline solution of high specific activity of (n, f)^{99}Mo (18.5 GBq , 500 mCi) , in the form of $Na_2{}^{99}MoO_4$, was taken into a lead shielded fume hood. The vial was then de-capped. Solution in the vial was transferred inside a specially designed lead shielded solvent extraction set-up (Fig. 4.4) by applying vacuum. The ^{99}Mo solution was further added with a 20 ml of 5N NaOH. The resulting solution inside the lead shielded extractor was agitated by drawing air through the bottom of extractor using a vacuum pump.

The above mentioned ^{99}Mo solution contains activity of decay product ^{99m}Tc in transient radioactive equilibrium with its parent isotope ^{99}Mo. From this solution, ^{99m}Tc can be recovered into the organic phase by solvent extraction using MEK as organic extractor. Extraction of ^{99m}Tc into organic phase was carried out by adding 30 ml of MEK into extraction set-up using vacuum for transferring the organic solvent. The aqueous phase and the organic phase were vigorously agitated for 15-20 minutes by drawing air through the bottom of the extraction system. The two phases were allowed to settle for 5 minutes for clear phase separation. The organic layer (containing recovered ^{99m}Tc) forms the top layer and aqueous layer (containing leftover ^{99}Mo) forms the bottom layer. The two layers were separately collected. The MEK layer (containing ^{99m}Tc) was further mixed with 500 mL of diesel and injected into heat-exchanger systems for radiotracer investigation.

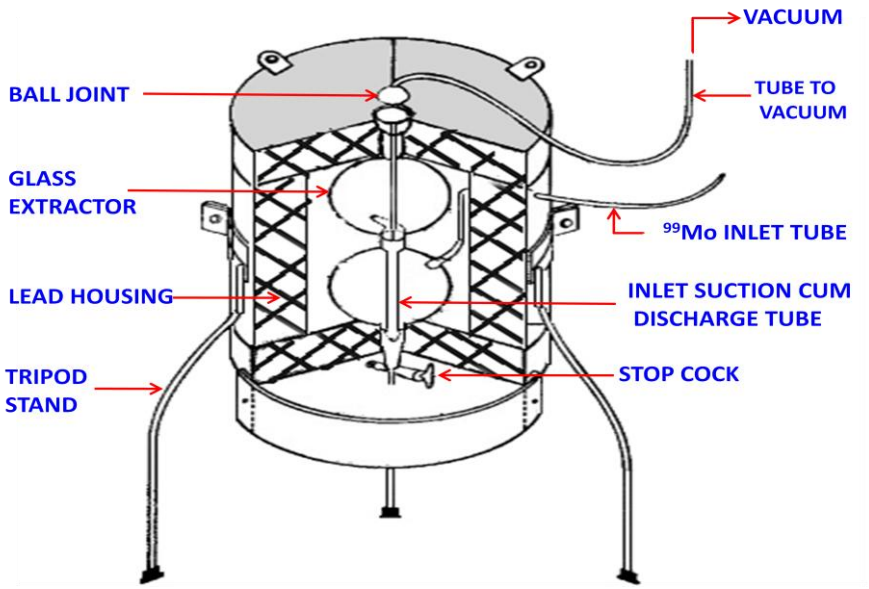

Fig. 4.4 *Lead shielded solvent extraction set-up*

4.2.3 Preparation of ^{99}Mo-ABO radiotracer dissolved in diesel

The ^{99}Mo containing aqueous layer from the previous extraction (section 4.2.2) was again transferred to the solvent extraction set-up by a vacuum action. Subsequently, 10 mg of molybdenum carrier, in the form of sodium molybdate, was added to this solution. The resulting solution was acidified by adding concentrated nitric acid to make final acidity around 3.5 M. The resulting solution was agitated for 30 minutes. Molybdenum in the aqueous solution was then quantitatively precipitated with the drop wise addition of 21 mL of alfa-benzoinoxime (ABO) solution (2 mg L^{-1} in ethanol). The resulting mixture was then mixed with 30 mL chloroform and agitated by drawing air through the mixture. The ^{99}Mo-ABO precipitate got dissolved into the chloroform layer. The mixture was allowed to settle for 5 minutes. The chloroform layer containing ^{99}Mo activity in the form of Mo-ABO complex, forms the bottom layer which was separately collected and dissolved with500 mL diesel for use in leak detection study in heat exchangers of DHDT unit.

4.2.4 Description of Heat exchanger system

In the present case, there are four heat exchangers in series viz. 09-EE-002A/B and 09-EE-003A/B as shown schematically in Fig. 4.5. Crude diesel feed is introduced through the shell inlet of 09-EE-003A and travels sequentially through the shells of 09-EE-003B, 09-EE-002A and 09-EE-002B to the reactor, which contains catalyst for desulfurization of feed. The diesel product that is emerging from the reactor flows counter current through the tubes of heat-exchangers in the following order: 09-EE-002B → 09-EE-002A → 09-EE-003B → 09-EE-003A. During its passage from the heat-exchangers, heat is transferred from product diesel stream to crude diesel stream via thermal conduction through the metalic interface. The feed flowing in the shell side is at higher pressure than the diesel flowing in the tube side as tabulated in Table 4.1. Since the sulphur content in the product diesel was higher than expected (>50 ppm), it was suspected that the feed is leaking into the final diesel product. Hence, a radiotracer study was planned to identify the leaky heat exchanger. Fig 4.6 shows the pictures of the heat-exchangers undertaken for radiotracer investigation.

4.2.5 Radiotracer Investigation

A first radiotracer injection was carried out using ^{99}Mo-ABO complex in organic phase. Fig. 4.7 shows the actual view of strategically placed and well shielded NaI(Tl) based radiation detectors around heat-exchangers for signal acquisition. The pressure inside the feed inlet to the pump was 490-588 KPa. The radiotracer was injected as a sharp pulse using a specially fabricated injection system as shown in Fig. 4.8, into the inlet of the feed pump. The radiotracer was first poured into the injection system and then it was pushed to the main diesel feed stream by pressurizing it with nitrogen gas at about 980 KPa.

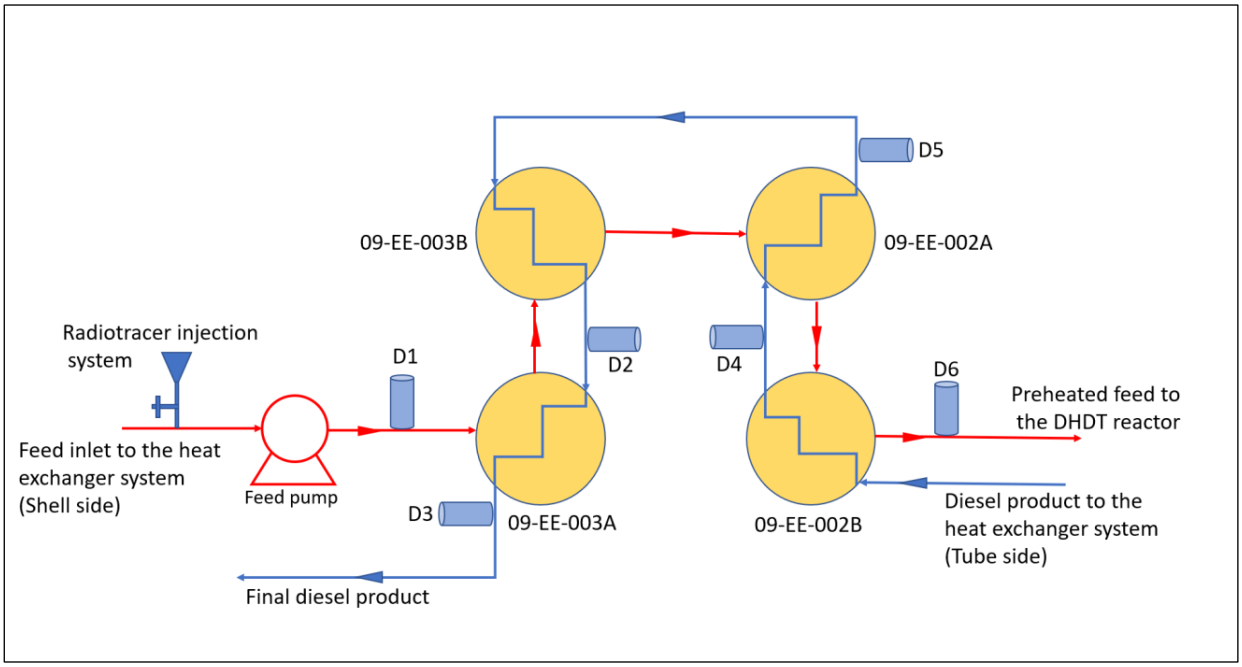

Fig. 4.6 *Schematic of heat exchanger system showing injection system, feed pump and strategically located radiation detectors*

Fig. 4.6 *Picture showing two out of the four heat-exchangers*

Table 4.1 *Characteristics of heat exchangers being studied*

Tag No.		**09-EE-002 A / B**	**09-EE-003 A / B**
Description		Hot combined Feed Exchanger	Cold combined Feed Exchanger
Service	Shell	Hydrocarbons, H_2 , H_2S	Hydrocarbons, H_2 , H_2S
	Tube	Hydrocarbons, H_2 , H_2S	Hydrocarbons, H_2 , H_2S
Operating pressure (MPa)	Shell	11.96	12.06
	Tube	10.66	10.36
Operating temperature (^oC)	Shell Inlet	195	80
	Shell Outlet	354	195
	Tube Inlet	408	234
	Tube Outlet	291	148

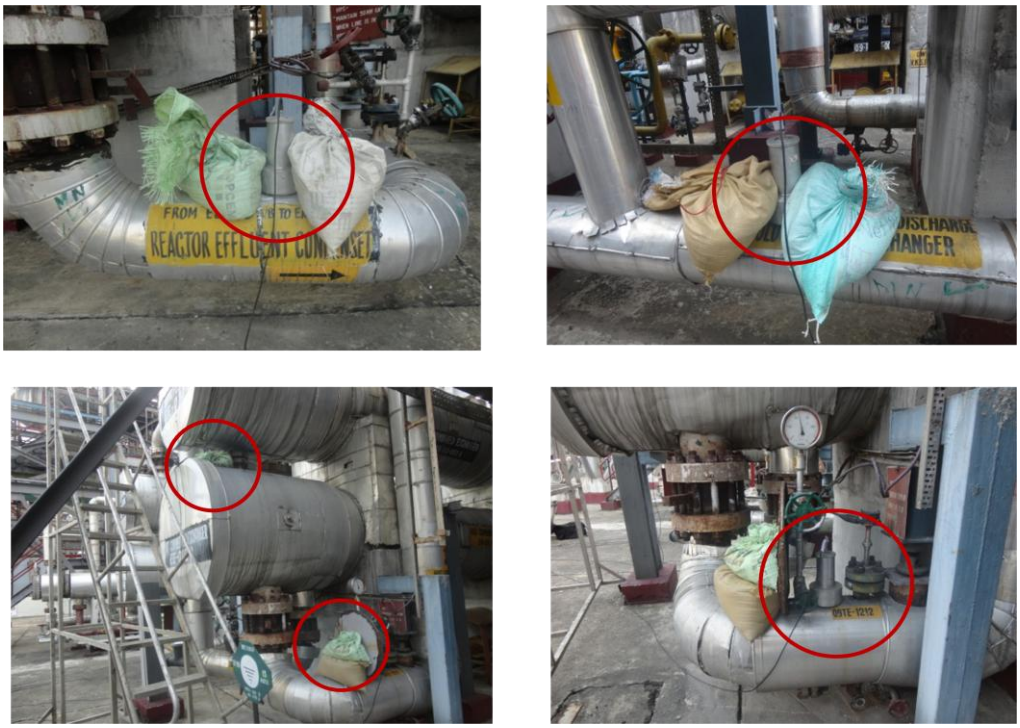

Fig. 4.7 *Picture showing strateagically placed colimated detectors*

Table 4.2 *Detector locations*

Detector No.	Detector location
D1	Shell Inlet of 09-EE-003A
D2	Tube Outlet of 09-EE-003B
D3	Tube Outlet of 09-EE-003A
D4	Tube Outlet of 09-EE-002B
D5	Tube Outlet of 09-EE-002A
D6	Shell Outlet of 09-EE-002B

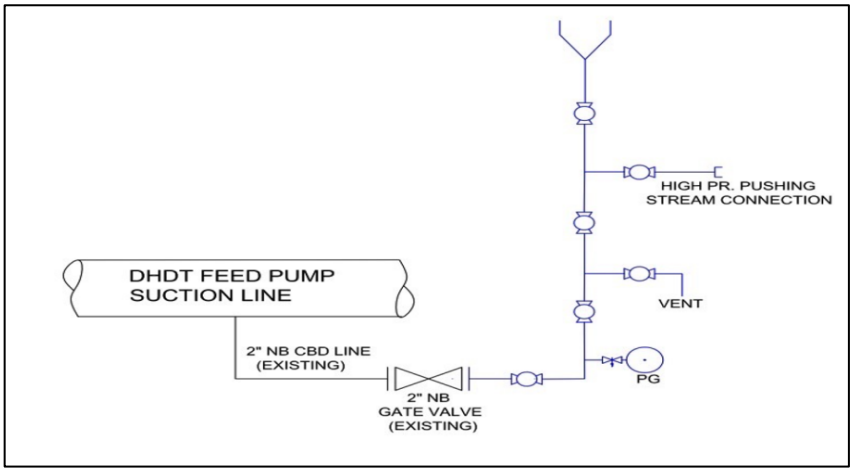

Fig. 4.8 *Schematic of the radiotracer injection system*

After completion of the ^{99}Mo-ABO radiotracer investigation is over, the same procedure of injection and subsequent detection was repeated with the radiotracer ^{99m}Tc dissolved in MEK. The flow of radiotracer in the heat exchanger system, was monitored using six strategically placed NaI(Tl) scintillation detectors. These all detectors were well shielded using an approximately 5 cm thick lead collimator and thermally insulated with Bakelite jacket (Fig. 4.7). Table 4.2 indicates the location of different detectors placed around the serially connected heat exchanger. The online count-rate data recorded by each detector was fed into an electronic device called *multi input data acquisition system*

(MIDAS) which offers simultaneous on-line collection of signal received from several detectors and their graphical visualization in real time through a display unit.

4.3 Results and Discussion

Recovery of ^{99m}Tc activity in MEK phase from an aqueous solution of ^{99}Mo/ ^{99m}Tc using solvent extraction method is a well known technique and has been used to avail ^{99m}Tc from ^{99}Mo-^{99m}Tc radioisotope generator [131]. During the extraction process, ^{99m}Tc goes into the organic phase (MEK) from alkaline aqueous layer, and hence gets separated from its parent isotope (^{99}Mo). The recovered ^{99m}Tc activity in organic phase forms a homogenous solution upon mixing with diesel. The resulting solution is suitable for radiotracer based industrial application [130]. The aqueous alkaline layer which contains left-over ^{99}Mo activity in the form of $^{99}MoO_4^{2-}$, was acidified with concentrated HNO_3 thereby converting ^{99}Mo activity in aqueous layer into a cationic species $^{99}MoO_2^{2+}$, which can be can be selectively precipitated by forming a complex compound with alfa-benzoin oxime (ABO) (Fig. 4.9) [132].

$$^{99}MoO_4^{2-}{}_{(aq.)} \xrightarrow{HNO_3} {}^{99}MoO_2^{2+}{}_{(aq.)} \xrightarrow{\text{ABO (2 \% in Ethanol)}} MoO_2[ABO]_2 \downarrow$$

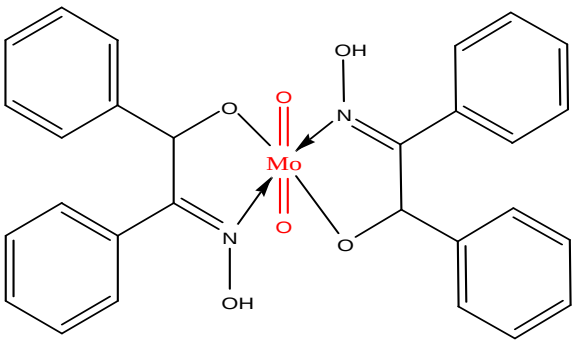

Fig. 4.9 *Mo-ABO complex*

In this present study, 3 M HNO_3 was added to the alkaline aqueous solution containing ^{99}Mo activity. The resulting solution was agitated for 30 minutes to ensure the formation of the desired molybdenum species (MoO_2^{2+}) suitable for complexation with ABO. Further, ABO solution (Mo: ABO weight ratio of 1:10) was added to the aqueous layer resulting in the formation of Mo-ABO complex, suitable for mixing with the organic phase.

Both the radiotracers were separately injected in to the system and their passage were monitored online through scintillation detectors. Radiotracer data was acquired for every 100 milliseconds. Data points for each detector were separately plotted and are shown in Fig. 4.10 to Fig. 4.21. A comparative study of detectors response to carefully analyze the results is shown in Fig. 4.22, Fig. 4.23, Fig. 4.24 and Fig. 4.25. These figures which depict the inlet/ outlet time of radiotracer in the heat-exchanger system and the indication of leakage.

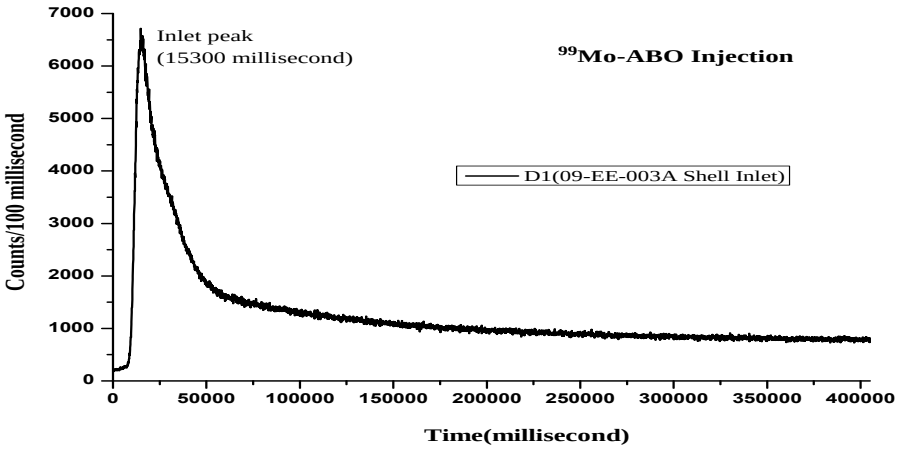

Fig. 4.10 *Response curve for D1 (^{99}Mo-ABO injection)*

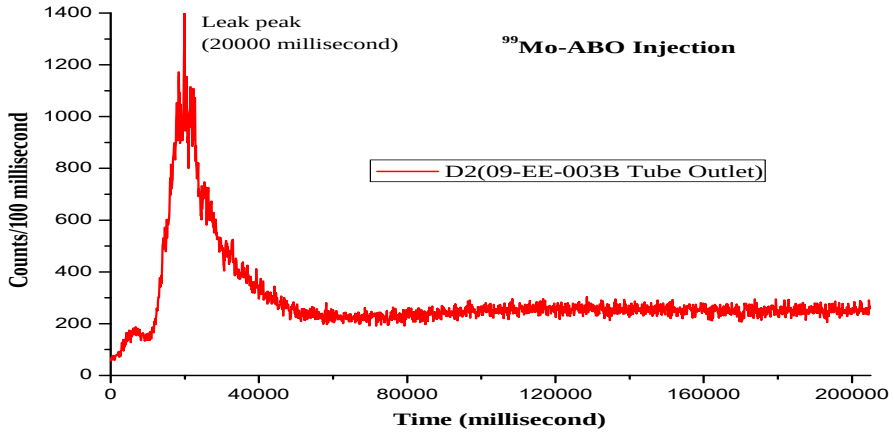

Fig. 4.11 *Response curve for D2 (^{99}Mo-ABO injection)*

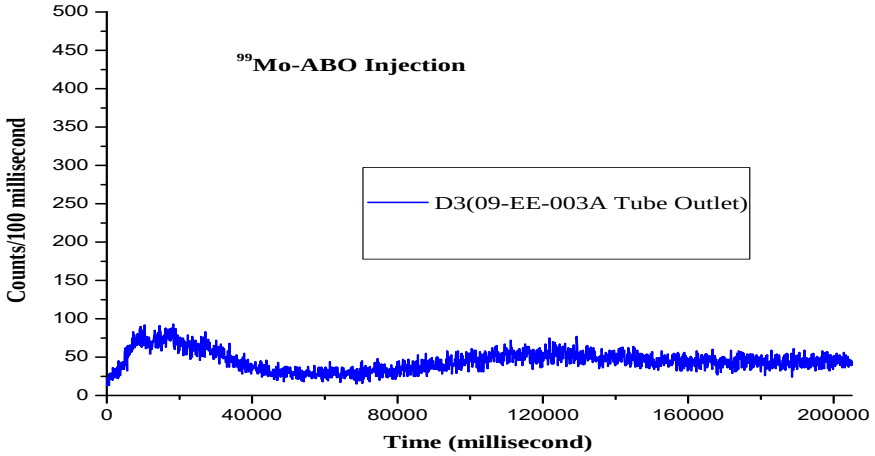

Fig. 4.12 *Response curve for D3 (^{99}Mo-ABO injection)*

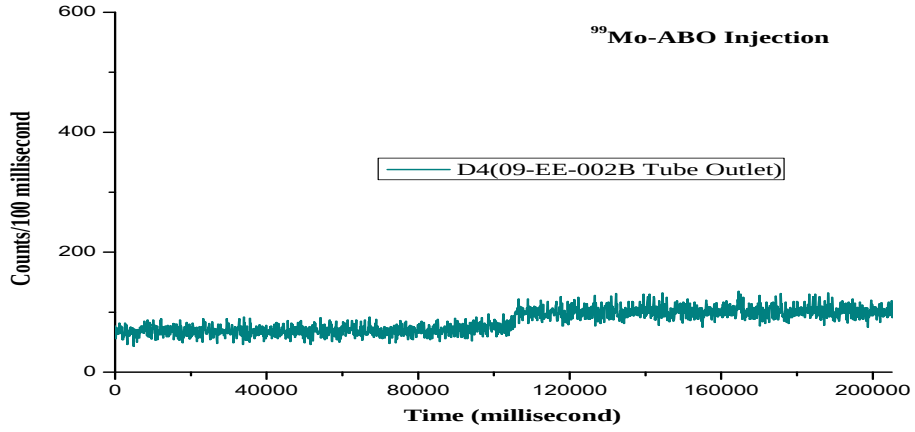

Fig. 4.13 *Response curve for D4 (^{99}Mo-ABO injection)*

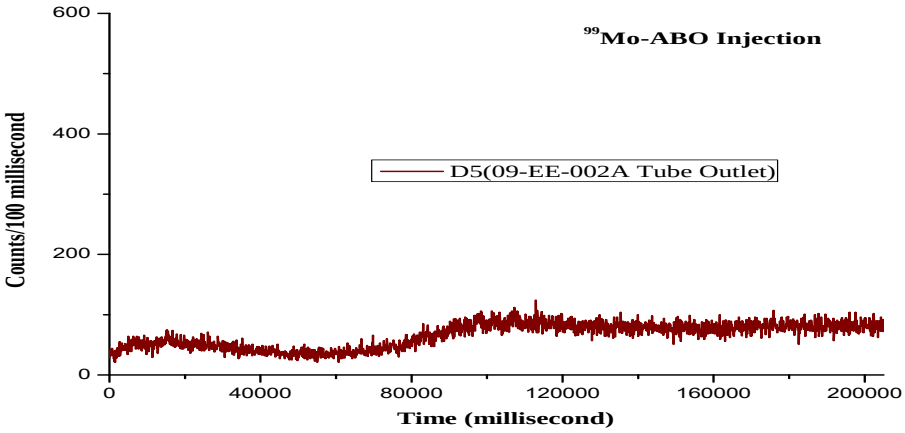

Fig. 4.14 *Response curve for D5 (^{99}Mo-ABO injection)*

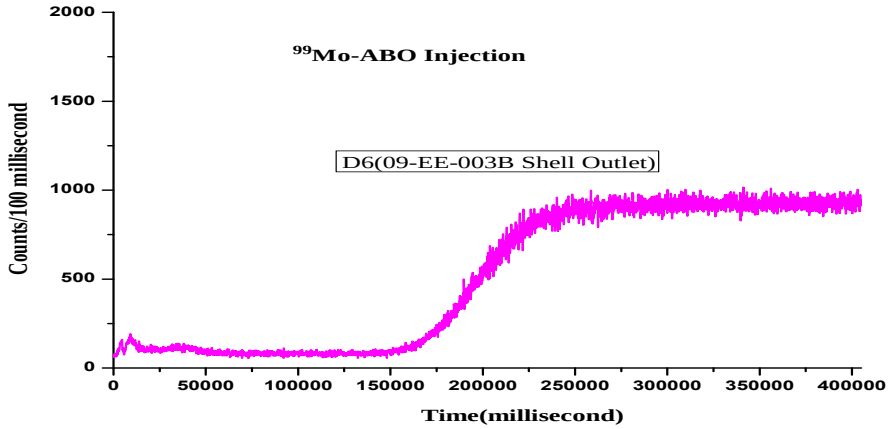

Fig. 4.15 *Response curve for D6 (^{99}Mo-ABO injection)*

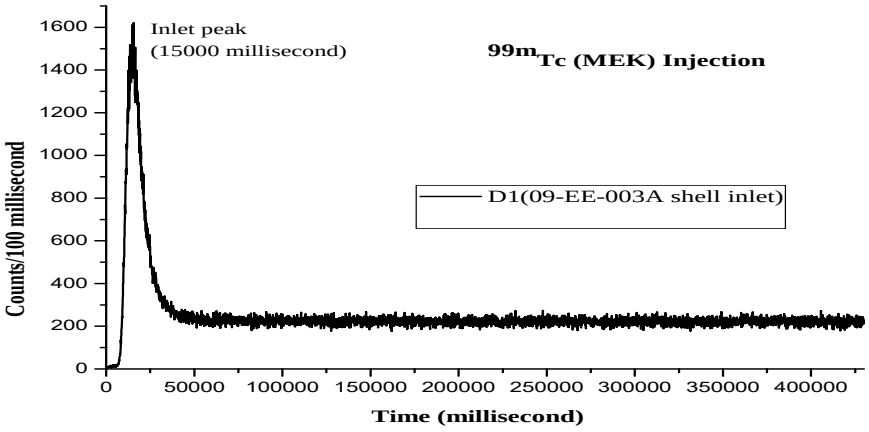

Fig. 4.16 *Response curve for D1 (^{99m}Tc-MEK injection)*

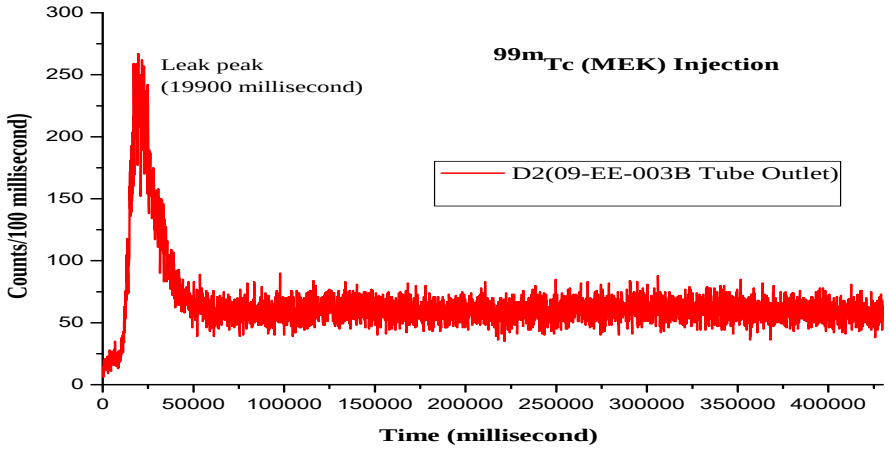

Fig. 4.17 *Response curve for D2 (^{99m}Tc-MEK injection)*

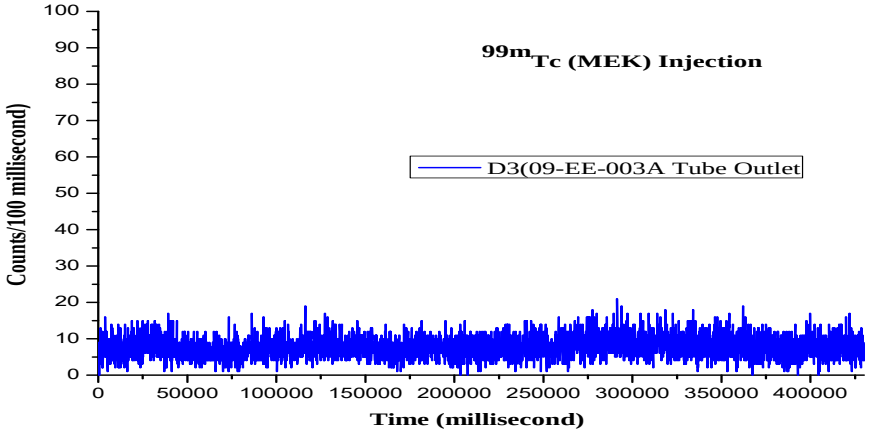

Fig. 4.18 *Response curve for D3 (^{99m}Tc-MEK injection)*

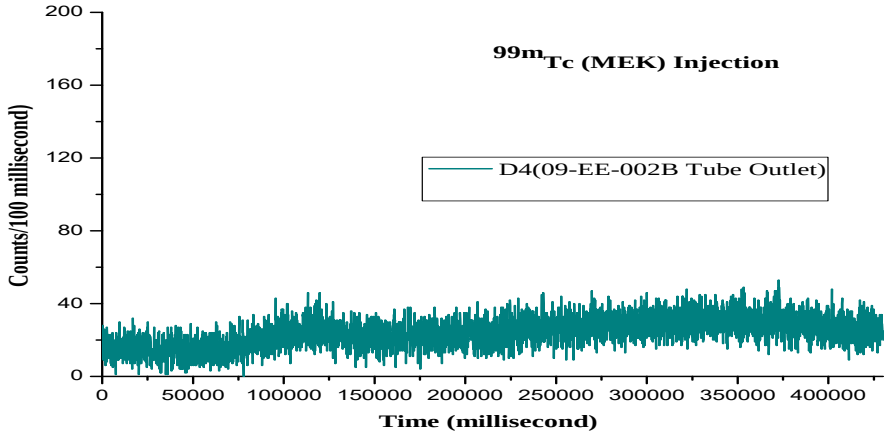

Fig. 4.19 *Response curve for D4 (^{99m}Tc-MEK injection)*

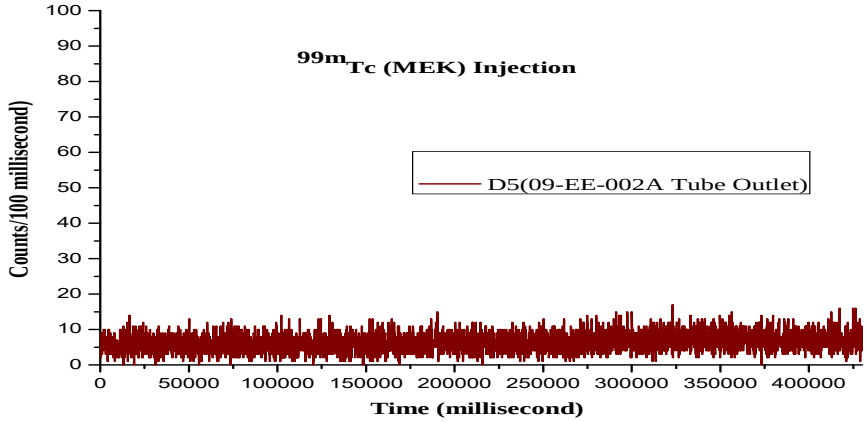

Fig. 4.20 *Response curve for D5 (^{99m}Tc-MEK injection)*

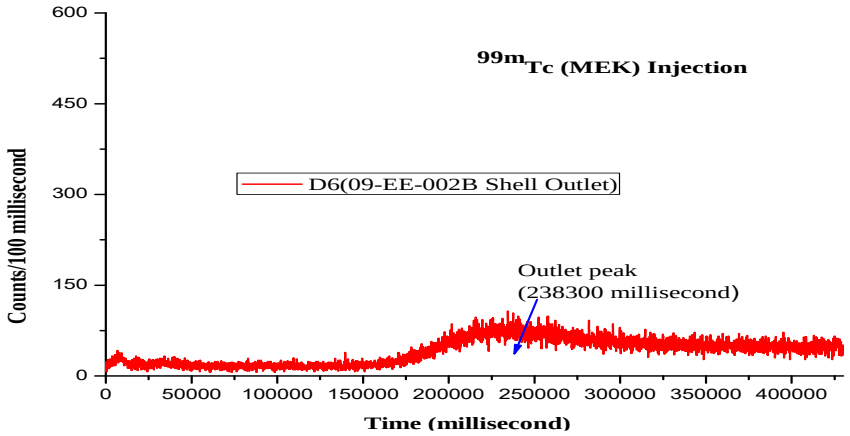

Fig. 4.21 *Response curve for D6 (^{99m}Tc-MEK injection)*

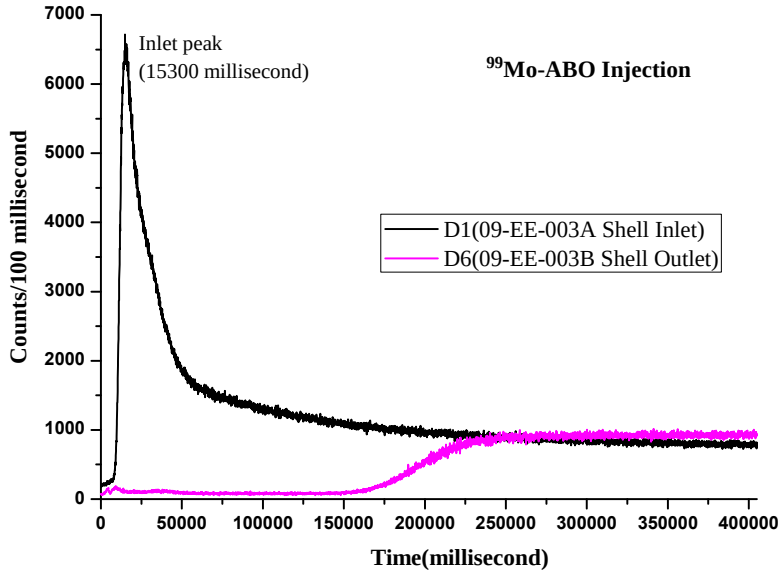

Fig. 4.22 *Detector response curve of D1 (shell inlet) and D6 (shell outlet)*

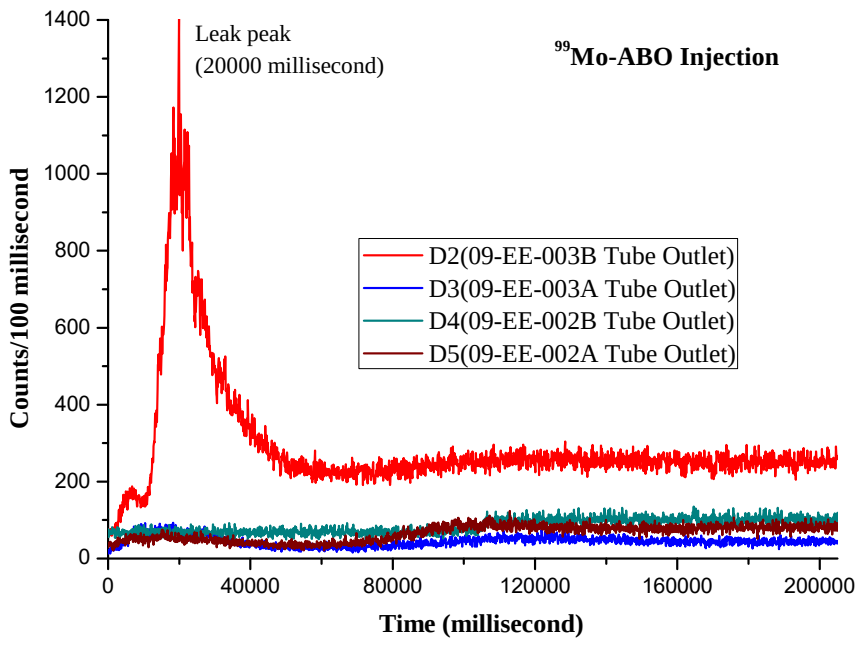

Fig. 4.23 *Detector response curve of D2, D3, D4 and D5 showing leak peak in the 09-EE-003B*

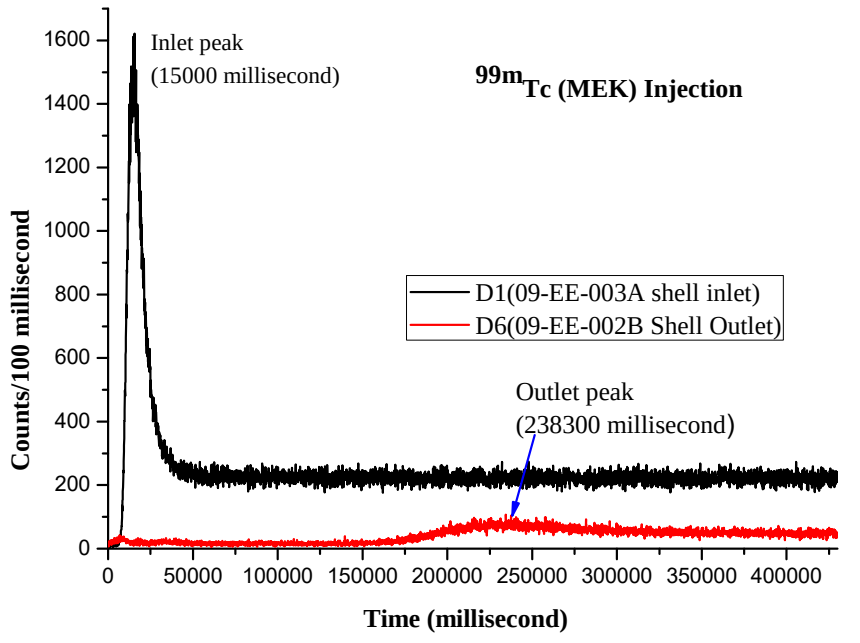

Fig. 4.24 *Detector response D1 (curve of shell inlet) and D6 (shell outlet)*

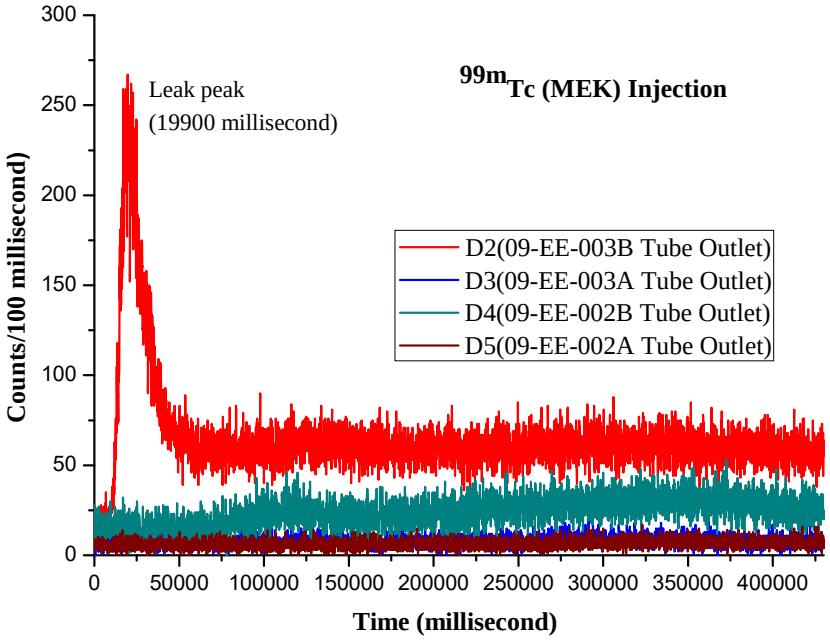

Fig. 4.25 *Detector response curves of D2, D3, D4 and D5 located at tube outlets of the heat exchangers showing leak peak in the 09-EE-003B*

The first radiotracer study was carried out by injecting ^{99}Mo-ABO complex dissolved in diesel. The peak observed at a time of 15300 millisecond in the response curve (Fig. 4.22) of detector D1 shows the instantaneous entry of the radiotracer into the shell side of heat exchanger 09-EE-003A. The time response curve of detector D6 (Fig. 4.22) shows the exit of the radiotracer from the shell outlet of heat exchanger 09-EE-002B. The output curve of D6 is stabilized after attaining a maximum value which indicates the adsorption of the radiotracer nearby the outlet pipe. Time response curves of the detectors D2, D3, D4 and D5 are collectively shown in Fig. 4.23. The peak observed at a time of 20000 millisecond in the time response curve of detector D2 corresponds to the leakage in the heat exchanger 09-EE-003B. The difference between inlet peak and leak peak was around 4.7 s. However, no peak was observed in the response curve of D3,

D4 and D5 in the heat exchangers 09-EE-003A, 09-EE-002A/2B respectively. A slight rise of the signal was observed in all the detectors at around 80000 millisecond which may be attributed to the cross-detection of radiotracer travelling in shell side of adjacent heat exchangers. However, this rise is insignificant as compared to the leak peak observed.

A second radiotracer injection was carried out by injecting ^{99m}Tc dissolved in diesel. The peak observed at a time of 15000 millisecond in the response curve of detector D1 (Fig. 4.24) shows the instantaneous entry of the radiotracer into the shell side of heat exchanger 09-EE-003A. The peak observed at a time of 238300 millisecond in the response curve of detector D6 (Fig. 4.24) shows the exit of the radiotracer from the shell side of heat exchanger 09-EE-002B, with the approximate residence time of the radiotracer in the system being 223 seconds. Fig. 4.25 shows the response of the detectors D2, D3, D4 and D5 placed at the tube outlets of the all the heat exchangers. Appearance of the peak at a time of 19900 millisecond in the time response curve of detector D2 indicates the leakage in the heat exchanger 09-EE-003B. The difference between inlet peak & leak peak was around 4.9 s. Time response curve of the detector D3, D4 and D5 shows absence of any leakage in the heat exchangers 09-EE-003A, 09-EE-002A/2B respectively.

From the above response curves of both the experiments, it is clear that signals recorded with ^{99}Mo-ABO radiotracer is stronger than that recorded with ^{99m}Tc, although the activity was same (18.5GBq). This may be attributed to the higher gamma energy of ^{99}Mo which renders high penetration through the pipe walls.

After passing through the heat exchangers, the diesel gets collected inside large storage tanks. The injected radiotracer gets diluted to a great extent with the diesel in

storage tanks (capacity > 10000 m^3) and decays to below detection limit till it reaches to the retail distribution centers.

4.4 Conclusion

Two radiotracers based on ^{99}Mo and ^{99m}Tc radioisotopes, were successfully prepared in organic phase for their intended use as industrial radiotracer. In DHDT unit of a leading petroleum refinery, ^{99}Mo radiotracer in the form of ^{99}Mo-ABO complex was injected to identify the leaky heat exchanger from a set of the four heat exchangers in series. The radiotracer investigation with ^{99}Mo based radiotracer indicates the leakage in heat exchanger 09-EE-003B.The results were replicated by using the radiotracer ^{99m}Tc in organic phase, indicating the reproducibility of the results and utility of ^{99}Mo-ABO complex radiotracer for such studies.^{99}Mo based radiotracer was found advantageous over ^{99m}Tc due to its high gamma energy and more penetration through the pipe walls.

Thesis abstract of Mr. Abhishek Kumar Sharma

Enrol No. CHEM01201204015

Radiochemical Separation and Purification of Molybdenum-99 for Medical and Industrial Applications

Thesis Abstract

Worldwide, artificial radioisotopes are being utilized for wide ranging societal application in the field of healthcare, industry, agriculture and research. Molybdenum-99 ($T_{1/2}$: 66 hrs) is one of the widely produced radioisotope worldwide due to huge medical utility of its daughter isotope ^{99m}Tc ($T_{1/2}$: 6 hrs.). ^{99m}Tc is used for SPECT based nuclear diagnostic imaging of various disorder/ diseases in human body, and said to be the work-horse of nuclear imaging. Large scale production of ^{99}Mo is carried out either by neutron activation route [^{98}Mo(n, γ)^{99}Mo] or by fission route [^{235}U(n, f)^{99}Mo]. The former production route leads to low specific activity of product ^{99}Mo, whereas later route leads to very high specific activity of ^{99}Mo which is a desirable feature for its medical utility.

The work carried out in this thesis is aims towards following goals:(i) Development of a novel method for production high specific activity, medical grade fission ^{99}Mo from thermal neutron irradiated U-Al alloy; (ii) Synthesis, radiolabelling and bio-evaluation of ^{99m}Tc labelled Fatty acid molecules for their use as SPECT based myocardial imaging agents; (iii) Development of ^{99}Mo based organic soluble industrial radiotracer.

The U-Al alloy target was irradiated for seven days followed by one day of cooling. The ^{99}Mo present in the target was recovered and purified by means of sequential radiochemical processing which involves the following steps: Alkaline dissolution, filtration, removal of aluminium matrix by precipitating, removal of radioiodine by precipitation, removal of ^{103}Ru, separation of ^{99}Mo by Mo-ABO precipitation and final purification by ion-exchange resin column (Amberlyst A-26). Towards medical application; ^{99m}Tc fatty acid based myocardial metabolic imaging agents were synthesized and evaluated in suitable animal model. Two fatty acid-HYNIC conjugates (11C-FA-HYNIC and 12C-FA-HYNIC) were synthesized and were labelled with ^{99m}Tc, using Tricine, EDDA and TPPTS as co-ligands. The bio-distribution studies of radio-labelled complexes in Swiss mice showed reasonable myocardial uptake. Towards industrial application of ^{99}Mo, an industrial radiotracer in organic phase was developed and tested for its efficacy. Starting with the aqueous alkaline solution of high specific activity (n,f)^{99}Mo, a radiotracer in the form of ^{99}Mo-ABO complex, suitable for mixing with organic phase was developed. The developed ^{99}Mo-ABO radiotracer was successfully evaluated for identifying the leaky component of a leading petroleum refinery.

Overall, the work carried out in this thesis resulted in development of a novel method for production of high specific activity, medical grade ^{99}Mo. Towards medical application of ^{99m}Tc in the form of fatty acid based myocardial SPECT imaging agents have been prepared and their potential were explored. Towards industrial application of ^{99}Mo, ^{99}Mo-ABO complex in organic phase was developed as industrial radiotracer and successfully used for identification of leaky heat-exchangers of a petroleum refinery.

Summary and outlook

The present thesis deals with the radiochemical separation and purification of high specific activity fission ^{99}Mo and its applications in healthcare and industry. Importance of ^{99}Mo stems out from the utility of its daughter radioisotope, ^{99m}Tc, which is the most widely used radioisotope in the field of diagnostic nuclear medicine. Annually, about 30 million medical diagnostic procedures are carried out worldwide using ^{99m}Tc.Commercial scale production of ^{99}Mo is carried out either by neutron activation of ^{98}Mo or by fission of ^{235}U. The former route produces low specific activity of ^{99}Mo, whereas the later route provides very high specific activity of ^{99}Mo, a desirable feature for making of alumina sorbent based ^{99}Mo-^{99m}Tc column chromatography generator.

Chapter one gives the general introduction about the production and use of artificial radioisotopes in the field of healthcare and industry. Artificial radioisotopes are produced either in nuclear reactor or in charge particle accelerator. This chapter also describes various routes of ^{99}Mo production, different types of ^{99}Mo-^{99m}Tc generators, radiopharmaceuticals prepared using ^{99m}Tc with brief description of myocardial metabolic agents for cardiac imaging. This chapter also contains a brief description of industrial applications of radioisotope.

The second chapter deals with the development of a radiochemical separation method for production of high specific activity medical grade ^{99}Mo.A radio-chemical method was developed for the separation and purification of (n,f)^{99}Mo from thermal neutron irradiated U-Al alloy target. A U-Al alloy target was irradiated in DHRUVA reactor for seven days followed by two days of cooling. The ^{99}Mo present in the target was recovered and purified by means of sequential radiochemical processing which involves the following steps: Alkaline dissolution, filtration, removal of aluminium matrix by precipitating $Al(OH)_3$,^{131}I removal by precipitation, removal of ^{103}Ru by

boiling-off RuO_4, separation of ^{99}Mo by Mo-ABO precipitation and final purification by ion-exchange resin column (Amberlyst A-26).The purity level of purified ^{99}Mo was assayed and was found suitable for making ^{99}Mo-^{99m}Tc radioisotope generators.

The third chapter deals with medical application of ^{99m}Tc, the daughter of ^{99}Mo. Towards medical application; ^{99m}Tc fatty acid based myocardial metabolic imaging agents were synthesized and evaluated in suitable animal model. Two fatty acid-HYNIC conjugates (11C-FA-HYNIC and 12C-FA-HYNIC) were synthesized in good yield. Further, these conjugates were labelled with ^{99m}Tc, using Tricine, EDDA and TPPTS as co-ligands to produce four set of radiolabelled complexes. The bio-distribution studies of radio-labelled complexes in Swiss mice showed reasonable initial myocardial uptake for all four ^{99m}Tc tracers with 12C-EDDA complex exhibiting maximum uptake and retention in the myocardium. This study documents the advantages of the HYNIC BFCA in designing fatty-acid based radiotracers for myocardial imaging.

The fourth chapter is focused towards industrial application of ^{99}Mo.Starting with the aqueous alkaline solution of high specific activity (n,f)^{99}Mo, a radiotracer in the form of ^{99}Mo-ABO complex, suitable for mixing with organic phase was developed. The developed ^{99}Mo-ABO radiotracer was successfully evaluated for identifying the leaky component of DHDT unit of a leading petroleum refinery. Results were replicated with ^{99m}Tc in organic phase as another radiotracer, showing reproducibility of results.

Overall, the work carried out in this thesis resulted in development of a novel radiochemical separation method for production of high specific activity, medical grade ^{99}Mo. Towards medical application of ^{99m}Tc in the form of fatty acid based myocardial SPECT imaging agents have been prepared and their potential were explored. Towards industrial application of ^{99}Mo, ^{99}Mo-ABO complex in organic phase was developed as

industrial radiotracer and successfully used for identification of leaky heat-exchangers of petroleum refinery.

Towards the development of high specific activity ^{99}Mo, using (n,γ) route, Molybdenum di-sulfide nano particles hold a great promise as target material for Szilard Chalmers reaction. It would be interesting to synthesize these nano-particles and use them to increase the specific activity of (n,γ)^{99}Mo exploiting Szilard Chalmer method. Towards the development of myocardial metabolic imaging agents, synthesis of HYNIC conjugated ethoxy fatty acid compounds, their radiolabelling with ^{99m}Tc followed by bio-evaluation of the radiopharmaceuticals will be an interesting work. Considering the successful application of ^{99}Mo-ABO in leak detection in heat exchangers in petroleum industry, it would be worthwhile to explore this radiotracer in other industrial applications in future.

References:

1. D. D. Sood, A. V. R. Reddy and N. Ramamoorthy, *Fundamentals of Radiochemistry*, IANCAS Publications.
2. S. Glasstone, Sourcebook on Atomic Energy, 3rd Ed., Affiliated East West Press Pvt. Ltd. (1967).
3. G.R. Choppin and J. Rydberg, Nuclear Chemistry: Theory and Applications, Pergamon Press, Oxford (1980).
4. INTERNATIONAL ATOMIC ENERGY AGENCY, Cyclotron Produced Radionuclides: Principles and Practice, Technical Reports Series No. 465, IAEA, Vienna (2009).
5. Mra, Pillai & Dash, Ashutosh & Knapp, F. (2012). Sustained Availability of Tc-99m: Possible Paths Forward. Journal of nuclear medicine: official publication, Society of Nuclear Medicine. 54. 10.2967/jnumed.112.110338.
6. P.S. Rao, Guest Editor "Nuclear Agriculture and Biotechnology", IANCAS Bulletin, 15(1) (1999).
7. H.N. Wagner Jr., Z. Szabo, J.W. Buchanan, Principles of Nuclear Medicine, 2nd Edition (1995).
8. Therapeutic Applications of Radiopharmaceuticals, IAEA-TECDOC 1228 (2001), IAEA, Vienna.
9. E.A. Evans, M. Muramatsu, Radiotracer Techniques and Applications, Marcel Dekker, New York (1977).
10. Industrial and Environmental Applications of Nuclear Analytical Techniques, IAEA-TECDOC-1121, IAEA, Vienna (1999).

11. W.D. Ehmann and D.E. Vance, Radiochemistry and Nuclear Methods of Analysis, John Wiley & Sons (1992).

12. H.J. Arnikar, Isotopes in the Atomic Age, Wiley Eastern Ltd., New Delhi (1989).

13. Radiochimica Acta Volume 70-71 issue s1 1995 Stöcklin, G.; Qaim, S. M.; Rösch, F. The Impact of Radioactivity on Medicine Metallic.

14. Radiochimica Acta Volume 100 issue 8-9 2012 Qaim, Syed M. -- The present and future of medical radionuclide production.

15. NTERNATIONAL ATOMIC ENERGY AGENCY, Manual for Reactor Produced Radioisotopes, IAEA-TECDOC-1340, IAEA, Vienna (2003).

16. E.K. Hyde, Fission Phenomenon in The Nuclear Properties of Heavy Elements, Prentice-Hall Press, Englewood Cliffs, New Jersey (1964).

17. S. Humphry Jr., Principle of Charged Particle Acceleration, Wiley-Interscience, New York (1989).

18. IAEA Training Course Manual for "Research Reactor Utilisation for Production and Applications of Radioisotopes", BARC/IAEA, Mumbai, India (1989).

19. Radioisotope Production and Quality Control, IAEA Technical Report Series 128, IAEA, Vienna (1971).

20. K. Cohen, "The Theory of Isotope Separation", McGraw Hill, New York (1951).

21. W.R. Nitske, The Life of Wilhelm Conrad Röntgen-Discoverer of X-rays, The University of Arizona Press, USA (1971).

22. A. Romer, The Discovery of Radioactivity and Transmutation, Dover, New York (1964).

23. H. Becquerel, *Comp. Rend.*, **122** (1896) 420, 501.

24. P. Curie and Mme S. Curie, *Compt. Rend.*, **127** (1898) 175.

25. T.J. Trenn, The Self Splitting Atom - The History of Rutherford- Soddy Collaboration, Taylor and Francis Ltd., London (1977).

26. F. Joliot and I. Curie, *Nature*, **133** (1934) 201.

27. Frontiers in Nuclear Chemistry, Eds. D.D. Sood, A.V.R. Reddy and P.K. Pujari, IANCAS Publication, Mumbai (1996).

28. R.D. Evans, The Atomic Nucleus, Tata-McGraw-Hill Book Co.,NewYork (1978).

29. Kaplan, Nuclear Physics, 2nd Ed., Addision Wesley, Cambridge, Massachusetts (1963).

30. G. Friedlander, J.W. Kennedy, E.S. Macias and J.M. Miller, Nuclear and Radiochemistry, 3rd Ed., John Wiley & Sons Inc., New York (1981).

31. H. Langevin-Joliot, In Artificial Radioactivity, Eds. K.N. Rao and H.J. Arnikar, Tata-McGraw Hill, New Delhi (1985).

32. B.L. Cohen, Concepts of Nuclear Physics, Tata McGraw-Hill (1971).

33. I. Kaplan, Nuclear Physics, 2nd Ed., Addision Wesley, Cambridge, Massachusetts (1963).

34. Introduction to Radiochemistry, A.V.R. Reddy and D.D. Sood, IANCAS Publication, Mumbai (1997).

35. W. Scharf, Particle Accelerators and their Uses, Harwood Academic, New York (1986).

36. Directory of Cyclotron used for Radionuclide Production in Member States, IAEA-TECDOC-1007, IAEA, Vienna (1998).

37. Nuclear Chemistry, Vol. 1 and 2, Ed. L. Yaffe, Academic Press, New York (1968).

38. G.I. Bell, S. Glasstone, 'Nuclear Reactor Theory', Van Nostrand, Reinhold, New York (1970).

39. J.R. Marsh, 'Introduction to Nuclear Engineering', Addison Wesley, Reading (1977).

40. S. Glasstone, A. Sesonke, `Nuclear Reactor Engineering', Van Nostrand Reinhold, New York (1987).

41. I.R. Cameron, 'Nuclear Fission Reactors', Plenum Press, New York (1982).

42. INTERNATIONAL ATOMIC ENERGY AGENCY, Non-HEU Production Technologies for Molybdenum-99 and Technetium-99m, Nuclear Energy Series No. NF-T-5.4, IAEA, Vienna (2013).

43. INTERNATIONAL ATOMIC ENERGY AGENCY, Technetium-99m Radiopharmaceuticals: Manufacture of Kits, Technical Reports Series No. 466, IAEA, Vienna (2008).

44. Dash A, Chakravarty R. Radionuclide generators: the prospect of availing PET radiotracers to meet current clinical needs and future research demands. *Am J Nucl Med Mol Imaging*. 2019;9(1):30–66. Published 2019 Feb 15.

45. R.J. Kowalsky and J.R. Perry, Radiopharamceuticals in Nuclear Medicine Practice, Appletons Lange (1987).

46. Modern Trends in Radiopharmaceuticals for Diagnosis and Therapy, IAEA-TECDOC 1029, IAEA, Vienna (1998).

47. Radiopharamaceuticals and Hospital Radiopharmacy Practices, Eds. N. Ramamoorthy, V. Shivarudrappa, A.A.Bhelose, BRNS, BRIT-DAE, Mumbai (2000).

48. N.P. Alazraki and F.S. Mishkin, Fundamentals of Nuclear Medicine, Society of Nuclear Medicine, New York (1984).

49. D.D. Sood, "Changing Scenarios in Isotope Production and Utilisation", IANCAS Bulletin, 14(1) (1998) vii.

50. Isotopes and Radiation Technology in Industry, Eds. S.M. Rao and K.M. Kulkarni, NAARRI, Mumbai (1994).

51. R.J. Woods and A.K. Pikaev, Applied Radiation Chemistry: Radiation Processing, Wiley Interscience (1994).

52. Applications of Radioisotopes and Radiation in Industrial Development, Eds. D.D. Sood, A.V.R. Reddy, S.R.K. Iyer, S. Gangadharan and Gursharan Singh, NAARRI, Mumbai (1998).

53. A.K. Sharma, Guest Editor "Preservation of Food by Ionising Radiation", IANCAS Bulletin, 14(1) (1998).

54. G. Harderson, Use of Nuclear Techniques in Soil Plant Relationships, Training Course Series No.2, IAEA, Vienna (1990).

55. IAEA Technical Report Series 336, IAEA, Vienna (1992).

56. Arino, H., Cosolito, F.J., George, K.D., Thornton, A.K., (1976). Preparation of a primary target for the production of fission products in a nuclear reactor. U.S. Patent 3,940,318.

57. Ariono, H., Kramer, H.H., Mcgovern, J.J., Thornton, A.K., (1974). Production of high purity fission product Molybdenum-99. U.S. Patent 3,799,883.

58. Burill, K.A., Harrison, R.J., (1989). Development of ^{99}Mo process at CRNL. IAEA TECDOC 515. Chalk River Nuclear Laboratories, Canada, pp. 35–46.

59. Hammermair, A., Reich, E., Bogl, W., (1986). Chemical, radiochemical and radio-nuclidic purity of eluates from different commercial fission ^{99}Mo/^{99m}Tc gen-erators. Eur. J. Nucl. Med. 12, 41–46.

60. Hwang, D.S., Choung, W.M., Kim, Y.K., Park, J.H., Park, S.J., (2002). Separation of ^{99}Mo from a simulated fission product solution by precipitation with α-benzoin oxime. J. Radioanal. Nucl. Chem. 254, 255–262.

61. Lewis, R.E., 1971. Production of high specific activity molybdenum-99 for prepara-tion of technetium-99m generators. Int. J. Appl. Radiat. Isot. 22, 603–605.

62. Mcdonald, M.J., Carson, S.D., Naranjo, G.E., Wemple, J.A., 2000. Challenges of extracting and purifying fission-produced molybdenum-99. Ind. Eng. Chem. Res. 39, 3146–3150.

63. Marques, R.O., Cristini, P.R., Fernandez, H., Marziale, D., 1989. Operation of the installation for fission ^{99}Mo production in Argentina. IAEA TECDOC 515. Direccion de Radioisotops Radiaciones, Argentina, pp. 23–33.

64. Mushtaq, A., Iqbal, M., Muhammad, A., 2009. Management of radioactive waste from molybdenum-99 production using low enriched uranium foil target and modified CINTICHEM process. J. Radioanal. Nucl. Chem. 281, 379–392.

65. Nair, A.G.C., Das, S.K., Deshmukh, S.M., Prakash, Satya, 1992. Carrier free separation of ^{99}Mo from ^{233}U fission products. Radiochim. Acta 57, 29–31.

66. Pfenning, G., Nebexius, H.K., Eggebest, W.S., 1998. Chart of Nuclides, 6th edition Farschungszentrum Karlrusche GmbH

67. Sameh, A.A., Ache, H.J., 1989. Production techniques of fission ^{99}Mo. IAEA TECDOC 515. Institut fur Radiochemie, Federal Republic of Germany, pp. 47–64.

68. Shikata, I., Iguchi, A., 1986. Production of ^{99}Mo and its applications in nuclear medicine. J. Radioanal. Nucl. Chem. 102 (2), 533–550.

69. Tucker, W.D., Greene, M.W., Weiss, A.J., Murrenhoff, A., 1958. Methods of purification of some carrier-free radioisotopes involving sorption on alumina. BNL-3746.

70. Vandegrift, G.F., Conner, C., Hofman, G.L., Leonard, R.A., Mutalib, A., Sedlet, J., Walker, D.E., Wiencek, T.C., Snelgrove, J.L., 2000. Modification of targets and processes for conversion of ^{99}Mo production from high-to low-enriched uranium. Ind. Eng. Chem. Res. 39, 3140–3145.

71. Van der Walt, T.N., Coetzee, P.P., 2004. The isolation of ^{99}Mo from fission material for use in the 99Mo/99mTc generator for medical use. Radiochim. Acta 92, 251–257.

72. Villiers, W.V.Z. de, 2003. Manual for reactor produced radioisotopes. IAEA TECDOC 1340. The South African Nuclear Energy Corporation Ltd., South Africa, pp. 139.

73. Vinberg, N., Kristensen, K., 1980. Fission Mo-99/Tc-99m generators – a study of their performance and quality. Eur. J. Nucl. Med. 5, 435–438.

74. Eur J Nucl Med (1981) 6:191-200; L.E. Feinendegen, K. Vyska, Chr. Freundlieb, A. Hock t, H.J. Machulla, G. Kloster, and G. Stocklin; Non-Invasive Analysis of Metabolic Reactions in Body Tissues, the Case of Myocardial Fatty Acids.

75. K. Yoshinaga and N. Tamaki, Curr. Opin. Biotechnol., 2007, 18, 52–59.

76. N. Tamaki, K. Morita, Y. Kuge and E. Tsukamoto, J. Nucl. Med., 2000, 41, 1525–1534.

77. M. Schwaiger and R. Hicks, J. Nucl. Med., 1991, 32, 565–578.

78. M. R. Schelbert, Ann. Nucl. Med., 1994, 8, 91–100.

79. R. A. Goldstein, M. S. Klein, M. J. Welch and B. E. Sobel, J. Nucl. Med., 1980, 21, 342–348.

80. S. Y. Chan, R. C. Brunken, M. E. Phelps and H. R. Schelbert, J. Nucl. Med., 1991, 32, 665–672.

81. F. F. Knapp Jr. and J. Kropp, Eur. J. Nucl. Med., 1995, 22, 361–381.

82. F. F. Knapp Jr., K. R. Ambrose and M. M. Goodman, Eur. J. Nucl. Med., 1986, 12, S539–S544.

83. E. Cazzola, E. Benini, M. Pasquali, P. Mirtschink, M. Walther, H. J. Pietzsch, L. Uccelli, A. Boschi, C. Bolzati and A. Duatti, Bioconjugate Chem., 2008, 19, 450–460.

84. A. Mathur, S. Subramanian, M. B. Mallia, S. Banerjee, G. Samuel, H. D. Sarma and M. Venkatesh, Bioorg. Med. Chem., 2008, 16, 7927–7931.

85. P. Mirtschink, S. N. Stehr, H. J. Pietzsch, R. Bergmann, J. Pietzsch, G. Wunderlich, A. C. Heintz, J. Kropp, H. Spies, W. Kraus, A. Deussen and M. Walther, Bioconjugate Chem., 2008, 19, 389–393.

86. M. Walther, C. M. Jung, R. Bergmann, J. Pietzsch, K. Rode, K. Fahmy, P. Mirtschink, S. Stehr, A. Heintz, G. Wunderlich, W. Kraus, H. J. Pietzsch, J. Kropp, A. Deussen and H. Spies, Bioconjugate Chem., 2007, 18, 216–230.

87. A. C. Heintz, C. M. Jung, S. N. Stehr, P. Mirtschink, M. Walther, J. Pietzsch, R. Bergmann, H. J. Pietzsch, H. Spies, G. Wunderlich, J. Kropp and A. Deussen, Nucl. Med. Commun., 2007, 28, 637–645.

88. T. Uehara, T. Uemura, S. Hirabayashi, S. Adachi, K. Odaka, H. Akizawa, Y. Magata, T. Irie and Y. Arano, J. Med. Chem., 2007, 50, 543–549.

89. T. Chu, Y. Zhang, X. Liu, Y. Wang, S. Hu and X. Wang, Appl. Radiat. Isot., 2004, 60, 845–850.

90. Y. Magata, T. Kawaguchi, M. Ukon, N. Yamamura, T. Uehara, K. Ogawa, Y. Arano, T. Temma, T. Mukai, E. Tadamura and H. Saji, Bioconjugate Chem., 2004, 15, 389–393.

91. G. S. Jones Jr., D. R. Elmaleh, H. W. Strass and A. J. Fichman, Bioorg. Med. Chem. Lett., 1996, 6, 2399–2404.

92. G. S. Jones Jr., D. R. Elmaleh, H. W. Strass and A. J. Fichman, Nucl. Med. Biol., 1994, 21, 117–123.

93. R. H. Mach, H. F. Kung, P. Jungwiwattanaporn and Y. Guo, Nucl. Med. Biol., 1991, 18, 215–226.

94. M. J. Abrams, M. Juweid, C. I. tenKate, D. A. Schwartz, M. M. Hauser, F. E. Gaul, A. J. Fuccello, R. H. Rubin, H. W. Strauss and A. J. Fischman, J. Nucl. Med., 1990, 31, 2022–2028.

95. M. E. Ultee, G. J. Bridger, M. J. Abrams, C. B. Longley, C. A. Burton, S. Larsen, G. W. Henson, S. Padmanabhan, F. E. Gaul and D. A. Schwartz, J. Nucl. Med., 1997, 38, 133.

96. J. W. Babich, H. Solomon, M. C. Pike, D. Kroon, W. Graham, M. J. Abrams, R. G. Tompkins, R. H. Rubin and A. J. Fischman, J. Nucl. Med., 1993, 34, 1967.

97. C. Decristoforo and S. J. Mather, Bioconjugate Chem., 1999, 10, 431–438.

98. C. Decristoforo, L. Melendez, J. K. Sosabowski and S. J. Mather, J. Nucl. Med., 2000, 41, 1114–1119.

99. C. Decristoforo and S. J. Mather, Eur. J. Nucl. Med., 1999, 26, 869–876.

100. M. Bangard, M. B´eh´e, S. Guhlke, R. Otte, H. Bender, H. R. Maecke and H. J. Birsack, Eur. J. Nucl. Med., 2000, 27, 628–637.

101. C. Decristoforo, S. J. Mather, W. Cholewinski, E. Donnemiller, G. Riccabona and R. Moncayo, Eur. J. Nucl. Med., 2000, 27, 1318–1325.

102. S. Liu, A. R. Harris, M. C. Ziegler, D. S. Edwards and N. E. Williams, Bioconjugate Chem., 2002, 13, 881–886.

103. S. Liu, D. S. Edwards, M. C. Ziegler, A. R. Harris, S. J. Hemingway and J. A. Barrett, Bioconjugate Chem., 2001, 12, 624–629.

104. S. Liu, W. Hsieh, Y. Jiang, Y. Kim, S. G. Sreerama, X. Chen, B. Jia and F. Wang, Bioconjugate Chem., 2007, 18, 438.

105. B. Jia, J. Shi, Z. Yang, B. Xu, Z. Liu, H. Zhao, S. Liu and F. Wang, Bioconjugate Chem., 2006, 17, 1069–1076.

106. P. Laverman, E. T. M. Dams, W. J. G. Oyen, G. Storm, E. B. Koenders, R. Prevost, J. W. M. van der Meer, F. H. M. Corstens and O. C. Boerman, J. Nucl. Med., 1999, 40, 192.

107. Y. M. Zhang, N. Liu, Z. H. Zhu, M. Rusckowski and D. J. Hnatowich, Eur. J. Nucl. Med., 2000, 27, 1700–1707.

108. D. J. Hnatowich Jr., P. Winnard, F. Virzi, M. Fogarasi, T. Santo, C. L. Smith, C. R. Cantor and M. Rusckowski, J. Nucl. Med., 1995, 36, 2306–2314.

109. S. Liu, D. S. Edwards, R. J. Looby, A. R. Harris, M. J. Poirier, J. A. Barrett, S. J. Heminway and T. R. Carroll, Bioconjugate Chem., 1996, 7, 63–70.

110. D. S. Edwards, S. Liu, M. C. Ziegler, A. R. Harris, A. C. Crocker, S. J. Heminway, J. A. Barrett, G. J. Bridger, M. J. Abrams and J. D. Higgins, Bioconjugate Chem., 1999, 10, 884–891.

111. D. S. Edwards, S. Liu, J. A. Barrett, A. R. Harris, R. J. Looby, M. C. Ziegler, S. J. Heminway and T. R. Carroll, Bioconjugate Chem., 1997, 8, 146–154.

112. S. Liu, D. S. Edwards and A. R. Harris, Bioconjugate Chem., 1998, 9, 583–595.

113. C. Decristoforo, I. Santos, H. J. Pietzsch, J. U. Kuenstler, A. Duatti, C. J. Smith, A. Rey, R. Alberto, E. von Guggenberg and R. Haubner, Q. J. Nucl. Med. Mol. Imaging, 2007, 51, 33–41.

114. L. K. Meszaros, A. Dose, S. C. G. Biagini and P. J. Blower, Inorg. Chim. Acta, 2010, 363, 1059–1069.

115. C. A. Otto, L. E. Brown, D. M. Wieland and W. H. Beierwaltes, J. Nucl. Med., 1981, 22, 613–618.

116. S. Liu, Top. Curr. Chem., 2005, 252, 117–153.

117. A. Boschi, L. Uccelli, A. Duatti, C. Bolzati, F. Refosco, F. Tisato, R. Romagnoli, B. P. Giovanni, V. Katia and B. P. Andrea, Bioconjugate Chem., 2003, 14, 1279–1288.

118. International Atomic Energy Agency (IAEA) (1990), Guidebook on radioisotope tracers in industry, Technical reports series No. 316,Vienna, Austria

119. Samantray, J.S., Sunil Goswami, Sharma, V.K., Jayashree Biswal, & Pant, H.J. (2014). Leak detection in a high-pressure heat exchanger system in a refinery using radiotracer technique. Journal of Radioanalytical and Nuclear Chemistry, 302(2), 979-982

120. International Atomic Energy Agency (IAEA) (2009) Training course series No. 38.Guidebook on leak detection in heat exchangers and underground pipelines using radiotracers, Vienna, Austria

121. Charlton J.S. (1986), Radioisotope Techniques for Problem Solving in Industrial Process Plants, Leonard Hill, Glasgow and London

122. J. Thýn (1989) Radioisotope Techniques for Process Optimization, Isotopenpraxis Isotopes in Environmental and Health Studies, 25:4, 144-151

123. Pant , H., Kundu , A. & Nigam , K. (2011). RADIOTRACER APPLICATIONS IN CHEMICAL PROCESS INDUSTRY. Reviews in Chemical Engineering, 17(3), pp. 165-252

124. Radiotracer residence time distribution method for industrial and environmental applications, IAEA Training Course Series No. 31, Vienna (2008)

125. Chapter I: Bromine Isotopes. Decay Schemes of Br-80m and Br-82 and Their Properties for Impulse Counting and Autoradiography, Acta Radiologica, 53:sup190, 15-22,(1960)

126. McAuley, R., Lull, R. & Ice, R. Eur J Nucl Med (1985), Bromine-82 contamination in fission product ^{99m}Tc-generator eluate, Volume 10, pp 60-62

127. J. Thýn (1981), Chemical process analysis with nuclear technique, The International Journal of Applied Radiation and Isotopes, Volume 32, Issue 10,1981,Pages 733-746

128. Ramamoorthy, N.Ananthakrishnan, M., Ananthakrishnan, M., & Nandakumar, A.N. (Eds.). (2001). Proceedings of NAARRI international conference on applications of radioisotopes and radiation technology in the 21st century. India: National Association for Applications of Radioisotopes and Radiation in Industry

129. Mohd Yunos MAS, Hussain SA, Sipaun SM (2019), Industrial radiotracer application in flow rate measurement and flowmeter calibration using ^{99m}Tc and ^{198}Au nanoparticles radioisotope, Applied Radiation and Isotopes, Volume 143, 2019, Pages 24-28

130. Ram, Ramu & Chakravarty, Rubel & Pamale, Yugandhara & Dash, Ashutosh & Venkatesh, Meera (2009). An Alumina Based ^{99}Mo-^{99m}Tc Generator to Produce ^{99m}Tc in Organic Medium Suitable for Industrial Radiotracer Applications. Chromatographia. 69. 497-501. 10.1365/s10337-008-0931-9

131. O. P. D. Noronha (1986) Solvent Extraction Technology of ^{99}Mo–^{99m}Tc Generator System 1. An Indian Experience: Process Design Considerations, Isotopenpraxis Isotopes in Environmental and Health Studies, 22:2, 53-57

132. Hwang, D.S., Choung, W. M., Kim, Y. K., Park, J. H., Park, S.J., (2002), Separation of ^{99}Mo from a simulated fission product solution by precipitation with α-benzoin oxime. J. Radioanal. Nucl. Chem., 254, 255-262